

PRODUCTION AND MOVEMENT OF N₂O IN THE FULL SOIL PROFILE

By

Iurii Shcherbak

A DISSERTATION

Submitted to
Michigan State University
in partial fulfillment of the requirements
for the degree of

Crop and Soil Sciences - Doctor of Philosophy

2013

ABSTRACT

PRODUCTION AND MOVEMENT OF N₂O IN THE FULL SOIL PROFILE

By

Iurii Shcherbak

Nitrous oxide (N₂O) is a major greenhouse gas and cultivated soils are the dominant anthropogenic source. In this dissertation, I examine some aspects of N₂O where knowledge is lacking: diffusion of N₂O through the soil profile; production of N₂O in soils below the A or Ap horizon in relation to irrigation, tillage, and fertilization; and patterns of N₂O response to nitrogen (N) fertilizer rate.

In Chapter 2, I measure diffusion by comparing single and inter-port diffusivity determinations using sparse sampling after sulfur hexafluoride (SF₆) and N₂O tracer injections at Kellogg Biological Station in SW Michigan. In general, the sparse method provided accurate measurements of soil diffusivity. Injection port diffusivities of SF₆ and N₂O had poorer agreement in the summer ($r^2=0.49$) than in the fall ($r^2=0.96$), likely due to less uniform soil moisture in summer. The low N₂O to SF₆ diffusivity ratio (0.67 compared to 1.82 in free air) suggests that water solubility of N₂O plays a significant role in retarding its movement in the soil. Movement of SF₆ is not obscured by dissolution in water, making SF₆ a superior tracer compared to N₂O. Results show it is possible to estimate N₂O diffusivity with sparse measurements; accuracy can be improved with knowledge of soil moisture and texture in the immediate vicinity of the ports.

In Chapter 3, I estimate the influence of crop and management practices on subsoil N₂O production in intensively managed cropping systems in a series of experiments also at KBS. N₂O concentrations showed a saturating increase with depth except immediately after fertilization and

in the winter when concentrations were highest in the surface horizon. Variability of N₂O concentrations declined with depth, in agreement with more constant soil conditions. Total N₂O fluxes from direct measurements and estimates by the concentration gradient method showed good agreement, with correlations ranging from 0.55-0.73. N₂O production in subsoil horizons as estimated from concentration gradients is significant, with over 50% of total N₂O produced in moderately fertilized rainfed treatments. In highly fertilized sites where added N exceeded plant N requirements only a small fraction of total N₂O was produced in lower horizons. Dry conditions deepened the maximum N₂O production depth. Results show that the fraction of total N₂O produced in subsoil is controlled by the N and moisture status of the soil profile.

Knowledge of a more precise fertilizer N₂O emission response could improve global and regional N₂O assessments and help to design more efficient mitigation strategies. Evidence now suggests that the emission response is not linear, as assumed by IPCC methodologies, but rather exponentially increases with fertilization. In Chapter 4, I performed a meta-analysis to test the generalizability of these findings. I selected published studies with at least three N fertilizer rates otherwise identical. From 78 available studies (231 site-years), I calculated the change in N₂O emission factors (Δ EFs) as the change in the percentage of applied N converted to N₂O emissions. I found that Δ EF grew with N additions for synthetic fertilizers, for a majority of the crop types examined, and for soils with high organic carbon content, low mean annual temperatures, or low pH. Nitrogen-fixing crops had a significantly higher Δ EF than non-fixing crops. My results suggest a general trend of exponentially increasing N₂O emissions as N fertilizer rates increase to exceed crop N needs. Use of this knowledge in global and regional greenhouse gas inventories could provide a more accurate assessment of fertilizer-derived N₂O emissions and help further close the global N₂O cycle.

ACKNOWLEDGMENTS

I thank my adviser Dr. G. Philip Robertson for guidance through this dissertation work. His patience and constructive criticism helped me withstand the pressures of graduate work and see this project to completion. I am also grateful to my committee members, Bruno Basso, Stephen K. Hamilton, Alexandra N. Kravchenko, for many helpful discussions of experimental design and other suggestions on early drafts. I thank faculty colleagues and fellow graduate students for invaluable discussions and feedback during the development of the experiments and analysis. I am grateful to Kevin Kahmark, Stacey VanderWulp, Cathy McMinn, Leilei Ruan, and Sven Bohm for suggestions on analytical techniques, help with building equipment, sampling, and laboratory analyses. I thank Joe Simmons for agronomic management advice and guidance. I thank Jane Schuette and Volodymyr Shcherbak for help with figure preparation. I thank Melissa Yost for help in acquiring and Leilei Ruan for help with Chinese translations of primary papers for Chapter 4. Funding was provided by the US National Science Foundation Doctoral Dissertation Improvement Grant (DEB 1110683), Long-term Ecological Research (DEB 1027253), and Graduate STEM Fellows in K-12 Education (DGE 0538509) programs, the US DOE Office of Science (DE-FCO2-07ER64494) and Office of Energy Efficiency and Renewable Energy (DE-ACO5-76RL01830), and MSU AgBioResearch.

TABLE OF CONTENTS

LIST OF TABLES	vii
LIST OF FIGURES	viii
CHAPTER 1	
Thesis Introduction	1
SUBSOIL DENITRIFICATION	2
NONLINEARITY OF N₂O EMISSIONS WITH N INPUT	4
REFERENCES	8
CHAPTER 2	
Determining the Diffusivity of Nitrous Oxide in Soil Using In Situ Tracers	11
ABSTRACT	11
INTRODUCTION	12
MATERIALS AND METHODS	15
Site description	15
Soil Profile Gas Sampling	16
Nitrous oxide consumption in the soil	17
Tracer injection and data collection	18
Diffusivity calculations	20
RESULTS	23
N₂O Consumption Experiment	23
Field experiments	24
DISCUSSION	25
N₂O consumption	25
Diffusivity of a relatively soluble gas	26
Diffusivities measured by SF₆ and N₂O tracers	27
Diffusivities of rainfed and irrigated treatments	28
Single-port vs. inter-port diffusivities and comparison with models	29
CONCLUSION	30
REFERENCES	42
CHAPTER 3	
The Importance of Subsoil N₂O Production in Response to Tillage, Fertilizer and Irrigation Effects at a Site in Michigan USA	47
ABSTRACT	47
INTRODUCTION	47
METHODS	52
Site description	52

Experimental Approach	52
<i>Monolith Lysimeters Experiment</i>	53
<i>Soil profile gas probes</i>	55
N₂O surface flux and N₂O production by depth	57
RESULTS	58
Monolith Lysimeters Experiment	59
ILTER Resource Gradient Experiment	59
ILTER Main Cropping System Experiment	60
DISCUSSION	61
Patterns of N₂O concentrations with soil depth	61
Predicting soil N₂O fluxes to the atmosphere from profile N₂O concentrations and diffusivity	62
The contribution of different soil depths to seasonal N₂O fluxes	63
CONCLUSION	65
REFERENCES	76
CHAPTER 4	
A Meta-analysis of the Nonlinearity of Direct Annual N₂O Emissions in Response to Nitrogen Fertilization	81
ABSTRACT	81
INTRODUCTION	82
MATERIALS AND METHODS	85
Study Selection and Data Extraction	85
<i>Emission Factor Change Rates (ΔEFs)</i>	86
Analysis	86
Comparison with previous studies	88
RESULTS	88
DISCUSSION	91
REFERENCES	105
APPENDICES	110
APPENDIX A	111
APPENDIX B	118
APPENDIX C	127
APPENDIX D	131

LIST OF TABLES

Table 1.1. Summary of annual denitrification rates in agricultural soils (from Barton et al. 1999).	6
Table 2.1. Relative soil gas diffusivity (D_p/D_o) models following the Buckingham–Currie power-law function. Model references are as compiled in Jassal et al. (2005), Resurreccion et al. (2010), and Blagodatsky and Smith (2012).	32
Table 2.2. Kellogg Biological Station Long-Term Ecological Research Site soil textures (Kalamazoo and Ostemo Series). Texture is based on % of fraction less than 2 mm (from Crum and Collins 1995). pH values assume no liming is performed at the site.	33
Table 3.1. Horizon depths in the Monolith Lysimeters of Kalamazoo loam soil at KBS (From Aiken 1992). Monolith Lysimeter labels refer to Figure 3.1.	66
Table B.1. Mean and median ΔEF values for different site-year groups by various experimental and sampling factors with the respective standard errors.	118
Table B.2 a. T-test results for paired differences between mean ΔEF groups by crop.	120
Table B.2 b. T-test results for paired differences between mean ΔEF groups by N fertilizer type.	120
Table B.2 c. T-test results for paired differences between mean ΔEF groups by experimental factors.	121
Table B.2 d. T-test results for paired differences between mean ΔEF groups by sampling factors.	121
Table B.3 a. Experimental factor associations in contingency tables.	122
Table B.3 b. Sampling factor associations in contingency tables.	122
Table B.4. Locations for the studies included in the analysis.	123
Table B.5. Variables collected in Dataset S2.	126

LIST OF FIGURES

- Figure 1.1. Major controls on denitrification from cellular (right) to landscape scales. (From Robertson, 2000). 7
- Figure 2.1. Soil profile gas probe with ports at 12, 24, 36, 60, and 90 cm depths. Diameter of the probe is 6.4 mm and not shown to scale. For interpretation of the references to color in this and all other figures, the reader is referred to the electronic version of this dissertation. 34
- Figure 2.2. Replicate (top view) consists of 7 soil profile gas probes arranged in 2 equilateral triangles with 90 cm sides and an additional injection sampler. Values above probes indicate port used for gas injection (in addition to sampling). Unmarked probes were used for sampling only. 35
- Figure 2.3. Mean N₂O to SF₆ ratio over time in summer and fall microcosm experiments. Only microcosms retaining more than 60% of original SF₆ have been retained. Error bars are lower and upper boundaries of the 95% confidence interval for the median. 36
- Figure 2.4. Comparison of SF₆ and N₂O diffusivities. Each replicate observation is a separate point. Straight line is the regression line with best slope through the origin. 37
- Figure 2.5. SF₆ and N₂O diffusivities modeled for ports used for injections. SF₆ is in the left column and N₂O is in the right column. Treatments are Rainfed and Irrigated. Within each treatment there are values for 5 experimental dates arranged chronologically: June 20, June 27, July 03, October 29, and November 1. Only diffusivities with r^2 above 0.85 for SF₆ and 0.6 for N₂O are included. 38
- Figure 2.6. Comparison of SF₆ diffusivities obtained from simulations involving only ports used for tracer injections with a) corresponding diffusivities for the ports used to inject tracers when diffusivities at other ports are taken into account ($r^2=0.99$) and b) median diffusivities for ports at the same depth that were not used to inject tracers ($r^2=0.45$). 39
- Figure 2.7. Poor fit of common diffusivity models with measured SF₆ diffusivity in this study. Lines are models that best fit: Penman 1940 (Pn), Millington 1959 (MI), and Millington-Quirk 1961 (MQ). 41
- Figure 3.1. Diagram of field plots established at the Kellogg Biological Station in 1986 to investigate N supply and tillage effects on soil-plant interactions. Intact-profile 67

monolith lysimeters are located in plots 2, 6, 9, and 13 (From Aiken 1992).	
Figure 3.2. Schematic diagram of monolith lysimeter with instrumentation ports for nondestructive sampling of soil atmosphere, soil solution, soil moisture, and soil temperature. All units are in cm.	68
Figure 3.3. Schematic representation (top view) of nondestructive probes in a soil profile layer in a monolith lysimeter.	69
Figure 3.4. Soil profile gas probe installed at 60° angle with sampling depths at 10, 20, 30, 50, and 75 cm (from Shcherbak and Robertson, in press).	70
Figure 3.5. Mean seasonal N ₂ O concentration profiles observed in the experiments. Atmospheric concentration is 0.38 ppm _v . a) Tilled and no-till Monolith Lysimeters treatments. b) Rainfed and irrigated Resource Gradient Experiment treatments. c) Poplar, Alfalfa, Early-successional community, and Mown grassland (never tilled) systems of the LTER Main Cropping System Experiment (MCSE).	71
Figure 3.6. Average temporal autocorrelations of concentrations at different depths and temporal autocorrelation of surface fluxes of N ₂ O. Autocorrelations close to one indicate N ₂ O concentrations (or fluxes) with low temporal variability, whereas autocorrelations close to or below zero indicate highly variable and unstable values. a) Tilled and no-till Monolith Lysimeter treatments. b) Rainfed and irrigated and Resource Gradient Experiment treatments.	72
Figure 3.7. Change in correlation between N ₂ O surface fluxes and soil N ₂ O concentrations with distance between measurement depths for rainfed and irrigated Resource Gradient Experiment treatments. Each point represents a correlation of N ₂ O concentrations at two different depths in 2011 vs. absolute differences between the depths.	73
Figure 3.8. Comparison of total seasonal N ₂ O emissions measured by static or automatic chamber method and modeled from N ₂ O concentration and diffusivity at 10 cm depth. a) Tilled and no-till Monolith Lysimeter treatments. b) Rainfed and irrigated Resource Gradient Experiment treatments. c) Poplar, Alfalfa, Early-successional community, and Mown grassland (never tilled) systems of the LTER MCSE.	74
Figure 3.9. Annual relative N ₂ O production by depth as calculated from concentrations and modeled diffusivity. a) Tilled and no-till Monolith Lysimeter treatments. b) Rainfed and irrigated Resource Gradient Experiment treatments with rate of N input (0-246 kg N ha ⁻¹) indicated next to the treatment. c) Poplar, Alfalfa, Early-successional community, and Mown grassland (never tilled) systems of the LTER MCSE.	75
Figure 4.1. Locations for the studies included in the analysis.	97

Figure 4.2. Histogram of emission factor change rates (Δ EFs) that indicate percentage of EF change per 1 additional kg N ha ⁻¹ of fertilizer input. Zero, positive, and negative Δ EFs indicate, respectively, a linear, faster-than-linear, and slower-than-linear rate of N ₂ O emissions increase with N input. Δ EFs < -0.02 are not shown for clarity.	98
Figure 4.3. Mean Δ EF with standard errors by type of a) crop, b) fertilizer type, and c) other experimental factors. *, **, and *** indicate difference from 0 at p=0.05, 0.01, and 0.001, respectively. Different letters indicate significant differences between mean Δ EFs for groups of site-years by particular factor.	99
Figure 4.4. a) Comparison of IPCC 1% linear emission model, the Hoben et al. (2011) model, and a model of average upland grain crop emissions from the current meta-analysis; and b) Relative N ₂ O emission reductions for the three models when N application rates are reduced by 50 kg N ha ⁻¹ from three baseline N fertilization scenarios: 200, 150, and 50 kg N ha ⁻¹ .	102
Figure 4.5. Comparison of uncertainties between IPCC Tier 1 (1%), and range of six models from Philbert et al. (2012) and mean quadratic model for all site years without N-fixing crops and the bare soil site. Each of the three models is presented with 95% CI range across 0-300 kg N ha ⁻¹ fertilizer input. IPCC Tier 1 95% CI is 0.3-3%. Philbert et al. (2012) 95% CI for model uncertainty is included with and without parameter uncertainty.	104
Figure A.1. Daily precipitation measured at Kellogg Biological Station Long-Term Ecological Research Site for 2011.	111
Figure A.2. Average daily soil moisture content for 0-25 cm depth in rainfed (Rain) and irrigated (Irr) treatments of the N fertilizer gradient site in 2011.	112
Figure A.3. Mean daily soil temperature at 10 cm depth (Soil) and air temperature (Air) and N fertilizer gradient site in 2011. Differences between rainfed and irrigated treatments are less than 1 °C.	113
Figure A.4. N ₂ O concentration profile in Resource Gradient Experiment Irrigated treatment with 101 kg N ha ⁻¹ input rate on DOY 172 in 2011.	114
Figure A.5. N ₂ O concentration profile in Monolith Lysimeter Conventional Tillage treatment with in plot CT6 on DOY 66 in 2011.	115
Figure A.6. Temporal autocorrelation with depth of modelled water content for days of N ₂ O concentration measurements in Monolith Lysimeter No Till treatment in plot CT6 in 2011.	116
Figure A.7. Temporal autocorrelation with depth of modelled soil temperature for days of	117

N₂O concentration measurements in Monolith Lysimeter No Till treatment in plot CT6 in 2011.

- Figure C.1. Effect of nitrogen (N) input rate on total N₂O emissions and emission factors (EFs) for a) linear, b) slower-than-linear, and c) faster-than-linear response type. 127
- Figure C.2. ΔEF plotted against mean EF for each site-year in meta-analysis. Best linear regression line is plotted $\Delta EF = -0.00045 + 0.0024EF$. Standard error of the linear parameter is 0.0003. 128
- Figure C.3. Graph of mean ΔEF by type of sampling factor. 129
- Figure C.4. Relationship between ΔEF and adjusted r^2 of the quadratic function fit is absent. 130

CHAPTER 1

Thesis Introduction

Nitrogen has the most complex biogeochemical cycle of all the elements essential for life. Since the last century, natural rates of active nitrogen fixation have been severely distorted by human activity. In particular, industrial fixation via the Haber-Bosch process and the cultivation of leguminous crops have added to the biosphere 150 Tg yr^{-1} in additional inputs of reactive nitrogen (Robertson and Vitousek 2009). Almost all pathways within the nitrogen cycle have been drastically changed through additions of biologically active nitrogen (e.g. nitrate, ammonia), which makes it even more difficult to quantify the fate of nitrogen inputs. Vitousek et al. (2009) note that one of the major constraints to reducing this uncertainty is the scarcity of farm-scale nitrogen budgets. Galloway (2004) points out that the relative importance of storage versus the production of N_2 via denitrification is arguably the largest uncertainty that exists for nitrogen budgets at almost any scale.

Denitrification represents one of the major pathways that active nitrogen leaves the site of application, along with leaching, volatilization, and runoff, and is the major process in soils capable of returning nitrogen to its inert form of dinitrogen (N_2) gas (Robertson and Groffman 2014).

Denitrification flux rates are extremely variable due to their dependency at many levels on temporally and spatially variable factors (Table 1.1). Microsite, field, and regional factors are usually considered (Robertson 2000 and Figure 1.1). Microsite level factors include soil temperature, redox status (soil moisture or oxygen concentration are usually used as proxies for this factor), nitrate, and soluble organic carbon concentrations. Field scale factors are agricultural practices and soil type. Regional factors are represented by temperature and moisture regimes.

Denitrification releases two long-lived components to the atmosphere: N_2 and nitrous

oxide (N_2O). N_2 is an inert gas comprising approximately 78% of the modern atmosphere, which makes direct measurements of its fluxes from soil very difficult. Nevertheless, accurate assessment of N_2 fluxes from agricultural soils could help our understanding of the global nitrogen cycle by providing correct values for fluxes among soils, atmosphere, and the ocean.

Nitrous oxide is a potent greenhouse gas (GHG) with a 100-year global warming potential of 298 (IPCC 2007). Agriculture is the single most important source of N_2O , accounting for about two thirds of global anthropogenic emissions (Robertson 2004). On a micro-scale, N_2O is produced from nitrate and transformed to N_2 during denitrification by separate enzymatic reactions, with the potential for some N_2O to escape to the atmosphere (Robertson and Groffman 2014).

SUBSOIL DENITRIFICATION

Denitrification processes in soil have been studied for more than a century, with most attention being devoted to topsoil denitrification, i.e. top 10-20 cm of soil. More than 12,000 articles mention surface soil denitrification in Web of Science database. About thirty articles are available on subsoil denitrification and only a few are from agricultural sites. As noted later, subsoil denitrification could sometimes be a significant or even a major source of N_2O and N_2 in the soil profile.

Chapters 2 and 3 of this dissertation are directed at answering the question “How large is denitrification at depth in soil and how does this vary with land-use, and more specifically, with agricultural practices?” Answering this question will help to reduce significant uncertainties about the rates of $\text{N}_2/\text{N}_2\text{O}$ emissions (Galloway et al. 2004). It will also help modern modeling approaches more accurately represent temporal and spatial distributions of denitrification fluxes; modeling today succeeds only in simulating averages across seasonal time scales. Knowing that

subsoil denitrification is significant changes flux estimations: the whole profile needs to be considered instead of only of the surface horizon (with arbitrary thickness of 10, 5, or even 2 cm). Considering denitrification of the entire profile could lead to less variable N_2/N_2O emissions estimates, which will not only decrease uncertainties in global nitrogen budgets, but also give more precise estimates of global warming impact of particular agricultural practices and agriculture overall.

Experiments in the second chapter measure the speed of N_2O movement in the soil profile, which forms the basis for the transformation of N_2O concentrations in the profile into fluxes to the atmosphere from the soil surface. In the third chapter I answer the general question “How large is denitrification at depth in the soil profile and how does subsoil denitrification vary with land-use, and more specifically, with agricultural practices?” I address this question in a corn / soybean / wheat rotation at the KBS LTER site in southern Michigan.

My main objective is to test the global hypothesis that nitrous oxide production at depth is significant and patterns change significantly along the soil profile and with land use because of predictable underlying changes in primary controls: nitrate and dissolved organic carbon (SOC) availability, soil temperature, and soil redox potential.

I subdivide this global hypothesis into three specific hypotheses tested with experiments described in chapters:

- H1** Significant denitrification occurs at depth in arable soils because subsoil layers have significant levels of nitrate and higher average moisture content compared to surface soils, with DOC a limiting factor for the reaction.
- H2** Tillage, irrigation, and N fertilizer application rate have significant impact on N_2O concentrations in the soil and, in turn, on subsoil N_2O fluxes due to agricultural disturbances like plowing and compaction of the overlying surface soils, as well as

additions of N and carbon.

H3 Different cropping systems will have different patterns of subsoil N₂O concentrations and fluxes for the same reason as in H₂ – differences in soil disturbances.

Experimental results from my site represent only specific groups of soil and climate conditions. With proper calibration, modeling allows extrapolating results to a much wider group of soils and climates, thus providing a way to apply results in many practical situations. Such extrapolation of the specific outcome is possible because many parts of integrated plant-soil-atmosphere models have already been tested for a variety of environmental conditions, which means that only the gas flux prediction module still requires validation.

NONLINEARITY OF N₂O EMISSIONS WITH N INPUT

Total added N fertilizer from all sources is the most important single predictor of N₂O emissions from cultivated land (Millar et al. 2010). There are different models that describe N fertilizer effect on N₂O emissions. Better knowledge of N₂O emission response to N fertilizer is essential for improving global emission budgets of N₂O, and understanding efficient mitigation strategies for emission reduction is an important task.

The N₂O emission factor (EF) is the percentage of applied N converted to N₂O emissions additional to emissions from the non-fertilized field. Global EFs for fertilizer-induced direct N₂O emissions have been determined by Bouwman (1990), Eichner (1990), Bouwman (1996), Mosier et al. (1998), Bouwman et al. (2002a, b), and Stehfest and Bouwman (2006). The current global mean value, derived from over 1000 field emissions measurements of N₂O, is ~0.9% or 0.009 (Bouwman et al. 2002b, Stehfest and Bouwman 2006). This value is an approximate average of synthetic fertilizer (1.0%) and animal manure (0.8%) induced emissions, and was rounded by the

IPCC to 1% or 0.01 due to uncertainties and the inclusion of other N inputs e.g., crop residues (Novoa and Tejeda 2006) and SOM mineralization (IPCC 2007). In short, for every 100 kg of N input, 1.0 kg of N in the form of N₂O–N is assumed to be emitted directly. Constant EF assumes a linear relationship between N fertilizer rate and N₂O emissions that is indifferent to biological thresholds, which might occur, for example, when the availability of inorganic N exceeds the requirements of competing biota such as plants and soil heterotrophs (Erickson et al. 2001).

However, a growing number of studies (e.g., Hoben et al. 2011, McSwiney and Robertson 2005), including the meta-analyses and associated models that informed the IPCC default EF (Tier 1) of 1% (Bouwman et al. 2002a, b, Stehfest and Bouwman 2006), indicate that emissions of N₂O respond non-linearly to increasing N fertilization rate across a range of fertilizer, climate, and soil type, and that therefore EFs vary with respect to N addition. In chapter 4 of this dissertation I investigated the rate of N₂O EF change with N application increase to test the IPCC (2007) assumption of constant EF.

This research will lead to a better understanding of the nitrogen cycle and provide the potential for developing recommendations directed at mitigation of N₂O's impact on climate change as well as other problems associated with reactive N in the environment (Robertson and Vitousek 2009).

Table 1.1. Summary of annual denitrification rates in agricultural soils (from Barton et al. 1999)

<i>System</i>	<i>Observations</i>	<i>Range</i> (<i>kg N ha⁻¹ year⁻¹</i>)
Unfertilized, not irrigated	14	0-17.4
N-fertilized, not irrigated	49	0.5-110
N-fertilized, irrigated	7	49-239
<i>Total</i>	<i>70</i>	<i>0-239</i>

REFERENCES

REFERENCES

- Barton L, McLay CDA, Schipper LA, and Smith CT (1999) Annual denitrification rates in agricultural and forest soils: a review. *Australian Journal of Soil Research* 37:1073-1093.
- Bouwman AF (1990) in *Soils and the greenhouse effect*, ed Bouwman AF (John Wiley and Sons, Chichester, UK), pp 61-127.
- Bouwman AF (1996) Direct emission of nitrous oxide from agricultural soils. *Nutr. Cycl. Agroecosyst.* 46(1):53-70.
- Bouwman AF, Boumans LJM, Batjes NH (2002a) Emissions of N₂O and NO from fertilized fields: Summary of available measurement data. *Glob. Biogeochem. Cycle* 16(4):6.1-6.13.
- Bouwman AF, Boumans LJM, Batjes NH (2002b) Modeling global annual N₂O and NO emissions from fertilized fields. *Glob. Biogeochem. Cycle* 16(4):28.1-28.8.
- Eichner MJ (1990) Nitrous-oxide emissions from fertilized soils - summary of available data. *J. Environ. Qual.* 19(2):272-280.
- Hoben JP, Gehl RJ, Millar N, Grace PR, Robertson GP (2011) Nonlinear nitrous oxide (N₂O) response to nitrogen fertilizer in on-farm corn crops of the US Midwest. *Global Change Biology* 17(2):1140-1152.
- Galloway JN, et al. (2004) Nitrogen cycles: past, present, and future. *Biogeochemistry* 70(2):153-226.
- IPCC (2007) *Climate Change 2007: The Physical Science Basis. Contribution of Working Group I to the Fourth Assessment Report of the Intergovernmental Panel on Climate Change.* ed Solomon S, D. Qin, M. Manning, Z. Chen, M. Marquis, K.B. Averyt, M. Tignor and H.L. Miller (eds.) (Intergovernmental Panel on Climate Change, Cambridge University Press, Cambridge, United Kingdom and New York, NY).
- McSwiney CP, Robertson GP (2005) Nonlinear response of N₂O flux to incremental fertilizer addition in a continuous maize (*Zea mays* L.) cropping system. *Global Change Biology* 11(10):1712-1719.
- Millar N, Robertson G, Grace P, Gehl R, Hoben J (2010) Nitrogen fertilizer management for nitrous oxide (N₂O) mitigation in intensive corn (Maize) production: an emissions reduction protocol for US Midwest agriculture. *Mitig. Adapt. Strateg. Glob. Chang.* 15(2):185-204.

- Mosier A, et al. (1998) Closing the global N₂O budget: nitrous oxide emissions through the agricultural nitrogen cycle - OECD/IPCC/IEA phase II development of IPCC guidelines for national greenhouse gas inventory methodology. *Nutr. Cycl. Agroecosyst.* 52:225-248.
- Novoa RSA, Tejeda HR (2006) Evaluation of the N₂O emissions from N in plant residues as affected by environmental and management factors. *Nutr. Cycl. Agroecosyst.* 75:29-46.
- Robertson GP (2000) Denitrification In *Handbook of Soil Science* ed. Sumner ME (CRC Press, Boca Raton, Florida, USA) pp C181-190
- Robertson GP (2004) Abatement of nitrous oxide, methane, and the other non-CO₂ greenhouse gases: the need for a systems approach In *The global carbon cycle: integrating humans, climate and the natural world* eds. Field CB, Raupach MR (Island Press, Washington,) pp 493-506.
- Robertson GP, Groffman PM (2014) Nitrogen transformations. In *Soil Microbiology, Ecology and Biochemistry* ed. Paul EA (4th Ed. Academic Press, Burlington, MA). In press.
- Robertson GP, Vitousek PM (2009) Nitrogen in Agriculture: Balancing the Cost of an Essential Resource. *Annual Review of Environment and Resources*, (Annual Reviews, Palo Alto), 34:97-125.
- Stehfest E, Bouwman L (2006) N₂O and NO emission from agricultural fields and soils under natural vegetation: summarizing available measurement data and modeling of global annual emissions. *Nutr. Cycl. Agroecosyst.* 74(3):207-228.
- Vitousek, et al. (2009) Nutrient imbalances in agricultural development. *Science* 324:1519-1520.

CHAPTER 2

Determining the Diffusivity of Nitrous Oxide in Soil Using In Situ Tracers.

ABSTRACT

Diffusion is a key process for understanding the movement of nitrous oxide (N₂O), carbon dioxide (CO₂), methane (CH₄), oxygen (O₂), and other biogeochemically important gases in soil. Soil gas diffusivity is highly variable, which makes the application of generic predictive models based on soil macrofeatures uncertain. In situ methods provide greater certainty but intensive sampling usually makes such determinations expensive. I compared single and inter-port diffusivity determinations using a sparse sampling alternative. I used 28 in situ profile probes with ports at 5 depths for pulsed sulfur hexafluoride (SF₆) and N₂O tracer injections at single ports followed by 2-3 measurements in 5 adjacent ports at an agricultural site in SW Michigan, USA. I repeated this procedure for 3 dates in the summer and 2 in the fall. In general, the sparse method provided accurate measurements of soil diffusivity. Estimated diffusivities of SF₆ and N₂O had poorer agreement in the summer ($r^2=0.49$) than in the fall ($r^2=0.96$), likely due to less uniform soil moisture in summer. The low N₂O to SF₆ diffusivity ratio (0.67 compared to 1.82 in free air) suggests that water solubility of N₂O plays a significant role in retarding its movement in the soil. Movement of the relatively insoluble SF₆ is not obscured by dissolution in water making SF₆ a superior tracer compared to N₂O. Median diffusivities in ports where the gas was injected were only moderately correlated ($r^2=0.45$) with diffusivities at the same depth measured by the inter-port method, likely due to an increase in the variability of diffusivity with distance from the injection port. Results show it is possible to estimate N₂O diffusivity with sparse measurements; accuracy can likely be further improved with knowledge of soil moisture and texture in the immediate vicinity of the injection and sampling ports, as uncertainty in water modeling is reduced.

INTRODUCTION

Knowledge of soil gas dynamics is important for understanding soil aeration and the movement of greenhouse and other important gases in soil, and as well for parameterizing biogeochemical models used for predicting global change impacts (Li 1992a, 1992b, del Grosso et al. 2006) and contaminant flows (Moldrup et al. 2000, Resurreccion et al. 2010). Diffusion is the dominant process controlling soil gas movement (Jin and Jury 1996, Werner et al. 2004). It is the result of the random movement of gas molecules and tends to equilibrate gas concentrations without requiring mass flow. Diffusivity of gases in soils is variable because of the complex structure of the pore network and changing soil moisture content.

Diffusion is usually characterized with a diffusivity or diffusion coefficient, which is a proportionality constant that connects the gas concentration gradient with diffusive flux (Lide 2010). The diffusivity coefficient is central to gas dynamics models, and in recent decades much effort has been devoted to developing practical and theoretical methods for measuring and estimating diffusivity under various conditions in undisturbed and repacked soils in the laboratory and in the field.

Most laboratory methods to measure the diffusivity coefficient employ a repacked or intact soil column that has injection and sampling ports along the column sampled 10-15 times over an injection period (Allaire et al. 2008). Diffusivity is then calculated either as the rate of gas disappearance from the injection chamber or as the rate of gas accumulation at the opposite end. While relatively straightforward, for repacked soil columns this method does not account for in situ diffusion through macropores that are destroyed on repacking and that can otherwise have a big influence on total diffusivity (Lange et al. 2009). Even intact soil columns are usually not large enough to include all macro features (Allaire and van Bochove 2007). This problem can be partly alleviated by instead measuring diffusion in intact soil monoliths in the lab (>0.5 m on a

side, Allaire et al. 2008). Monoliths are more difficult to keep at constant moisture, however, and are very labor and cost intensive, especially for heterogeneous sites. Large monoliths also cannot be readily replicated.

In situ field methods provide an attractive alternative that do not suffer from distorted macropore or other soil structure issues associated with laboratory determinations. Field measurements of gas diffusivity reviewed by Werner et al. (2004) include flux chamber, atmospheric tracer, instantaneous point-source single-port, instantaneous point source inter-port, and continuous point source inter-port methods.

The flux chamber method consists of a chamber that is placed with edges a few centimeters into the soil and that is then injected with a tracer gas. The tracer diffuses into the soil at a rate estimated by its disappearance from the chamber. This method works well for short measurement intervals and provides diffusivity measurements in soil surface layers.

The atmospheric tracer method (Weeks et al. 1982) relies on gas concentrations measured at several depths in the soil profile and historical gas concentrations in the atmosphere to estimate diffusivity. A one-dimensional diffusion equation uses atmospheric gas concentration at the surface and no flux at the water table as boundary conditions. The method is simple to implement as only two measurements at each depth are required, but is limited to environments where gases move very slowly, are not biologically active, and do not express large temporal or spatial variations.

The instantaneous point-source single-port method (Lai et al. 1976) uses the same port to introduce a tracer and remove samples. Diffusivity is calculated by analytical or numerical methods. The method is relatively simple to implement and analyze and requires low numbers of samples, but the measurement volume is poorly defined and some probe designs can disturb the soil during installation. These limitations make the method useful for fast determinations of

diffusivity, but many sampling ports are required because of sampling volume uncertainty.

The instantaneous point-source inter-port method (Nicot and Bennett 1998, Werner 2002) uses two or more ports. One is used for injection and others are sampled to determine the time to maximum concentration at different distances from the injection port. A better defined sampling volume allows fewer probes to estimate diffusion, but the method requires frequent sampling due to high sensitivity of diffusivity estimates to the time it takes gases to reach maximum concentration at some distance from the injection point.

The continuous point-source inter-port method (Kremer et al. 1988) also uses several ports, but the tracer is released from the injection port at a constant rate. This method allows for much simpler steady-state solutions to obtain the diffusivity constant and is presently the most reliable field-based method. However it requires that significant amounts of tracer be injected at a constant rate for long periods (up to several days depending on the inter-port distances), and that soil conditions do not significantly change before steady-state is achieved for the soil volume of interest.

Attempts have also been made to predict gas diffusivity from static soil characteristics that are more readily available or estimable. Most models of soil diffusivity use total soil porosity (Φ), the volume of air (ϵ), and pore geometry (tortuosity and connectivity) and have the general form $a\epsilon^b\Phi^{-c}$, where a, b, and c are numerical constants that account for pore geometry and are used to bring the model into agreement with the data (Table 1). Other models distinguish between inter- and intra-aggregate porosity and use more complicated relationships of diffusivity to soil characteristics, often additionally requiring knowledge of soil air volume at one or more matric potentials (e.g. ϵ_{100} – air volume at -100 cm H₂O pressure head, Moldrup et al. 2005) and representing diffusivity with a piecewise function where pieces relate to intervals of the water-filled porosity (Resurreccion et al. 2010).

Despite much effort, a universal predictor of diffusivity for many soil types and conditions has not been found (Jin and Jury 1996). Bruckler et al. (1989) concluded that such a predictor cannot exist because it would necessarily be dependent on complex pore geometry, which might not be possible to represent with soil parameters that are easily measured. For any given site large differences in diffusivities are obtained by different models and it is difficult to select the best one for the site on purely theoretical grounds. Many diffusivity models are also very sensitive to air filled volume and total porosity since they are raised to high powers in many popular models (Werner et al. 2004). Thus model selection for any given site is probably best informed by in situ measurements at the site of application using equipment that is easy to install and operate.

Here I describe an inexpensive soil atmosphere probe that can be used for in situ profile measurements of gas concentrations to yield diffusivity as a numeric solution of the diffusion equation. My specific objectives are 1) to test the applicability of in situ tracer measurement to determine diffusivity with inverse methods, 2) to test if measurements made with SF₆ are more appropriate than direct measurements with N₂O, and 3) to evaluate the effectiveness of single port vs. inter-port methods. To address the second objective I also measured N₂O consumption at depth. I then compare measured diffusivities against values provided by models from the literature.

MATERIALS AND METHODS

Site description

I measured diffusivities at the Resource Gradient Experiment at the W.K. Kellogg Biological Station Long-Term Ecological Research Site (KBS LTER, kbs.msu.edu/lter), located in southwest Michigan in the northeast portion of the U.S. Corn Belt (42° 24' N, 85° 24' W, with

average elevation 288 m). Mean annual temperature is 10 °C and annual rainfall averages 1027 mm/y with about half of the precipitation received as snow. Detailed weather and soil data for the 2011 growing season are in Figure A.1-A.3. Soils are a mixture of Kalamazoo (fine-loamy, mixed, semi-active, mesic Typic Hapludalfs) and Oshtemo (coarse-loamy, mixed, active, mesic Typic Hapludalfs) loams (Mokma and Doolittle 1993, Crum and Collins 1999) (Table 2).

The KBS LTER Resource Gradient Experiment provides a range of nitrogen fertilization levels under both rainfed and irrigated conditions in a corn–soybean–wheat rotation.

Experiments were performed in summer and fall 2012 with the field planted to soybean. Planting occurred on May 22 at 45 seeds m⁻² in 38 cm rows to a depth of 4 cm. Plots are 4.6 by 27.4 m arranged in 4 replicate blocks. In this study I used plots with 56 and 74 kg N/ha in rainfed plots and 37 and 93 kg N/ha in irrigated plots in one block.

Soil Profile Gas Sampling

I used 5-port soil profile gas probes to make tracer injections at different soil profile depths and to collect gas samples, which I then used to determine diffusivities. I compared diffusivities across treatments, injection depths, and seasons. I also compared measured diffusivities with the diffusivities from published models.

My 5-port soil profile gas probe (Figure 2.1) consists of a master tube made of stainless steel (90 cm long, ~6.4 mm o.d., ~4.8 mm i.d.) that contains 5 stainless steel sampling tubes (~1.6 mm o.d., 0.5 mm i.d.) that protrude 3 cm from the outer walls of the master tube at 12, 24, 36, 60, and 90 cm depths. Openings around the protrusions are sealed with air-tight silicon-based sealant to prevent gas diffusion into and out of the master tube. The upper ends of the sampling tubes each fitted with a brass reducer (Swagelok, Solon, Ohio, USA) and rubber septum for sampling access. The largest dead space for the port at 90 cm depth is about 1 ml.

To minimize the impact on future tracer concentrations, the protocol minimized the volume of gas taken. To draw a sample, I pierced a septum with a needle attached to a syringe and pumped the air inside the tube 3 times by drawing 10 mL of air and immediately injecting it back into the port. Then I injected 5 mL of soil gas sample and 5 mL of atmospheric air to 5.9 mL non-evacuated Exetainer vials originally containing air at atmospheric pressure to create overpressure. Samples were analyzed for N₂O and SF₆ as described above.

Nitrous oxide consumption in the soil

I performed microcosm experiments to determine the suitability of using N₂O directly as a non-consumable tracer for soil diffusivity determinations. If N₂O is consumed then it cannot be used to measure diffusivity reliably.

On 25 May 2012 I took 1 sample of 0-10 cm soil from the first four replicates of soybeans in the Conventional, No-till, Reduced input, Biologically based, Alfalfa, Poplar, Early Successional, and Mown Grassland (Never tilled) systems of the Main Cropping System Experiment at the Kellogg Biological Station (KBS) Long-Term Ecological Research Site (Robertson and Hamilton 2014), <500 m from the soil gas probe installations on the same soil type. Soil samples were put through a 4 mm sieve. Moisture contents of the soil were estimated by drying subsamples in an oven at 105°C. The next day two 200 g fresh weight subsamples were placed in a 1 L mason jar (Jarden, Rye, NY, USA). I added 75 mL of deionized water to completely saturate the soil, with one subsample receiving nitrate at 150 mg N kg⁻¹ soil. Jars were then sealed with lids with septa to allow for gas sampling and to each jar was added 1 mL of 45 nmole L⁻¹ SF₆ (1 ppm_v) and 1 mL of 2.23 μmole L⁻¹ N₂O (5% by volume). An additional 60 mL of laboratory air were added to each jar to create an initial overpressure. Headspace samples were taken 12, 24, 48, 72, 96, and 120 hours after the jars were sealed. At each

sampling I removed 5 ml of microcosm atmosphere to a 5.9 ml non-evacuated Exetainer vial (Labco Ltd., High Wycombe, UK) to which I then added 5 mL of air to over-pressurize during storage. Samples were analyzed within 10 days of collection.

Again, on 10 Oct., 2012, I took duplicate 6-cm diameter 1 m-deep soil cores from 2 rainfed and 2 irrigated locations on the Resource Gradient site with a hydraulic sampler (Geoprobe, Salina, KS). The locations of these samples were less than 2 m from corresponding soil gas probe installations as explained below. The next day three 300 g field moist samples from each core at depths 5-25, 35-50, and 75-90 cm were sieved and placed in duplicate jars that were then supplemented with 75 ml of deionized water and injected with SF₆ and N₂O as described above. I took a total of 9 headspace samples per jar 0, 4, 8, 13, 19, 27, 37, 50, and 74 hours after the jars were closed.

Samples were analyzed for SF₆ and N₂O using a gas chromatograph (Agilent 7890A) equipped with an auto-sampler (Gerstel MPS 2 XL). SF₆ and N₂O were separated with one of two Restek PP-Q 80/100 packed columns (length 3 m, ID 2 mm, OD 3.175 mm) and detected using a ⁶³Ni electron capture detector at 350°C. Carrier gas was 90% Ar and 10% CH₄ (Ultra High Purity Grade 5.0 with a Restek 21997 moisture trap and Restek 20601 oxygen scrubber) at a 10±0.5 mL/min flow rate. Oven temperature was 78°C during the first 5.5 min of the run, and then the column was back flushed and baked for 0.5 min (terminal temperature 105°C, increase rate 55°C/min). The analytical coefficient of variation was below 2% for SF₆ and N₂O.

Tracer injection and data collection

I installed 28 soil profile gas probes in Block 1 of the Resource Gradient Experiment. Seven probes were installed in each of 2 replicate rainfed and 2 replicate irrigated plots. Every probe was installed into a predrilled vertical well made with a 6.35 mm × 0.9-m length drill-bit

(Model A36.250; Associated Industrial Distributors, Crystal Lake, IL). Sampling depths were 12, 24, 36, 60, and 90 cm (Figure 2.1). The 7 probes per plot were installed in a configuration designed to check diffusivity not only in the vertical but also in the horizontal direction (Figure 2.2). I used two of the probes for gas injection at 90 cm depth, two for gas injection at 60 cm depth, one probe for gas injection at 36 cm depth, and two control probes were not used for gas injection. Probes were located at least 3 m from a plot edge. Each pair of probes used for injection at 60 and 90 cm was grouped with a control probe to form an equilateral triangle with 0.9 m side (Figure 2.2) so that the concentrations at the horizontal distance from the injection port could be measured. Installations were performed separately for summer and fall in the same plots with probes installed into a well of the same diameter at least 10 days before first sampling to allow soil to equilibrate post-installation and provide a good seal between sampling ports.

Experiments were performed over 5 dates in 2012: three in the summer (June 20, June 27, and July 03) starting 29 days after planting, and two in the fall (Oct. 29 and Nov. 1) shortly after harvest. Summer sampling occurred after three weeks without rain, whereas fall experiments followed about 14 cm of rain during October, which completely recharged the profile as it holds 12 cm of water m^{-1} . On each sampling date I sampled ports used for gas injection to determine background concentrations of N_2O and SF_6 . Direct measurement of baseline tracer concentrations eliminated the need to measure concentration of the precursors: nitrate and soluble organic carbon. I injected 2 mL of 45 nmole L^{-1} SF_6 (1 ppm_v) and later 2 mL of 44.6 $\mu\text{mole L}^{-1}$ N_2O (100% by volume) into the injection port with each gas followed by 8 mL of atmospheric air to flush the dead volume of the injection ports. Injections of each gas into 20 injection ports took about 10 minutes to complete. Following the injections, I took three sets of samples: 1) from 20 injection ports (taking 15 minutes), 2) from all 140 ports (taking 60 minutes), 3) from all 140 ports (taking 60 minutes). I allowed 15 minutes between the sampling

sets. I obtained 4 independent diffusivity estimates for the 36 cm injection depth, and 8 estimates for the 60 and 90 cm injection depths. A total of 20, 40, and 40 diffusivity values for injection depths at 36, 60, and 90 cm have been obtained, respectively.

Diffusivity calculations

I estimated only layered soil water content and temperature for 2012 with the System Approach to Land Use Sustainability (SALUS, Basso et al. 2006) model, parameterized and tested for the site earlier (Syswerda et al. 2012). I validated modeled averages for 0-25 cm soil depth with measured data for the same depth. I did not measure particle density and assumed it is 2.65 g/cm^3 . To calculate porosity I assumed bulk density below 69 cm stayed the same at 1.8 g/cm^3 . Using total porosity and modeled water content I estimated air-filled porosity (ϵ) to be used in diffusivity calculations.

I obtained diffusivity by numerical procedure performing an interval search for the diffusivity value, minimizing the sum of squared differences of measured tracer concentrations and tracer concentrations from the diffusion equation for the same position in space and time. The general form of a nonhomogeneous 3-dimensional diffusion equation in cylindrical coordinates is

$$\frac{\partial(\epsilon C)}{\partial t} = \frac{1}{r} \frac{\partial}{\partial r} \left(D r \frac{\partial C}{\partial r} \right) + \frac{1}{r^2} \frac{\partial}{\partial \varphi} \left(D \frac{\partial C}{\partial \varphi} \right) + \frac{\partial}{\partial z} \left(D \frac{\partial C}{\partial z} \right) + g \quad [1]$$

where r – radius,

φ – angular coordinate,

z – vertical coordinate,

ϵ – fraction of air-filled porosity,

$D = D(r, \varphi, z)$ – diffusivity of gas,

$g = g(t, r, \varphi, z)$ – production function,

$C = C(t, r, \varphi, z)$ – concentration of gas.

Because there was no production or consumption of SF₆ or N₂O (see Results) I assumed angular symmetry of concentrations. I assumed diffusion was constant at the same depth. I assumed porosity to stay constant for each depth for the duration of the experiment. Therefore, the equation simplifies to the 2-dimensional homogeneous form

$$\varepsilon \frac{\partial C}{\partial t} = \frac{D}{r} \frac{\partial}{\partial r} \left(r \frac{\partial C}{\partial r} \right) + \frac{\partial}{\partial z} \left(D \frac{\partial C}{\partial z} \right) \quad [2]$$

Initial concentrations were assumed to follow the 2 dimensional error function

$$C_{0,r,z} = \frac{v C_{inj}}{2\pi\sigma^2} e^{-\frac{1}{2\sigma^2}(r^2+(z-z_0)^2)} \quad [3]$$

where $C_{0,r,z}$ – initial concentration at point (r, z) ,

C_{inj} and V_{inj} – concentration and volume of the gas injected,

σ – a parameter equal to 4 cm,

$(0, z_0)$ – point of injection,

v – parameter, adjusted so that $\iint r C_{0,r,z} dr dz = V_{inj} C_{inj}$.

Concentrations at the border were assumed to be 0 at all times. The exact initial distribution is inconsequential, since the first sampling occurs at least 15 minutes after the injection and there were no abrupt changes in concentrations. In a general case this equation with initial and boundary conditions does not have an analytical solution, so I employed the alternating direction implicit method (Peaceman and Rachford, 1955). Equations that describe the process are

$$\varepsilon_j \frac{C_{i,j}^{n+\frac{1}{2}} - C_{i,j}^n}{\Delta t/2} = \frac{D_j}{r_i} \delta_r C_{i,j}^{n+\frac{1}{2}} + D_j \delta_{rr} C_{i,j}^{n+\frac{1}{2}} + \delta_z D_j \delta_z C_{i,j}^n + D_j \delta_{zz} C_{i,j}^n \quad [4]$$

$$\begin{aligned} \varepsilon_j \frac{C_{i,j}^{n+1} - C_{i,j}^{n+\frac{1}{2}}}{\Delta t/2} \\ = \frac{D_j}{r_i} \delta_r C_{i,j}^{n+\frac{1}{2}} + D_j \delta_{rr} C_{i,j}^{n+\frac{1}{2}} + \delta_z D_j \delta_z C_{i,j}^{n+1} + D_j \delta_{zz} C_{i,j}^{n+1} \quad [5] \end{aligned}$$

where $C_{i,j}^n$ – concentration at time $n\Delta t$, at radius $i\Delta r$, and depth $j\Delta z$,

Δr – step in radial direction,

Δz – step in vertical direction,

Δt – time step,

$$\begin{aligned} \delta_z D_j &= \frac{D_{j+1} - D_{j-1}}{2\Delta z}, \\ \delta_r C_{i,j} &= \frac{C_{i+1,j} - C_{i-1,j}}{2\Delta r}, \\ \delta_{rr} C_{i,j} &= \frac{C_{i+1,j} - 2C_{i,j} + C_{i-1,j}}{(\Delta r)^2}, \\ \delta_z C_{i,j} &= \frac{C_{i,j+1} - C_{i,j-1}}{2\Delta z}, \\ \delta_{zz} C_{i,j} &= \frac{C_{i,j+1} - 2C_{i,j} + C_{i,j-1}}{(\Delta z)^2}. \end{aligned}$$

The equations were run in a cycle from time 0 to T with a step Δt , where during each iteration diffusion is assumed to occur in a horizontal direction for the first equation and in a vertical direction for the second. During time step $n + 1$, terms from previous time steps $n + 1/2$ and n are considered known. Assembling unknown terms on the right-hand side yields a set of tridiagonal matrices that are solved (Thomas 1949) to find concentrations in the next time step.

I fit diffusivity parameters to the data using a program written in C# and run on the .NET 4.5 framework (Microsoft 2012, see supplemental materials for source code). The program executed a search in diffusivity parameter space with an objective function to minimize the sum of squared deviations between measured and simulated gas concentrations. Diffusivities ranged from 10^{-9} to $1.38 \cdot 10^{-5} \text{ m}^2/\text{s}$, with limits of diffusivity being diffusivity in water and in air,

respectively. I ran the diffusivity adjustment model involving only the region with the injection port for both N₂O and SF₆ and compared them.

I performed parametric (two-sided t-test) comparisons of diffusivities obtained for injection ports by depth, presence of irrigation and time of year (summer or fall). For 60 and 90 cm depths I compared SF₆ diffusivities for ports used for injections with median values of diffusivities for ports at the same depth that were only used for sampling. Statistical analyses were carried out in Wolfram Mathematica 9.0 (Wolfram Research 2012).

I performed full 5-port probe diffusivity adjustment for N₂O and SF₆. The parameter space in each case consisted of independent diffusivities for consecutive layers with borders at 0, 18, 30, 41, 69, 120 cm. A 4 cm border region between every two layers has diffusivity as a linear mixture of the layers. I compared diffusivities for injection ports in this procedure (full diffusivity) with corresponding injection port diffusivities in simplified procedure (one-port diffusivity). I then used resampling to compare median diffusivity of ports not used for gas injection (sampling port diffusivity) with median diffusivity of ports used for injection at the same depth (injection port diffusivity).

Using moisture content, temperature, and texture as inputs I obtained diffusivities using existing soil diffusivity models (Table 2.1) and compared those to diffusivities I obtained by my method.

RESULTS

N₂O Consumption Experiment

Headspace concentrations of N₂O relative to the inert tracer SF₆ did not significantly decline for the duration of the experiment, 77 h, in experiments with soil samples taken either in summer or fall (Figure 2.3): measured N₂O consumption was nil. I had to remove approximately half of the microcosm replicates where more than 40% of original SF₆ content was lost from a

jar due to a defective seal; the remaining dataset had significantly reduced variance.

Field experiments

Figure 2.4 compares soil gas diffusivity estimates for decreasing concentrations of injected N₂O to those for SF₆ for summer and fall samplings. SF₆ diffusivities have much better agreement with the concentration measurements (only 5% of runs have $r^2 < 0.85$) than N₂O diffusivities (60% of runs did not achieve $r^2 < 0.85$). I have removed 6 SF₆ diffusivity results with $r^2 < 0.85$ and 17 N₂O diffusivity results with $r^2 < 0.6$. However, SF₆ and N₂O diffusivities agreed reasonably well (Figure 2.4 a, $r^2 = 0.64$) when calculated only on remaining experiments. By season, SF₆ diffusivities were only weakly correlated with N₂O diffusivities in the summer experiments (Figure 2.4 b, $r^2 = 0.53$), while SF₆ and N₂O diffusivities had very high agreement in the fall experiments (Figure 2.4 c, $r^2 = 0.95$). The N₂O to SF₆ diffusivity ratio for the fall experiments was 1.24.

Diffusivities of SF₆ in the rainfed treatments were significantly ($p < 0.02$) higher than respective values for irrigated treatments for all depths in summer tests (Figure 2.5) while differences for diffusivities at 90 cm injection depth were also significant for the fall samples. N₂O diffusivities had similar differences between respective rainfed and irrigated treatments, but larger variability and exclusion of some diffusivity values led to weaker results ($p = 0.10 - 0.15$). The soil layers show a declining difference between rainfed and irrigated treatment diffusivities with depth. Diffusivities of SF₆ in the rainfed treatment significantly declined with depth ($p < 0.03$) in the summer, with the first sampling date having a lower significance at $p = 0.1$ a minimum power of pairwise comparisons between diffusivities at 36, 60, and 90 cm depths.

SF₆ diffusivities involving only the injection port almost perfectly coincided with diffusivities for the injection port obtained from full scale simulations (Figure 2.6 a, $r^2 = 0.99$).

Single-port vs. inter-port SF₆ diffusivity comparisons yielded a weak correlation (Figure 2.6 b, $r^2 = 0.4$). N₂O diffusivities followed the same trends, but are much more variable and do not show significant differences.

In my experiments models of diffusivity based on soil moisture content do not have strong predictive ability for diffusivities since they all use soil moisture as a main predictor, which is only weakly correlated with my diffusivity measurements (Figure 2.7).

DISCUSSION

Overall results suggest that the point source single port method is adequate for diffusivity measurements and that the point source inter-port method does not improve results (as noted in Figure 2.6 b) despite a better defined sampling volume. I also found that diffusivity is not easily measured directly with N₂O, probably due to its greater solubility in water. SF₆ with its lower solubility is a superior tracer because its movement is not obscured by absorption and release by soil water. SF₆ diffusivity can be converted to N₂O diffusivity based on their mass differences.

N₂O consumption

N₂O dynamics in soil depend on its diffusion between the layers, as well as production and consumption of the gas. To use N₂O directly as a diffusivity tracer requires that N₂O dynamics be determined only by diffusion and not be lost or gained in the layers via biological activity. N₂O production in soil can be significant, but is not an obstacle for short term experiments because background concentrations usually change slowly and can be measured at the beginning of the experiment. Nevertheless, it is necessary to show that N₂O consumption in a given soil is insignificant in situ; otherwise measurements of diffusion could be an artifact of substantial N₂O consumption.

The ability of soils to consume N₂O has only been tested for a limited range of soil types and no comprehensive survey exists (Clough et al. 2005). While many researchers have found evidence for N₂O consumption in laboratory experiments (Clough et al. 1999), others have not (van Bochove et al. 1998). Some field experiments have a significant number of small negative fluxes that might indicate the possibility of consumption, but other explanations have been proposed as well. Interactions of N₂O with water complicate the in situ determinations of N₂O consumption at depth (Heincke and Kaupenjohann 1999).

Concentrations of N₂O relative to SF₆ did not decline in my laboratory incubations with soil samples taken in summer or fall (Figure 2.3) regardless of profile depth and even under optimal consumption conditions of a mixed slurry. This indicates that N₂O was not consumed to a measurable degree. This result allows us to consider using N₂O as an inert tracer for my short-term (<5 hours) and possibly longer in situ diffusivity experiments for these soils.

Diffusivity of a relatively soluble gas

Water content is a major determinant of gas diffusivity in soil by occupying pore space. Its influence becomes even more complex when the gas of interest is relatively soluble (e.g. N₂O) or reacts with water to form other compounds (e.g. CO₂). Below I derive a theoretical ratio of apparent diffusivities of two gases with different masses and solubility under equal concentration gradients and soil conditions. For equal gradients of concentrations in air or soil (if solubility and reactions with water can be ignored) two gases have the ratio of diffusivities approximately inversely proportional to the square root of their molar mass ratio ($D_2/D_1 \sim \sqrt{M_1/M_2}$). For example, for N₂O to SF₆ this ratio is 1.82 (SF₆ and N₂O masses are 146 g mol⁻¹ and 44 g mol⁻¹, respectively). Differences in the solubility of gases modify this relationship. To derive an adjustment factor for the diffusivities of the two gases with solubility

f_1 and f_2 (expressed as Bunsen absorption coefficients or ratios of equilibrated gas concentrations in water to concentration in the headspace) I assume that both gases achieve instantaneous equilibrium between air (a) and water (w) fractions of total porosity. The flux of the gas through the air-filled phase depends only on the concentration gradient and not the solubility. Since soluble gas has $(a + f_i w)$ of combined gas in water and air phases, the change in concentration will be slower by a factor $a/(a + f_i w)$ compared with an insoluble gas ($f_i = 0$) of the same molar mass. Since apparent diffusion is proportional to observed change in concentrations, the ratio of diffusivities (D_i) of the two gases is

$$\frac{D_2}{D_1} = \sqrt{\frac{M_1}{M_2} \frac{a + f_1 w}{a + f_2 w}} \quad [6].$$

Heincke and Kaupenjohann (1999) have reviewed in detail other factors that influence N₂O solubility, including temperature, salt concentration and type, pH of the solvent, and possibly dissolved organic matter. Clay content can also influence apparent solubility through adsorption effects.

Diffusivities measured by SF₆ and N₂O tracers

For SF₆ only 5% of the measured diffusivities had an $r^2 < 0.85$, whereas for N₂O over 60% of diffusivities lacked this fit. This difference is likely due to heterogeneous distribution of soil water that influences the diffusion of N₂O because of the relatively high N₂O solubility of 1.47 g L⁻¹ (Gevantman 2010) as compared to SF₆'s solubility of 0.036 g L⁻¹ (Friedman 1954).

Diffusivities of SF₆ and N₂O are highly correlated for the fall measurements but only weakly correlated for the summer. This is likely due to differences in soil moisture.

Heterogeneity of the water content is caused by variation of soil physical properties (texture,

aggregation, porosity), precipitation, and temperature (Allaire et al. 2008). During the growing season variation in water content is increased due to the heterogeneous distribution of roots; this variation is present in both rainfed and irrigated treatments, despite the higher overall water content in the irrigated treatment.

The slope of the best fit line for the ratio of N_2O and SF_6 diffusivities combines the effects of mass and solubility differences and possible other differences in their interaction with the medium. The lower slope of only 0.67 for fall (Figure 2.4) compared to the ratio of diffusivities in free air indicates that the high solubility of N_2O has a major influence on its apparent diffusivity. Fall diffusivity ratios of N_2O and SF_6 are consistent because water content was more uniform after the soil profile had been recharged and no plant uptake influenced the distribution of water, as shown by modeling with SALUS. Substituting measured diffusivity ratio, molar mass ratio, and air filled porosity (1–10% modeled in SALUS) into Eq. [6] I obtain the ratio of water to air N_2O concentrations of 0.1-0.6 (at 32-40% porosity based on a bulk density of 1.6-1.8), a value that is lower than equilibrium partitioning (0.6-0.8 at temperatures of 13-23°C). This suggests that N_2O is a poor choice of tracer gas, since it behaves differently from N_2O produced in soil that is in equilibrium with soil water. This might not be true for air-filled porosity values above 10%, where N_2O will be more in equilibrium with water, behaving similarly to N_2O produced in the soil. Therefore, using SF_6 as a tracer gas and then applying modifications to adjust diffusivity for mass and solubility differences between SF_6 and N_2O (or another soluble gas of interest) is a more appropriate strategy for soils with low air-filled porosity.

Diffusivities of rainfed and irrigated treatments

Comparing SF_6 and N_2O diffusivities from rainfed and irrigated treatments (Figure 2.5)

agrees with the general prediction that diffusivity will grow with air-filled porosity since the diffusivity of gases in air is usually several orders of magnitude greater than their diffusivity in water. So, a larger diffusivity in rainfed compared to irrigated treatments in the summer is likely due to the greater percentage of soil pores occupied by air in the rainfed treatment. The irrigated treatment did not receive any additional water after the summer, so its water content was mostly equilibrated and diffusivity differences between the two treatments that were present in the summer disappeared in the fall, except for the deepest layer, which was not completely saturated by November in the rainfed treatment. Smaller differences between SF₆ and N₂O diffusivities of rainfed and irrigated treatments in deeper layers are likely also caused by a similarity in water content even in the summer due to the relative scarcity of roots at 90 cm depth. The decrease in SF₆ diffusivities of rainfed treatment in the summer are also caused by the modeled decrease in air-filled porosity with depth.

Single-port vs. inter-port diffusivities and comparison with models

Diffusivities for ports not used for injection have much higher variability than diffusivities for ports used for gas injection. The main reason for this is that spatial variability compounds with more layers between injection and measurements (Figure 2.6 b).

It is usually more practical to use diffusivity models instead of in situ measurements, especially in projects that do not allow the use of convenient tracers. Modeling informed by in situ data is an optimal approach in this case. I calculated diffusivities using modeled soil air and moisture content to compare with results from existing diffusivity models. Existing models yielded poor fits (Figure 2.7) and this failure is attributable to 1) the fact that moisture was not measured in the immediate vicinity of the ports, 2) the natural variability of diffusivity due to soil macro features, and 3) the poor ability of generic soil diffusivity models to predict diffusivity

on a particular site without prior calibration.

Overall my results show that the single-port pulse injection method with SF₆ as an inert tracer provides a viable approach for obtaining quick estimates of gas diffusivity for a particular site. Adjusting predictive diffusivity models with measurements for use at a specific site is simple and does not require a significant expenditure of resources. Using SF₆ as a tracer avoids complications related to the high solubility of N₂O and its production and perhaps consumption in a given soil.

My method could be improved and better applied in other soils with more precise estimates of moisture and temperature, making them more informative to generic soil diffusivity models on the site of interest. With additional resources, the continuous-injection method is likely to provide more precise estimates of N₂O diffusivity for any given soil by achieving a stationary SF₆ concentration profile and simplifying analytical procedures. For general use, however, my method provides estimates that should be sufficient and an improvement over static models for parameterizing most quantitative biogeochemical models.

CONCLUSIONS

1. I found no evidence of N₂O consumption in my site either in summer or fall.
2. The point source single-port method with sparse measurements yielded reliable estimates of diffusivity; the inter-port method did not improve precision.
3. Diffusivity estimates were higher in rainfed than irrigated treatments during the summer measurements, likely due to lower soil moisture under rainfed conditions. Likewise, in the fall when there were no modeled soil moisture differences between treatments at 36 and 60 cm, diffusivities were similar.
4. Measurements performed with SF₆ to estimate N₂O diffusivity were more appropriate

than direct measurements with N₂O, which may be subject to the incomplete equilibration of N₂O with soil water.

5. My diffusivity estimates with modeled water content did not have strong agreement with published diffusivity models that are very sensitive to proper determination of the water content, which I could not directly measure at the injection points.

Table 2.1. Relative soil gas diffusivity (D_p/D_o) models following the Buckingham–Currie power-law function. Model references are as compiled in Jassal et al. (2005), Resurreccion et al. (2010), and Blagodatsky and Smith (2012).

Model	Formula [†]
Buckingham (1904)	ε^2
Penman (1940)	0.66ε
Millington (1959)	$\varepsilon^{4/3}$
Marshall (1959)	$\varepsilon^{1.5}$
Millington and Quirk (1960)	$\varepsilon^{4/3}/\Phi^2$
Millington and Quirk (1961)	$\varepsilon^2/\Phi^{2/3}$
Moldrup et al. (2000)	$\varepsilon^{2.5}/\Phi$
Jassal (2005)	$1.18\varepsilon^{2.27}$
Moldrup et al. (2005)	$\Phi^2 (\varepsilon/\Phi)^{X_{100}}$ $X_{100} = 2 + \frac{\ln(\varepsilon_{100})}{4\ln(\varepsilon_{100}/\Phi)}$
Cannavo (2006)	$1.12\varepsilon^{2.13}$

[†] ε is the soil air content, ε_{100} is soil air content at -100 cm of matric potential, Φ is the total porosity

Table 2.2. Kellogg Biological Station Long-Term Ecological Research Site soil textures (Kalamazoo and Ostemo Series). Texture is based on % of fraction less than 2 mm (from Crum and Collins 1995). pH values assume no liming is performed at the site.

Horizon	Depth cm	Texture			Texture	CEC cmol ⁺ kg ⁻¹	Total C g kg ⁻¹	Total N g kg ⁻¹	pH	Bulk Density Mg m ⁻³
		Sand	Silt	Clay						
<i>Kalamazoo series: Fine-loamy, mixed mesic Typic Hapludalfs</i>										
Ap	0-30	43	38	19	Loam	8.4	12.85	1.31	5.5	1.6
E	30-41	39	41	20	Loam	11.5	3.25	0.53	5.7	1.7
Bt ₁	41-69	48	23	29	Sandy clay loam	15.3	2.25	0.42	5.3	1.8
2Bt ₂	69-88	79	4	17	Sandy loam	4.1	0.67	0.42	5.2	nd
2E/Bt	88-152	93	0	7	Sand	2.3	0.2	0.18	5.6	nd
<i>Oshtemo series: Coarse-loamy, mixed, mesic Typic Hapludalfs</i>										
Ap	0-25	59	27	14	Sandy loam	7.1	9.67	1.04	5.7	1.6
E	25-41	64	22	14	Sandy loam	6.8	2.52	0.43	5.7	1.7
Bt ₁	41-57	67	13	20	Sandy clay loam	8.1	1.99	0.4	5.8	1.8
2Bt ₂	57-97	83	4	13	Sandy loam	6.4	1.28	0.53	5.8	nd
2E/Bt	97-152	92	0	8	Sand	2.4	0.25	0.18	6	nd

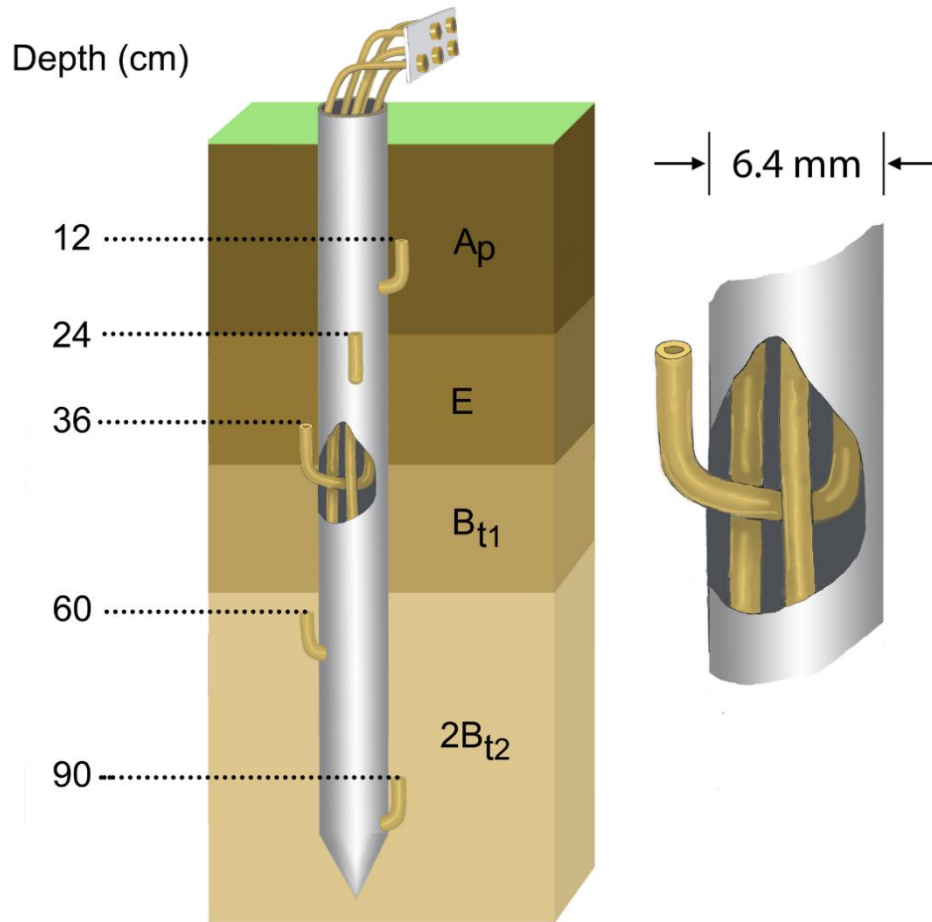


Figure 2.1. Soil profile gas probe with ports at 12, 24, 36, 60, and 90 cm depths. Diameter of the probe is 6.4 mm and is not shown to scale. For interpretation of the references to color in this and all other figures, the reader is referred to the electronic version of this dissertation.

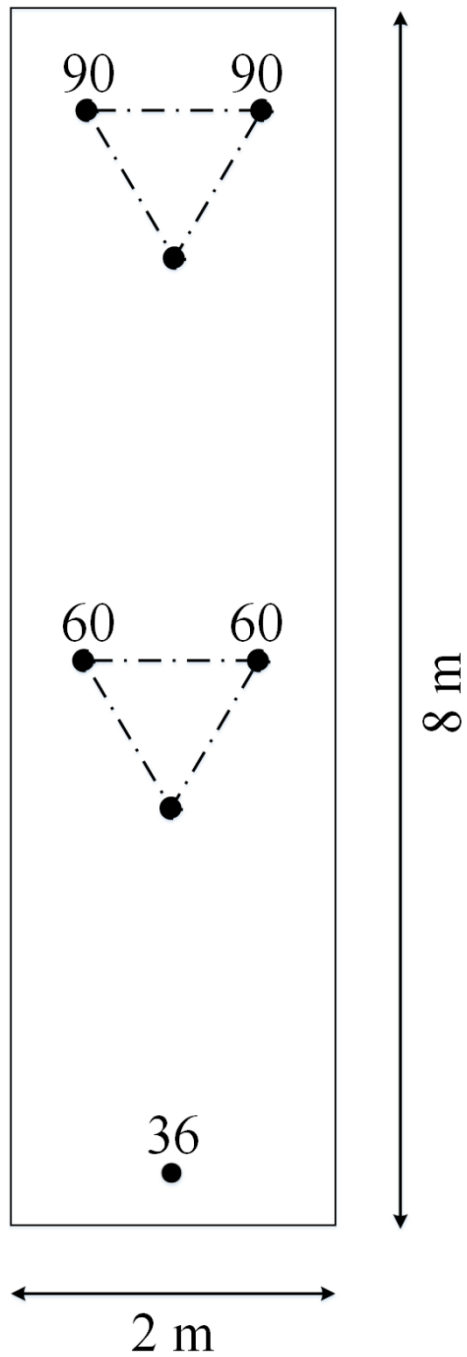


Figure 2.2. Replicate (top view) consists of seven soil profile gas probes arranged in two equilateral triangles with 90 cm sides and an additional injection sampler. Values above probes indicate port used for gas injection (in addition to sampling). Unmarked probes were used for sampling only.

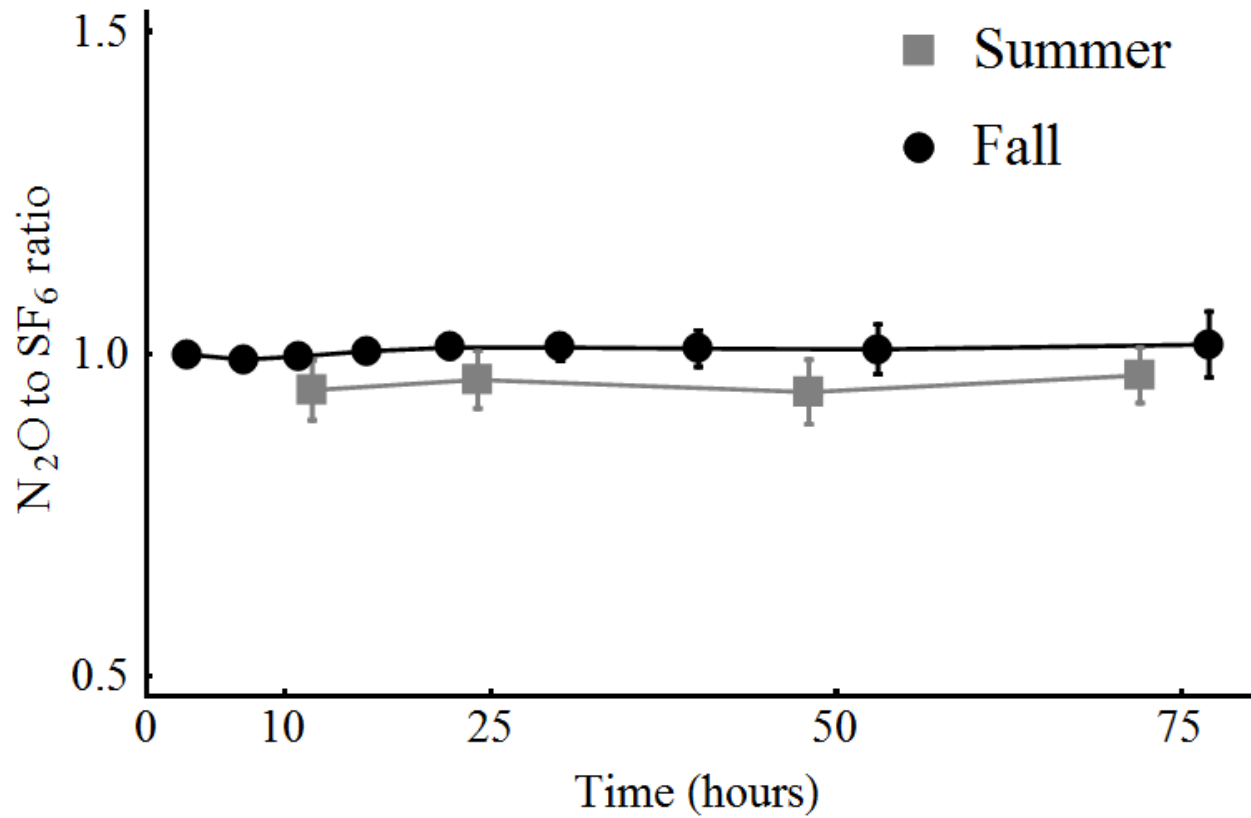


Figure 2.3. Mean N₂O to SF₆ ratio over time in summer and fall microcosm experiments. Only microcosms retaining more than 60% of original SF₆ have been retained. Error bars are lower and upper boundaries of the 95% confidence interval for the median.

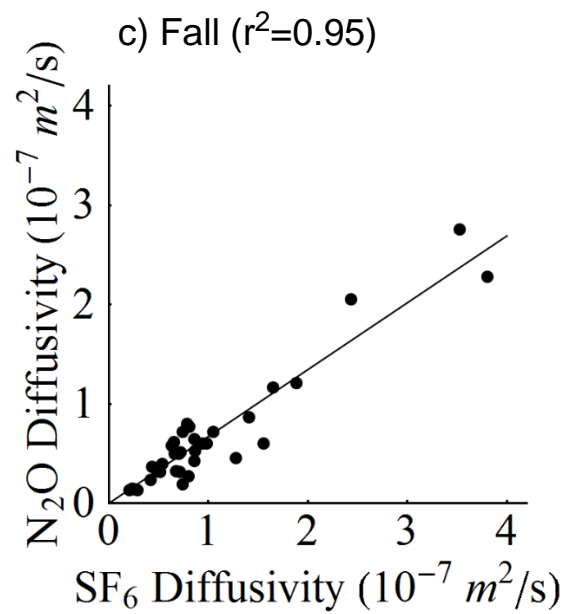
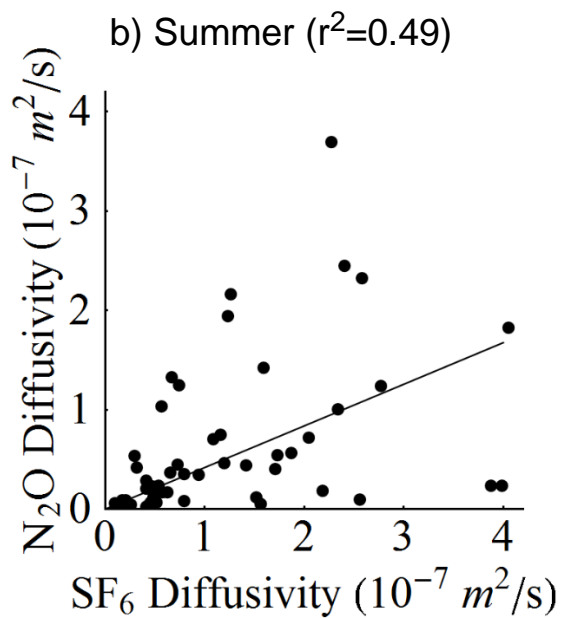
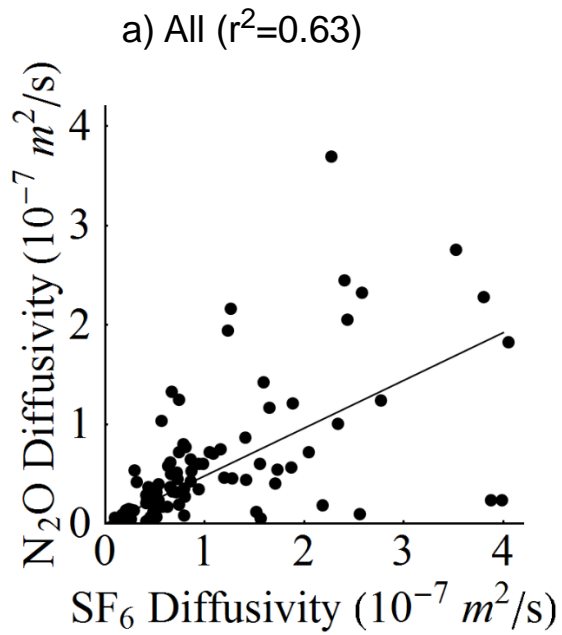


Figure 2.4. Comparison of SF₆ and N₂O diffusivities. Each replicate observation is a separate point. Straight line is the regression line with best slope through the origin.

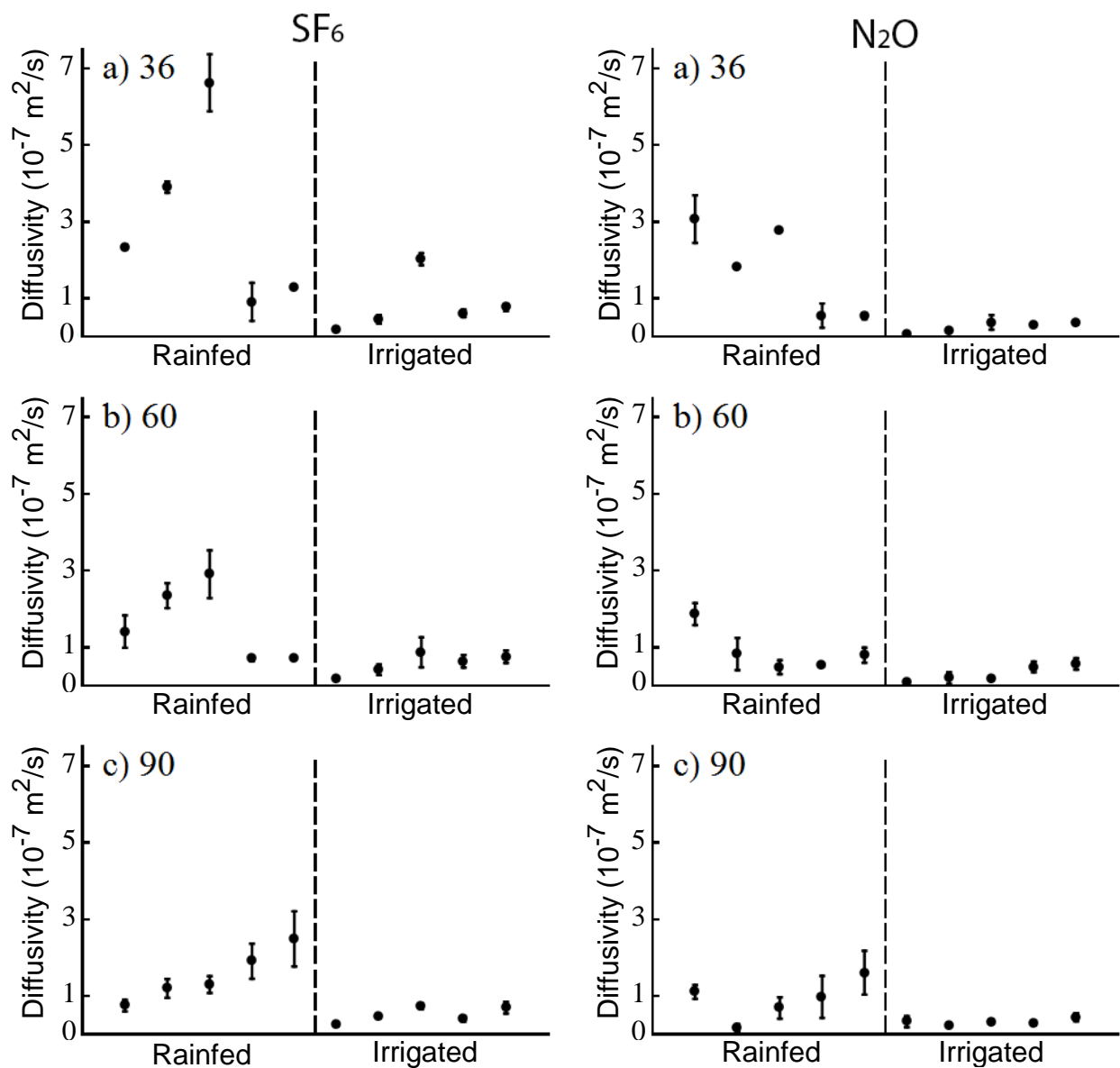


Figure 2.5. SF₆ and N₂O diffusivities modeled for ports used for injections. SF₆ is in the left column and N₂O is in the right column. Treatments are Rainfed and Irrigated. Within each treatment there are values for 5 experimental dates arranged chronologically: June 20, June 27, July 03, October 29, and November 1. Only diffusivities with r^2 above 0.85 for SF₆ and 0.6 for N₂O are included.

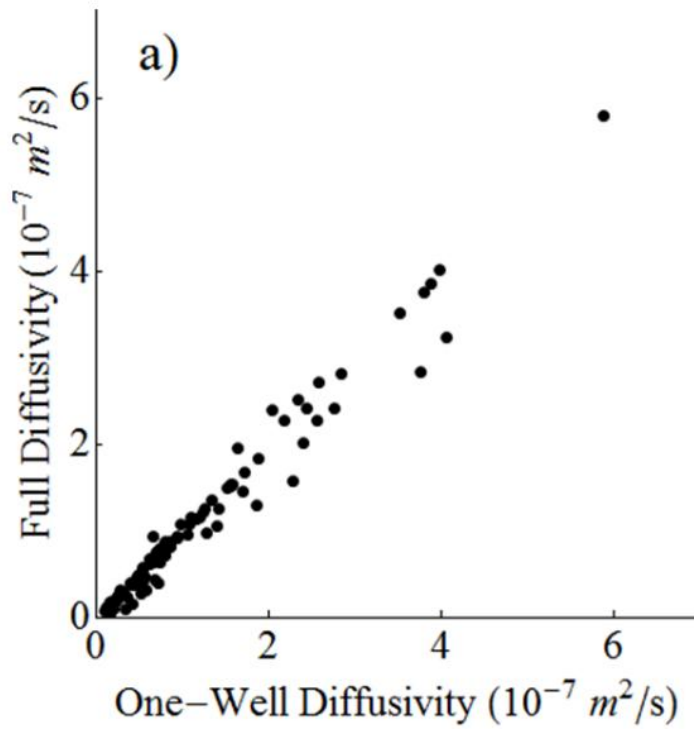
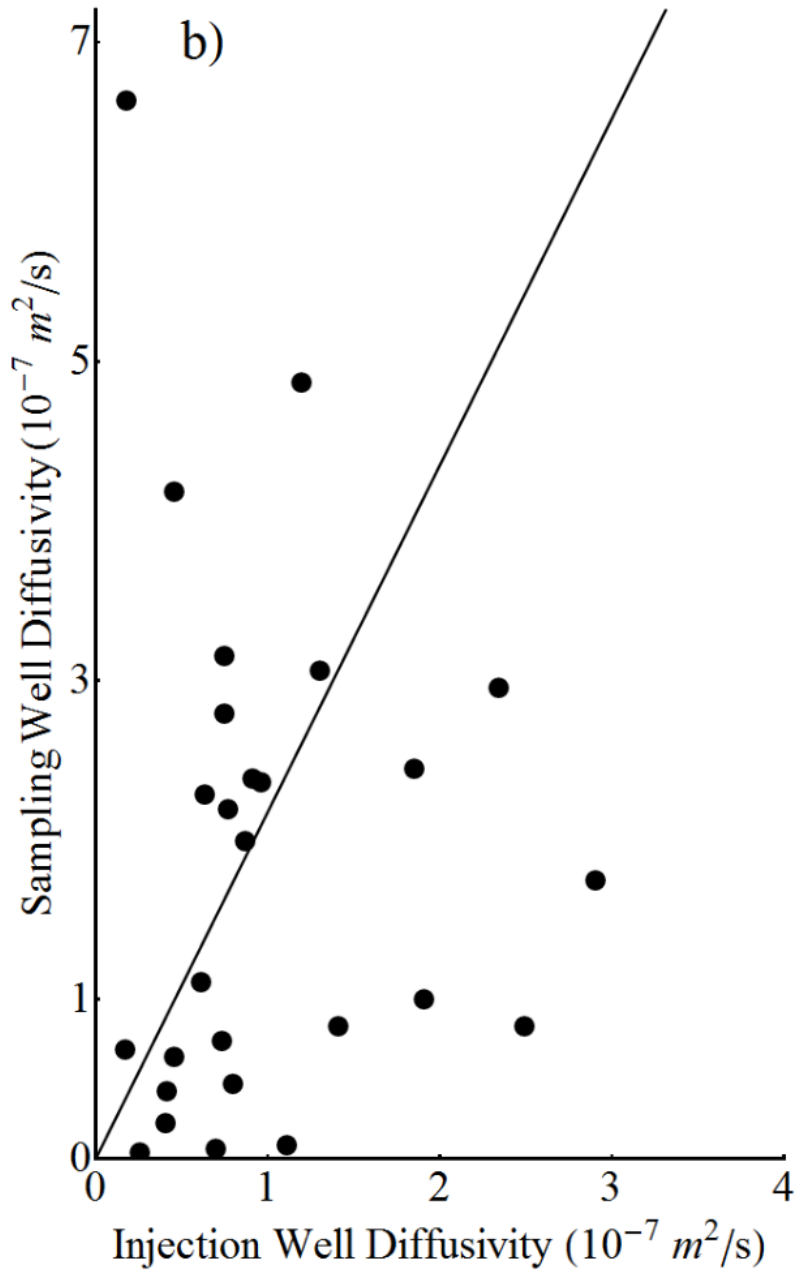


Figure 2.6. Comparison of SF_6 diffusivities obtained from simulations involving only ports used for tracer injections with a) corresponding diffusivities for the ports used to inject tracers when diffusivities at other ports are taken into account ($r^2=0.99$) and b) median diffusivities for ports at the same depth that were not used to inject tracers ($r^2=0.45$).

Figure 2.6. (Cont'd)



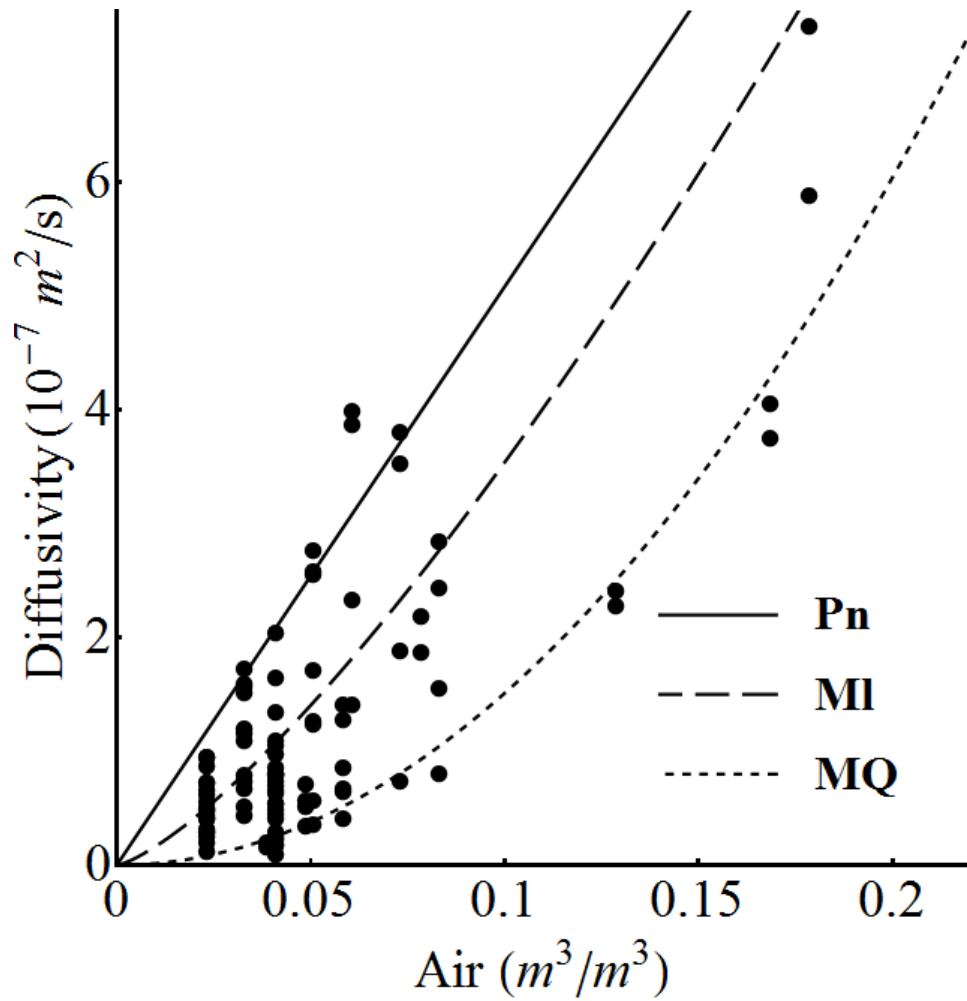


Fig 2.7. Poor fit of common diffusivity models with measured SF₆ diffusivity in this study. Lines are models that best fit: Penman 1940 (Pn), Millington 1959 (MI), and Millington-Quirk 1961 (MQ).

REFERENCES

REFERENCES

- Allaire, S.A. and E. van Bochove. 2006. Collecting large soil monoliths. *Canadian Journal of Soil Science* 86: 885-896.
- Allaire, S.E., J.A. Lafond, A.R. Cabral, and S.F. Lange. 2008. Measurement of gas diffusion through soils: comparison of laboratory methods. *Journal of Environmental Monitoring* 10: 1326-1336.
- Basso, B., J.T. Ritchie, P.R. Grace, and L. Sartori. 2006. Simulation of tillage systems impact on soil biophysical properties using the SALUS model. *Italian Journal of Agronomy* 1: 677-688.
- Blagodatsky, S. and P. Smith. 2012. Soil physics meets soil biology: Towards better mechanistic prediction of greenhouse gas emissions from soil. *Soil Biology & Biochemistry* 47:78-92.
- Bruckler, L., B.C. Ball, and P. Renault. 1989. Laboratory estimation of gas-diffusion coefficient and effective porosity in soils. *Soil Science* 147: 1-10.
- Buckingham, E. 1904. Contributions to our knowledge of the aeration of soils. U.S. Dept. of Agriculture, Bureau of Soils, Washington, D.C.
- Cannavo, P., F. Lafolie, B. Nicolardot, and P. Renault. 2006. Modeling seasonal variations in carbon dioxide and nitrous oxide in the vadose zone. *Vadose Zone Journal* 5: 990-1004.
- Clough, T.J., R.R. Sherlock, and D.E. Rolston. 2005. A review of the movement and fate of N₂O in the subsoil. *Nutrient Cycling in Agroecosystems* 72: 3-11.
- Crum, J.R. and H.P. Collins. 1999. KBS soils. W.K. Kellogg Biological Station Long-Term Ecological Research Project, Michigan State Univ., Hickory Corners, MI. Available at <http://lter.kbs.msu.edu/research/site-description-and-maps/soil-description/>.
- del Grosso, S.J., W.J. Parton, A.R. Mosier, M.K. Walsh, D.S. Ojima, and P.E. Thornton. 2006. DAYCENT national-scale simulations of nitrous oxide emissions from cropped soils in the United States. *Journal of Environmental Quality* 35: 1451-1460.
- Friedman, H.L. 1954. The solubilities of sulfur hexafluoride in water and of the rare gases, sulfur hexafluoride and osmium tetroxide in nitromethane. *Journal of the American Chemical Society* 76: 3294-3297.
- Gevantman, L. H. 2010. Solubility of selected gases in water In *Handbook of Chemistry and Physics, 90th Edition*, D.R. Lide, ed., CRC, p. 8-81.

- Heincke, M. and M. Kaupenjohann. 1999. Effects of soil solution on the dynamics of N₂O emissions: a review. *Nutrient Cycling in Agroecosystems* 55: 133-157.
- Jassal, R., A. Black, M. Novak, K. Morgenstern, Z. Nestic, and D. Gaumont-Guay. 2005. Relationship between soil CO₂ concentrations and forest-floor CO₂ effluxes. *Agricultural and Forest Meteorology* 130: 176-192.
- Jin, Y. and W.A. Jury. 1996. Characterizing the dependence of gas diffusion coefficient on soil properties. *Soil Science Society of America Journal* 60: 66-71.
- Kreamer, D.K., E.P. Weeks, and G.M. Thompson. 1988. A field technique to measure the tortuosity and sorption-affected porosity for gaseous-diffusion of materials in the unsaturated zone with experimental results from near barnwell, south-carolina. *Water Resources Research* 24: 331-341.
- Lai, S.H., J.M. Tiedje, and A.E. Erickson. 1976. In-situ measurement of gas-diffusion coefficient in soils. *Soil Science Society of America Journal* 40: 3-6.
- Lange, S.F., S.E. Allaire, and D.E. Rolston. 2009. Soil-gas diffusivity in large soil monoliths. *European Journal of Soil Science* 60: 1065-1077.
- Li, C.S., S. Frolking, and T.A. Frolking. 1992a. A model of nitrous-oxide evolution from soil driven by rainfall events .1. Model structure and sensitivity. *Journal of Geophysical Research-Atmospheres* 97: 9759-9776.
- Li, C.S., S. Frolking, and T.A. Frolking. 1992b. A model of nitrous-oxide evolution from soil driven by rainfall events .2. Model applications. *Journal of Geophysical Research-Atmospheres* 97: 9777-9783.
- Lide, D.R. 2010. Definitions of scientific terms. In *Handbook of Chemistry and Physics, 90th Edition*, D.R. Lide, ed., CRC, p. 2-49.
- Liu, D.L. and Y. Liu. 2006. Determination of N₂O in air, liquefied air and oxygen. *Chinese Journal of Analytical Chemistry* 34: 554-556.
- Marshall, T.J. 1959. The diffusion of gases through porous media. *Journal of Soil Science* 10: 79-82.
- Microsoft. 2012. Microsoft Visual Studio 2012. Microsoft, Redmond, WA
- Millington, R.J. 1959. Gas diffusion in porous media. *Science* 130: 100-102.
- Millington, R.J. and J.P. Quirk. 1960. Transport in porous media. *Transactions of 7th international Congress of Soil Science* 1: 97-106.
- Millington, R. and J.P. Quirk. 1961. Permeability of porous solids. *Transactions of the Faraday*

- Society* 57: 1200-1207.
- Mochalski, P. and I. Sliwka. 2008. Simultaneous Determination of Ne, Ar, CFC-11, CFC-12 and SF₆ in Groundwater Samples by Gas Chromatography. *Chemia Analityczna* 53: 651-658.
- Mokma, D.L. and J.A. Doolittle. 1993. Mapping some loamy Alfisols in southwestern Michigan using ground-penetrating radar. *Soil Survey Horizons* 34: 71-77.
- Moldrup, P., T. Olesen, P. Schjonning, T. Yamaguchi, and D.E. Rolston. 2000. Predicting the gas diffusion coefficient in undisturbed soil from soil water characteristics. *Soil Science Society of America Journal* 64: 94-100.
- Moldrup, P., T. Olesen, S. Yoshikawa, T. Komatsu, and D.E. Rolston. 2005. Predictive-descriptive models for gas and solute diffusion coefficients in variably saturated porous media coupled to pore-size distribution: I. Gas diffusivity in repacked soil. *Soil Science* 170: 843-853.
- Nicot, J.P. and P.C. Bennett. 1998. Shallow subsurface characterization of gas transport in a playa wetland. *Journal of Environmental Engineering-ASCE* 124: 1038-1046.
- Peaceman, D.W. and H.H. Rachford. 1955. The numerical solution of parabolic and elliptic differential equations. *Journal of the Society for Industrial and Applied Mathematics* 3: 28-41.
- Penman, H.L. 1940. Gas and vapour movements in the soil I. The diffusion of vapours through porous solids. *Journal of Agricultural Science* 30: 437-462.
- Resurreccion, A.C., P. Moldrup, K. Kawamoto, S. Hamamoto, D.E. Rolston, and T. Komatsu. 2010. Hierarchical, Bimodal Model for Gas Diffusivity in Aggregated, Unsaturated Soils. *Soil Science Society of America Journal* 74: 481-491.
- Robertson, G.P. and S.K. Hamilton. 2014. Conceptual and experimental approaches to understanding agricultural ecosystems: KBS long-term ecological research In *The ecology of agricultural ecosystems: research on the path to sustainability*. Pages xx-xx in S. K. Hamilton, J. E. Doll, and G. P. Robertson, eds., Oxford University Press, New York, New York, USA. In press.
- Syswerda, S.P., B. Basso, S.K. Hamilton, J.B. Tausig, and G.P. Robertson. 2012. Long-term nitrate loss along an agricultural intensity gradient in the Upper Midwest USA. *Agriculture Ecosystems & Environment* 149: 10-19.
- Thomas, L.H. 1949. Elliptic Problems in Linear Difference Equations over a Network. Watson Sci. Comput. Lab. Rept., Columbia University, New York
- van Bochove, E., N. Bertrand, and J. Caron. 1998. In situ estimation of the gaseous nitrous oxide diffusion coefficient in a sandy loam soil. *Soil Science Society of America Journal* 62:

1178-1184.

Weeks, E.P., D.E. Earp, and G.M. Thompson. 1982. Use of atmospheric fluorocarbons F-11 and F-12 to determine the diffusion parameters of the unsaturated zone in the southern high-plains of Texas. *Water Resources Research* 18: 1365-1378.

Werner, D., P. Grathwohl, and P. Hohener. 2004. Review of field methods for the determination of the tortuosity and effective gas-phase diffusivity in the vadose zone. *Vadose Zone Journal* 3: 1240-1248.

Werner, D. and P. Hohener. 2003. In situ method to measure effective and sorption-affected gas-phase diffusion coefficients in soils. *Environmental Science & Technology* 37: 2502-2510.

Wolfram Research. 2012. Wolfram Mathematica 9.0. Wolfram Research, Champaign, IL.

CHAPTER 3

The Importance of Subsoil N₂O Production in Response to Tillage, Fertilizer and Irrigation at a Site in Michigan USA

ABSTRACT

Nitrous oxide (N₂O) is a major greenhouse gas and cultivated soils are the dominant anthropogenic source. Potential N₂O production and consumption at depths deeper than the A or Ap horizon have been largely neglected in agricultural soils. I performed a series of experiments at a site in SW Michigan USA to estimate the influence of crop and management practices on subsoil N₂O production in intensively managed cropping systems. N₂O concentrations at depth were enriched up to 900 times atmospheric concentrations in the presence of irrigation and nitrogen (N) fertilization. N₂O concentrations showed a saturating increase with depth except immediately after fertilization and in the winter when concentrations were highest in the surface horizon. Variability of N₂O concentrations declined with depth in agreement with more constant soil moisture and temperature. Comparisons of total N₂O emissions from direct chamber flux measurements with estimates made by the concentration gradient method showed good agreement, with correlations ranging from 0.4-0.7. N₂O production in subsoil horizons is significant, contributing over 50% of total N₂O production in subsoils of moderately fertilized rainfed treatments. Subsoils of highly fertilized sites that exceed plant N requirements produced 25-35% of total N₂O emission. Dry conditions deepened the maximum N₂O production depth. Results show that the fraction of total N₂O produced in subsoil can be substantial and appears to be controlled by the N and moisture status of the soil profile and is unaffected by tillage.

INTRODUCTION

Nitrous oxide (N₂O) is a major greenhouse gas and cultivated soils produce ~84% of all

anthropogenic emissions (Robertson 2013). Emissions of N₂O from cultivated soils have been studied extensively for many years, with most attention directed towards emissions produced in the top few centimeters of surface soil. However, N₂O can also be produced and consumed at depths deeper than the A or Ap horizon.

Subsoil N₂O production has been studied in a variety of environments and depth ranges, but little in agricultural soils (Clough et al. 2006). Measurements of subsoil N₂O production are limited to a small number of experimental methods. Methods usually include either denitrification enzyme activity (DEA) assays (e.g., Castle et al. 1998, Kamewada 2007) to estimate total nitrogen gas production (N₂O + N₂), or measurements of N₂O emissions combined with soil profile isotopic concentrations of N₂O to estimate N₂O production (e.g., Clough et al. 1999, Van Groenigen et al. 2005b).

Sharp increases in N₂O concentrations with depth have been found in a number of sites. Van Groenigen et al. (2005a), Goldberg et al. (2009) and Wang et al. (2013) observed N₂O concentrations 20-30 times free-atmosphere concentrations at their deepest subsoil sampling points, suggesting an N₂O production rate in subsoil sufficient to maintain a very steep N₂O concentration gradient through the soil profile.

N₂O is produced by denitrification and nitrification in soil (Robertson and Groffman 2014). Denitrification potentials assayed by DEA usually decline substantially with soil depth. For example, Kamewada (2007) observed an abrupt drop in DEA in samples from an Andisol soil at depths between 0.5 and 1m, below which DEA was constant to 5 m. He concluded that subsoil denitrification was negligible. Other authors have also observed a substantial decrease in volumetric (per m³) or gravimetric (per kg) denitrification rates with depth in different environments (Hashimoto and Niimi 2001, Murray et al. 2004, Goldberg et al. 2008). However, even a 20-fold decrease could be significant – and even exceed surface soil rates – when

expressed on an areal (per m²) basis for the entire depth of the subsoil, which could be meters deep.

N₂O can also be produced by nitrification. Especially in forest surface soils nitrification can be a significant source of N₂O, and by extension subsoil N₂O might also be produced from nitrification. However, in most soils, including agricultural, only trace amounts of ammonium leach from surface horizons because of cation exchange processes that slow the movement of NH₄⁺ to deeper horizons and rapid uptake of ammonium in surface horizons by nitrifiers and plants. Nitrification is thus unlikely to be a significant source of subsoil N₂O (e.g., Page et al. 2002, Khalili and Nourbakhsh 2012).

Subsoil N₂O production could be especially important during dry periods, because surface horizons are too dry to produce N₂O (Goldberg and Gebauer 2009). And van Groenigen et al. (2005a) attributed high wintertime N₂O fluxes to subsoil denitrification when surface soils were frozen to a depth of several centimeters. The importance of subsoil N₂O production has been noted other studies in a variety of systems (Kammann et al. 2001, Addy et al. 2002, Well and Myrold 2002, Clough et al. 2006).

There are two fates for N₂O produced at depth: it can be consumed in place or it can diffuse to other locations in the profile, where it can also be consumed before diffusing elsewhere. Eventually N₂O not consumed will be lost to groundwater or emitted to the atmosphere. N₂O emitted at deeper depths has a higher chance of being consumed and transformed to N₂ due to a longer residence time in soil arising from a longer diffusion path (Castle et al. 1998). In any given soil layer diffusion is controlled by the N₂O gradient, soil porosity, water filled pore space (WFPS), and temperature (Shcherbak and Robertson 2014).

Goldberg (2008) concluded that N₂O was likely consumed during upward diffusion based on increasing δ¹⁵N values and decreasing N₂O concentrations, although precise estimates

of consumption were obscured by high diffusion rates. Clough et al. (1999) and Van Groenigen et al. (2005b) also combined *in situ* measurements of N₂O emissions to the atmosphere and soil profile concentrations with isotopic signatures of N₂O and found consumption during upward N₂O movement. WFPS rather than N or temperature primarily controlled N₂O production. In a repacked soil column, Clough et al. (2006) used ¹⁵N-N₂O to show that consumption could deplete 1/3 of the N₂O produced, although estimates of N₂O production and consumption in sieved subsoil columns may not reliably approximate subsoil processes in the field because sieving changes the structure of the soil and allows oxygen to diffuse to denitrification microsites faster, which can significantly impede its ability to denitrify (Robertson 2000) or change the molar ratio of N₂:N₂O produced by denitrification (Cavigelli and Robertson 2001).

The factors that control denitrification in subsoils are the same as those in surface soils. Robertson and Groffman (2014) identify three proximal factors that control denitrification at the cellular level: carbon (C), oxygen, and nitrate (NO₃⁻) concentrations (Chapter 1, Figure 3.1). A number of more distal factors, such as WFPS, vegetation, grazing, N fertilization, irrigation, other management operations, climate and soil type, influence oxygen, C, and NO₃⁻ to produce a very diverse range of denitrification rates in arable soils, from 0 to 250 kg N ha⁻¹ year⁻¹ (Barton et al. 1999, Robertson and Groffman 2014).

Subsoil denitrification in cropped soils is likely colimited by NO₃⁻, C, and WFPS (the latter determines O₂ availability). Soil nitrate concentrations in unfertilized systems in the range 1-10 mg NO₃⁻N kg dry soil⁻¹ have been reported to limit denitrification rate (Barton et al. 1999). Nitrate leached from surface soils (e.g. Syswerda et al. 2012) can raise subsoil NO₃⁻ concentrations to above 50 mg NO₃⁻N kg dry soil⁻¹ as evidenced by studies of groundwater next to heavily fertilized sites (Thorburn et al. 2003, Nisi et al. 2013).

Soil C most commonly limits denitrification in N-fertilized surface soils (Myrold and

Tiedje 1985, Myrold 1988, Weier et al. 1993) where nitrate availability is high. In subsoils C can also limit denitrification as shown by dissolved organic carbon (DOC) addition experiments (Weier et al. 1993, McCarty and Bremner 1992, Murray et al. 2004). Although low soil C and NO_3^- concentrations deeper in the soil may restrict denitrification, significant values occur at depths greater than 1m in forest soils with no amendments (Barkle et al. 2007, Funk et al. 1996). Castle et al. (1998) observed denitrification rates as high as $0.1\text{-}0.7 \text{ mg N}_2\text{O-N kg dry soil}^{-1} \text{ h}^{-1}$ in intact subsoil cores with no C or N additions. Manure application to topsoil can lessen the C limitation for subsoil denitrification, as shown by Bhogal and Shepherd (1997). Subsoil slurries (from long-term arable treatments in Iowa and SE England) amended with C or both C and N increased denitrification to $1\text{-}5.1 \text{ mg N}_2\text{O-N kg dry soil}^{-1} \text{ h}^{-1}$ at depth up to 2 m (Yeomans et al. 1992, Jarvis and Hatch 1994) on par with C and N amended surface soil denitrification rates (Hoffman et al. 2000, Bradley et al. 2011).

Oxygen depletion in soil is strongly controlled by WFPS, which controls soil aeration status by restricting oxygen movement in the soil. The WFPS threshold for denitrification depends on soil texture and is lower for finer textured soils. Barton et al. (1999) reported this threshold to be 74% to 83% in sandy and sandy loam soils, from 62% to 83% in loam soils, and from 50% to 74% WFPS in clay loam soils. Loam soils consequently tend to have higher annual rates of denitrification (as high as $110 \text{ kg N ha}^{-1} \text{ year}^{-1}$) than either sandy or clayey soils ($<10 \text{ kg ha}^{-1} \text{ year}^{-1}$).

In this study I examine subsoil N_2O production in intensively managed cropping systems at a site in the US Midwest on the same soil series 1) to identify patterns of N_2O concentrations with soil depth; 2) to test the ability to use profile N_2O concentrations and diffusivity measurements to predict soil N_2O fluxes to the atmosphere; and 3) to measure N_2O production and movement in the soil profile in order to estimate the relative contribution of different soil

depths to seasonal N₂O fluxes to the atmosphere as affected by tillage, irrigation, and N fertilizer input.

METHODS

Site description

I performed experiments at the Kellogg Biological Station (KBS) Long-Term Ecological Research (LTER) site, located in southwest Michigan in the northeast portion of the U.S. Corn Belt (42° 24' N, 85° 24' W, average elevation 288 m). Annual rainfall at KBS averages 1,027 mm y⁻¹ with an average snowfall of ~1.4 m. Mean annual temperature is 9.9 °C ranging from a monthly mean of -4.2 °C in January to 22.8 °C in July (Robertson and Hamilton 2014). Soils are co-mingled Kalamazoo (fine-loamy, mixed, semi-active, mesic Typic Hapludalfs) and Oshtemo (coarse-loamy, mixed, active, mesic Typic Hapludalfs) loams (Mokma and Doolittle 1993).

Experimental Approach

I used two experimental systems to address my objectives: in situ monolith lysimeters to test the effect of tillage on subsoil N₂O production and soil profile gas probes to test the effects of irrigation, N fertilizer input, and vegetation. Monolith lysimeters provided better resolution and more measured variables than soil profile gas probes. Probes, on the other hand, are easily installed in different locations without disturbing normal field operations and thus can be deployed extensively. I sampled monolith lysimeters from May 2010 to November 2011. I sampled soil profile gas probes in different treatments of the LTER Resource Gradient Experiment and the LTER Main Cropping System Experiment (MCSE) from May to November 2011.

Monolith Lysimeters Experiment

Field plots for monolith lysimeters were established in 1986 to study tillage and N supply effects on plant-soil interactions. Sixteen 27×40 m plots were randomly assigned within blocks to N fertilized vs. non-fertilized and till vs. no-till treatments in a randomized complete block design with 4 replicate blocks per treatment (Figure 3.1). I used four of these plots, in which monolith lysimeters were installed in 1990. A lysimeter was installed in each of two unfertilized no-till plots (NT6 and NT9 in Figure 3.1) and two unfertilized tilled plots (CT2 and CT13). The lysimeters (Figure 3.2) were installed in spring 1986 by excavating around 8 m^3 ($2.29 \times 1.22 \times 2.03$ m) pedons located at least 5 m from the edges of the respective plots. A stainless steel chamber was simultaneously lowered over the undisturbed portion of the pedon following the procedure of Brown et al. (1974). The intact pedon was temporarily capped, removed by crane as an assemblage, and inverted in order to weld onto the bottom of the pedon a 0.43 m extension that was then filled with C-horizon sand followed by a layer of pea gravel separated from the sand by a Teflon screen. The base of the extension was sloped to the center drain. The lysimeter assembly was then returned to its original upright position and surrounding soil was replaced by profile layer. Soil profile mappings of the excavation provide a detailed description of soil horizon depths (Table 3.1).

From 1985-2002 all plots were in a corn-soybean rotation and from 2004-2009 in a wheat-corn-soybean rotation. For this study in 2010 and 2011 all plots including over the lysimeters were planted to corn and N fertilizer was applied at the recommended rate of 145 kg N ha^{-1} (Warncke et al. 2004). Corn was planted in 3 rows across the top of each lysimeter at a standard row spacing of 70 cm with 15 cm between plants in the same row. Tillage within the two lysimeters assigned to till treatments was performed by hand-spading to mimic chisel plowing used elsewhere in the plots.

For each lysimeter, an outlet at depth provided drainage, and an access tunnel provided underground access to one side. Instruments to measure solute, gas, moisture, and temperature (Figure 3.3) within the entire volume of soil were installed 2 cm above and below the borders of major horizons directly below the center row of corn (Figure 3.2). I also measured N₂O flux from the surface of the soil profile.

Soil temperature in the profile was measured with type T (copper-nickel alloy junction) thermocouples (Scervini 2009) every 15 minutes at six soil depths (7, 20, 50, 75, 100, and 125 cm) with a 1°C limit of error. Soil moisture was measured with Time Domain Reflectometry (TDR, Cerny 2009) every 15 minutes at 5 depths (20, 25, 50, 55, and 75 cm) with paired 0.5 × 30 cm stainless steel rods as TDR wave guides. Each of the lysimeters was connected to a multiplexer that connected 5 pairs of rods. Two TDR units (Campbell Scientific TDR100) received measurements from four monolith lysimeters, with the closest lysimeters paired (CT2 paired with NT6, and NT9 with CT13, Figure 3.1) to keep distances within the 70 m limit of the instrument and avoid signal degradation. Data for temperature and moisture were stored in a Campbell Scientific datalogger CR10X.

Soil atmosphere was sampled using a system of stainless steel tubing. Tubes were installed at 10 different depths in the profile: 3, 7, 15, 20, 25, 50, 55, 75, 80, and 180 cm. All tubes were ~1.6 mm o.d., 0.5 mm i.d. Tubes for sampling at 3, 7, and 15 cm depths were installed vertically from the top of the profile. The rest of the tubes were installed horizontally with ends 30 cm from the lysimeter wall to avoid edge effects. Tubes were capped with septa inside the access tunnel, creating a system with a dead volume of ≤ 2 mL.

Nitrous oxide fluxes were measured at the top of the profile using the static chamber method. A closed-cover flux chamber was placed on the soil surface to trap soil gases emitted to the atmosphere. Chambers stayed open except for the period of measurement (~2 hours). During

this period samples from chamber headspace were taken every 30 min by inserting a syringe into the rubber septa and drawing 10 mL, which was placed in a 3.9 mL glass vial (Exetainer LABCO); overpressure avoided contamination during transport and storage (Kahmark and Millar 2008).

Gas measurements of soil atmosphere concentrations and surface fluxes were taken at the same locations twice per week with some additional measurements after major rain events and management operations. In both cases, a 10 mL syringe and non-coring needle were used for sampling. For each sample, an initial 10 mL volume was taken to flush the system's dead space and a second 10 mL volume was used to flush the 3.9 mL vial. A third 10 mL volume was added to the vial to create an overpressure to guard against leakage.

Gas samples were analyzed for N₂O, CO₂, and CH₄ using a gas chromatograph (Agilent 7890A) equipped with an auto-sampler (Gerstel MPS 2 XL). N₂O was separated with one of two Restek PP-Q 80/100 packed columns (length 3 m, ID 2 mm, OD 3.175 mm) and detected using a ⁶³Ni electron capture detector at 350°C. Carrier gas was 90% Ar and 10% CH₄ (Ultra High Purity Grade 5.0 with a Restek 21997 moisture trap and Restek 20601 oxygen scrubber) at a 10±0.5 mL/min flow rate. Oven temperature was 78°C during the first 5.5 min of the run, and then the column was back flushed and baked for 0.5 min (terminal temperature 105°C, increase rate 55°C/min) prior to the next sample.

Soil profile gas probes

I used soil profile gas probes that are fully described in Shcherbak and Robertson (2014). Each probe consisted of a 90 cm long 0.64 cm o.d. master tube that contained five stainless steel sampling tubes that protruded at different points along the master tube 3 cm from its outer wall. I installed the probes at a 60° angle to minimize the potential for vertical pores serving as channels

for preferential airflow. The sampling depths were 10, 20, 30, 50, and 75 cm (Figure 3.4). Gas sampling using soil profile gas probes was performed according to the same protocol as for gas probes in the monolith lysimeters.

The soil profile gas probes were placed in the LTER Resource Gradient Experiment and the LTER MCSE (Robertson and Hamilton 2014). The Resource Gradient Experiment is a randomized complete block design experiment with irrigation \times fertilizer treatments in 4 replicates. Rainfed and irrigated portions in each replicate include 9 fertilizer input levels planted to corn in 2011. Irrigation was sufficient to meet crop needs. For this study I selected a subset of plots with 6 fertilizer input levels (0, 67, 101, 134, 168, and 202 kg N ha⁻¹) in unreplicated rainfed and irrigated blocks equipped with automatic chambers that monitor gas fluxes from the soil surface. The 12 soil profile gas probes were each sampled 36 times during the season, with more intensive sampling after fertilization and with sampling frequency decreasing as the season progressed. Automatic chambers measured soil surface N₂O, CO₂, and CH₄ fluxes every 6 hours via a gas chromatograph installed in the field (Millar et al. 2013). Both rainfed and irrigated plots had replicated continuous measurements of surface temperature and moisture.

In the MCSE soil profile gas probes were installed in four replicates each of two perennial cropping systems and in two reference communities. The two perennial cropping systems were Alfalfa (*Medicago sativa* L., herbaceous) and hybrid Poplar (*Populus* sp., woody). The two reference communities were a minimally managed Early Successional community and a Mown Grassland (never tilled) community. Robertson and Hamilton (2014) provide more cropping system details. Each of the replicates had a soil profile gas probe installed as described above and sampled weekly at mid-growing season and then bi-weekly later in the season. I measured N₂O surface fluxes bi-weekly by the static chamber method together with surface horizon temperature and moisture.

N₂O surface flux and N₂O production by depth

I calculated average temporal autocorrelations and their standard errors for surface N₂O fluxes and N₂O concentrations at all depths to estimate temporal continuity. Autocorrelation close to one indicates high temporal continuity such that most measurements are very similar to the preceding measurement and the following measurement. Autocorrelation close to or below 0 indicates no continuity between measurements over time. I obtained average correlations and standard errors among N₂O fluxes and N₂O concentrations. Different levels of N input in the Resource Gradient Experiment were used as replicates for the calculations. I searched for an extinction parameter t minimizing sum of squared residuals for the e^{-td} correlation model, where d is the distance between the depths of measurements.

Daily N₂O flux in a given soil layer was calculated as N₂O diffusivity in that layer multiplied by the N₂O concentration gradient (Fick's First law), i.e. concentration increase per cm of increasing depth. I assumed for this calculation that daily concentration profiles are static. Total N₂O production (or consumption, if negative) plus a concentration change for a given layer is equal to N₂O flux into the layer less N₂O flux out of the layer. Previous laboratory experiments on soils from the MCSE and Resource Gradient Experiment sites show that consumption of N₂O during its diffusion towards the soil surface is likely nil (Figure 3 in Shcherbak and Robertson 2014). Diffusivity of N₂O was calculated based on modeled soil water content and the best fit diffusivity model (Millington 1959) most appropriate for the experimental site (Chapter 2, Shcherbak and Robertson 2014). Water content in each stratum estimated using the System Approach to Land Use Sustainability (SALUS) model (Basso et al. 2006) and calibrated with water content measured at 0-25 cm. SALUS model required soil conditions (soil texture, bulk density, carbon and nitrogen content, initial moisture), daily weather (rain, temperature, solar radiation), and agronomic management data in order to simulate

daily water balance. To bring the concentration profiles to a monotonic or unimodal shape where required I used a smoothing function of depth

$$N_2O(d) = N_2O_{atm} + C_1d + C_2(1 - e^{-C_3d}).$$

When concentration profiles were already uni-modal, I used linear interpolations of measured N₂O concentrations to create a concentration profile (N₂O concentration at 0 cm depth was assumed equal to the atmospheric N₂O concentration of 0.325 ppm_v). Seasonal N₂O production for each layer and N₂O surface flux was calculated by linear interpolation of respective daily values across the season.

RESULTS

I observed steep and consistent increases in N₂O concentrations with depth for 80-90% of the sampling period on all three sites (Figure 3.5): the Monolith Lysimeters Experiment, the Resource Gradient Experiment, and the MCSE. Mean seasonal N₂O concentrations increased with depth for every treatment in the three experiments.

Temporal autocorrelation of N₂O concentrations also increased with depth for all experimental treatments, starting as low as 0.1-0.2 for the top depth measured and reaching values as high as 0.8 for N₂O concentrations at the deepest horizons measured (Figure 3.6). Paired correlations among N₂O surface fluxes and N₂O concentrations are positive and significant. The correlations are highest for values measured at similar depths and significantly decline for values further apart (Figure 3.7).

Total annual N₂O emissions interpolated from chamber measurements and calculated from soil N₂O concentration profiles had high positive correlations for the three experiments (Figure 3.8). N₂O production declined with depth in all treatments (Figure 3.9). Surface soil layers (0-20 cm) produced >50% of total annual N₂O emissions for most treatments with some

exceptions in the Resource Gradient Experiment treatments. The exceptions were rainfed treatments with 0-135 kg N ha⁻¹ input and the irrigated treatment with 135 kg N ha⁻¹ input, where surface soil layer produced 25-40% of the annual N₂O emissions.

Monolith Lysimeters Experiment

N₂O concentrations in the monolith lysimeters usually increased with depth, but in the winter and early spring N₂O concentrations were highest in surface layers and decreased with depth (data not shown here; in Dataset S1). Mean annual N₂O concentrations were significantly higher in the No-till treatment than in the tilled treatment at every depth, reaching values of 7 and 3 ppm_v, respectively at 140 cm sampling depth (Figure 3.5 a).

Total N₂O emissions calculated from N₂O concentration gradients correlated well ($r^2 = 0.73$) with emissions directly measured by static chambers (Figure 3.8 a). Total N₂O emissions for tilled treatment were not statistically different from these for no-tillage when either measured directly ($p=0.16$) or calculated from concentrations and diffusivity estimates ($p=0.08$). The proportion of total N₂O emission produced in surface horizons was 40-60% across 2010-2011 and does not differ by tillage ($p=0.7$, Figure 3.9 a).

LTER Resource Gradient Experiment

Highest seasonal concentrations at each depth in fertilized treatments of the Resource Gradient Experiment occurred within 30-days following N fertilization. N₂O concentrations usually increased with depth, with the exception of the 246 kg N ha⁻¹ rainfed treatment on day 173 and 101 kg N ha⁻¹ irrigated treatment on days 173-186, where N₂O concentrations declined with depth. Rainfed treatments had higher mean seasonal N₂O concentrations than irrigated treatments for the entire profile and for all N input levels except for the 101 kg N ha⁻¹ treatment,

where N₂O concentrations reached 300 ppm_v on one day, and for one week N₂O concentrations were above 40 ppm.

Mean temporal autocorrelation for N₂O concentrations in the irrigated treatment is significantly above the mean for the rainfed treatment (p=0.002, Figure 3.7). Results show a significantly sharper decline for rainfed treatment correlations than for irrigated (p<0.01).

Measured total annual N₂O emissions increased with N fertilizer input for both rainfed and irrigated treatments (Figure 3.8 b) as did total annual N₂O emissions modeled from concentration gradient and diffusivity estimates. Correlations between measured and modeled emissions averaged 0.41; they were higher for rainfed (0.65) than for irrigated treatments (0.34). The fraction of total N₂O produced lower in the profile for rainfed treatments was large and declined with N fertilizer input. Modeled N₂O production indicated that irrigated treatments produced 80-95% of total modeled emissions in the top 20 cm of soil, with the exception of the 135 kg N ha⁻¹ fertilizer input level, where N₂O emissions from surface horizons were ~40% of total modeled emissions.

LTERR Main Cropping System Experiment

The Alfalfa system had much higher mean annual N₂O concentrations than the Poplar, Early-successional, and Mown grassland systems, which all had very low mean seasonal N₂O concentrations of below 0.7 ppm_v. Correlations between N₂O concentrations at two different depths declined with increased distance between the two depths. This decline in correlation with depth was significantly (p < 0.01) sharper for Poplar and Alfalfa systems than for the Successional systems.

Modeled total N₂O emissions were higher in Alfalfa than in the Poplar and Successional systems (Figure 3.8 c). Measured total N₂O emissions for Alfalfa and Poplar systems were

higher than successional communities. The correlations between measured and modeled annual N₂O emissions in the Alfalfa, Poplar and Successional systems is $r^2 = 0.55$. In the Alfalfa and Successional systems almost 90% of the total N₂O emission was produced in the top 20 cm horizon. In the Poplar system only 80% was produced in the surface horizon.

DISCUSSION

Patterns of N₂O concentrations with soil depth

I observed two distinct types of N₂O concentration profiles created by the relative rates of N₂O production and diffusion processes. The most common profile shape is a concentration increasing with depth showing saturation in deeper horizons. This pattern has also been observed by others (e.g. Clough et al. 2006, Goldberg et al. 2009) and occurs when diffusion is fast enough to carry produced N₂O to the atmosphere.

The other N₂O profile shape has the highest concentration near the surface and decreases or stays nearly constant with depth due to relatively slow diffusion. This happens in soils under two contrasting sets of conditions: in late spring or summer after N fertilization followed by sufficient rain (Figure A4), and in winter with surface emissions entrapped by water or ice (Figure A5). Conditions in the former case lead to intensive N₂O production concentrated at the top of the profile, with the possibility of N₂O concentration increase up to 100-1000 times the atmospheric concentration. Such N₂O concentration responses to N fertilization have been reported by Wang et al. (2013), who found maximum concentrations at shallowest sampling point (30 cm). N₂O production in winter is severely restricted in the surface horizon if it is saturated or blocked by ice. Highest N₂O production at the top of unfrozen part of the soil with extremely limited diffusion to the surface leads to highest concentration.

Daily and annual N₂O concentration profiles that increase with depth and show saturation

in deeper horizons have been reported before (Wang et al. 2013). Observed differences in mean annual N₂O concentrations between treatments are driven by daily N₂O concentration differences in the period of most intensive N₂O production after fertilizer input; at other times concentrations are relatively low and uniform. This shows the important role of management on belowground N₂O dynamics that lead to changes in N₂O fluxes to the atmosphere. The amount of mineral N in the profile influences the average annual N₂O concentrations in the profile: Alfalfa with intermediate N₂O concentrations likely has intermediate levels of mineral N in the profile, between those of the N-poor successional communities and those of N-fertilized corn.

Variability in N₂O concentrations reflects the spatial and temporal variability of soil conditions (temperature, moisture, and NO₃⁻ and soluble organic C concentrations) that declined with depth in SALUS model simulations (Figure A.6 and A.7). Autocorrelation results show that N₂O concentration variability declines with depth (Figure 3.6). Relative constancy of conditions below 70 cm explains autocorrelations close to one. Lower temporal and spatial variability in irrigated compared to rainfed treatments in the Resource Gradient Experiment follows from a more constant modeled moisture content under irrigation, as confirmed by temporal autocorrelation of N₂O concentrations and the correlation between N₂O fluxes and concentrations (Figure 3.6 a and 3.7, respectively).

Predicting soil N₂O fluxes to the atmosphere from profile N₂O concentrations and diffusivity

Total annual N₂O emissions measured directly and calculated from the N₂O concentration gradients and diffusion rates agree well for most treatments examined. Previous studies comparing direct N₂O emission measurements with calculations by the gas gradient method have had mixed success at best (Rolston et al. 1976, Yoh et al. 1997, and Maljanen et al.

2003). Jury et al. (1982) showed that surface N₂O flux measurements may not be quantitatively related to the rate of N₂O production in the profile due to the time lag caused by slow diffusivity and potential for N₂O consumption in some soils.

Total calculated N₂O emissions were higher than measured emissions in the Monolith Lysimeter treatments (Figure 3.8 a) probably due to overestimation of diffusivity of N₂O in the surface horizon of the profile. Both methods showed similar total N₂O emissions in tilled and no-till treatments possibly due to balancing somewhat wetter surface soil horizon under no-till by dryer subsoil horizons (Robertson et al. 2014), leading to greater N₂O production. Measured total annual N₂O emissions agreed with calculations by concentration gradient method, and increased with N inputs in the Resource Gradient Experiment in both rainfed and irrigated treatments. The MCSE alfalfa treatment has larger measured annual N₂O emissions than successional communities (p=0.001), but modeled N₂O fluxes did not show significant differences among the treatments (Figure 3.8 c).

The contribution of different soil depths to seasonal N₂O fluxes

My results show that subsoil N₂O production is important in a variety of management systems across the KBS landscape. Two major profile factors most influence total N₂O production and fractions of N₂O produced by depth: NO₃⁻ concentration and moisture content. Tillage does not appear to have an influence on the fraction of subsoil N₂O produced (Figure 3.9).

Soil profile NO₃⁻ concentration is one of the major drivers of total N₂O production and fractions produced in each soil horizon. High N inputs (168-246 kg N ha⁻¹) exceeding plant N requirements produce high N₂O fluxes from surface horizons in Resource Gradient Experiment due to very high inorganic N content during wet periods even if they are relatively short. In low

to moderate N fertilizer input ($0-135 \text{ kg N ha}^{-1}$) rainfed treatments in the Resource Gradient and Monolith Lysimeter Experiments (Figure 3.9 a and 3.9 b) the fraction of total N_2O produced in the subsoil is as high as 40-60%. In contrast with the low fertilization treatments of Resource Gradient Experiment, less intensive and minimal management systems at MCSE have only 10-20% of total annual N_2O production attributed to soil below the plow layer (Figure 3.9 c).

Water status of the soil profile and especially the surface horizon is another crucial factor in determining total N_2O production in the profile and the fractions produced in each horizon. In the irrigated treatments in the Resource Gradient Experiment (Figure 3.9 b) ~75% of N_2O production was concentrated in the surface horizon (except for the 135 kg N ha^{-1} treatment), which is a much larger fraction than in rainfed treatments with low to moderate N input. Dry surface horizons in rainfed treatments shifts N_2O production lower into horizons that are relatively wet. Clough et al. (2006) observed a similar N_2O production shift in unfertilized forest during summer drought. Tillage in the Monolith Lysimeter Experiments did not change the fraction of N_2O produced in subsoil (Figure 3.9 a).

My results show correspondence between total annual N_2O fluxes measured directly and modeled from concentration profiles, but there is room for improvement. Much of the difference between the two ways to estimate total N_2O flux may be sampling artefact. For example, one source of error is the difference in sampling time between measured and modeled fluxes that in my study was up to 3 hours during some sampling events. Another source of error in the large spatial variability of N_2O emissions; that emissions measured just a couple of meters away may differ considerably. In my study, the samples taken by the two methods were at a distance of up to 5 m. Finally, error may also result from errors in estimating moisture content and subsequent choice of gas diffusivity model. There are possible improvements to all those areas of potential error. An automatic system for sampling N_2O concentrations positioned close to and

synchronized with system for measurement of surface fluxes will reduce temporal and spatial discrepancy between the measurements. The automatic sampling system needs to have dead space and sampling volumes comparable with the manual system to minimize potential effects on gas in the soil (e.g. displacing it with atmospheric air). Additionally, direct measurements of moisture will bring improvements by eliminating error in modeling moisture.

My research suggests that we must consider not only surface but also subsoil conditions when trying to minimize greenhouse gas emissions from agricultural soil management. Models need to consider subsoil layers below the plow layer to improve simulation of daily and seasonal N₂O production, storage, movement, and emission to the atmosphere.

CONCLUSIONS

1. N₂O concentrations increased with depth in my agricultural soils except after fertilization when surface soil N₂O production was intense and in the winter when the profile was saturated or blocked by ice and snow.
2. Total annual N₂O fluxes measured directly and calculated by the concentration gradient method are in moderate agreement.
3. N₂O production in subsoil horizons is significant, with over 50% of total N₂O produced in subsoils of moderately fertilized rainfed treatments.
4. The fraction of total N₂O produced in subsoil at my site was controlled by the NO₃⁻ availability and moisture status of the soil profile, and was not affected by tillage.
5. Subsoils of sites fertilized at levels that well exceed plant N requirements produce a small fraction of total N₂O emission compared to the surface horizon.
6. Dry surface soil horizons in rainfed treatments shifted relative N₂O production into lower horizons where moisture was available.

Table 3.1. Horizon depths in the Monolith Lysimeters of Kalamazoo loam soil at KBS (From Aiken 1992). Monolith Lysimeter labels refer to Figure 3.1.

Soil layer	Monolith Lysimeter			
	CT2	CT13	NT6	NT9
	<i>cm</i>			
A _p	0-25	0-23	0-21	0-21
E	-	24-30	21-30	21-30
B _t	25-53	30-64	30-56	30-48
2B _{t2} B	53-73	64-84	56-66	48-55
2B _{t2} C	-	-	66-83	-
2B _{t3}	-	-	83-107	55-78
3E\B _t	73-	84-	107-	78-

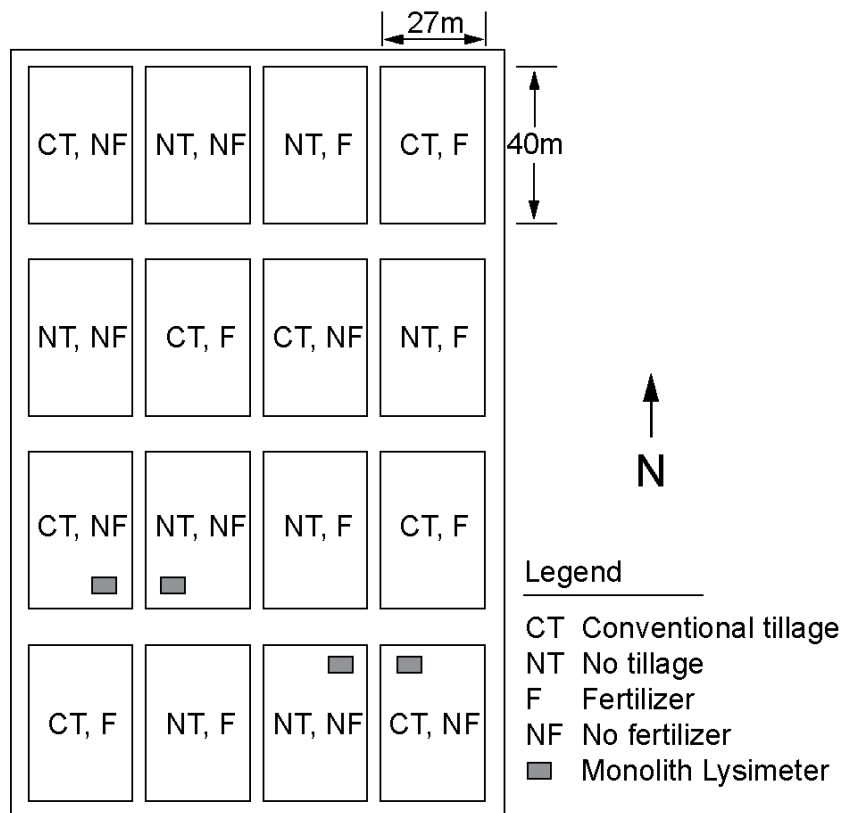


Figure 3.1. Diagram of field plots established at the Kellogg Biological Station in 1986 to investigate N supply and tillage effects on soil-plant interactions. Intact-profile monolith lysimeters are located in plots 2, 6, 9, and 13 (From Aiken 1992).

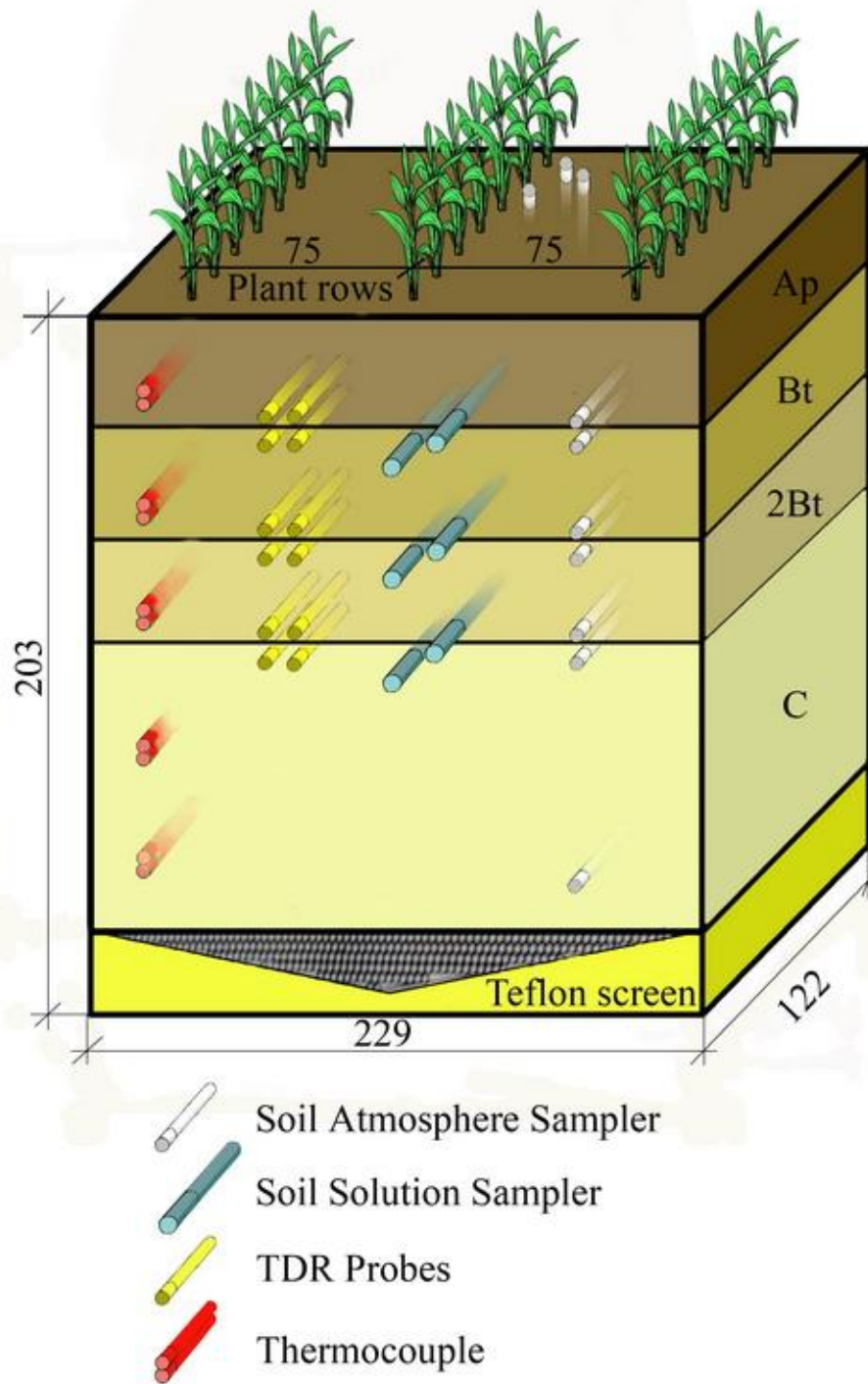


Figure 3.2. Schematic diagram of monolith lysimeter with instrumentation ports for nondestructive sampling of soil atmosphere, soil solution, soil moisture, and soil temperature. All units are in cm.

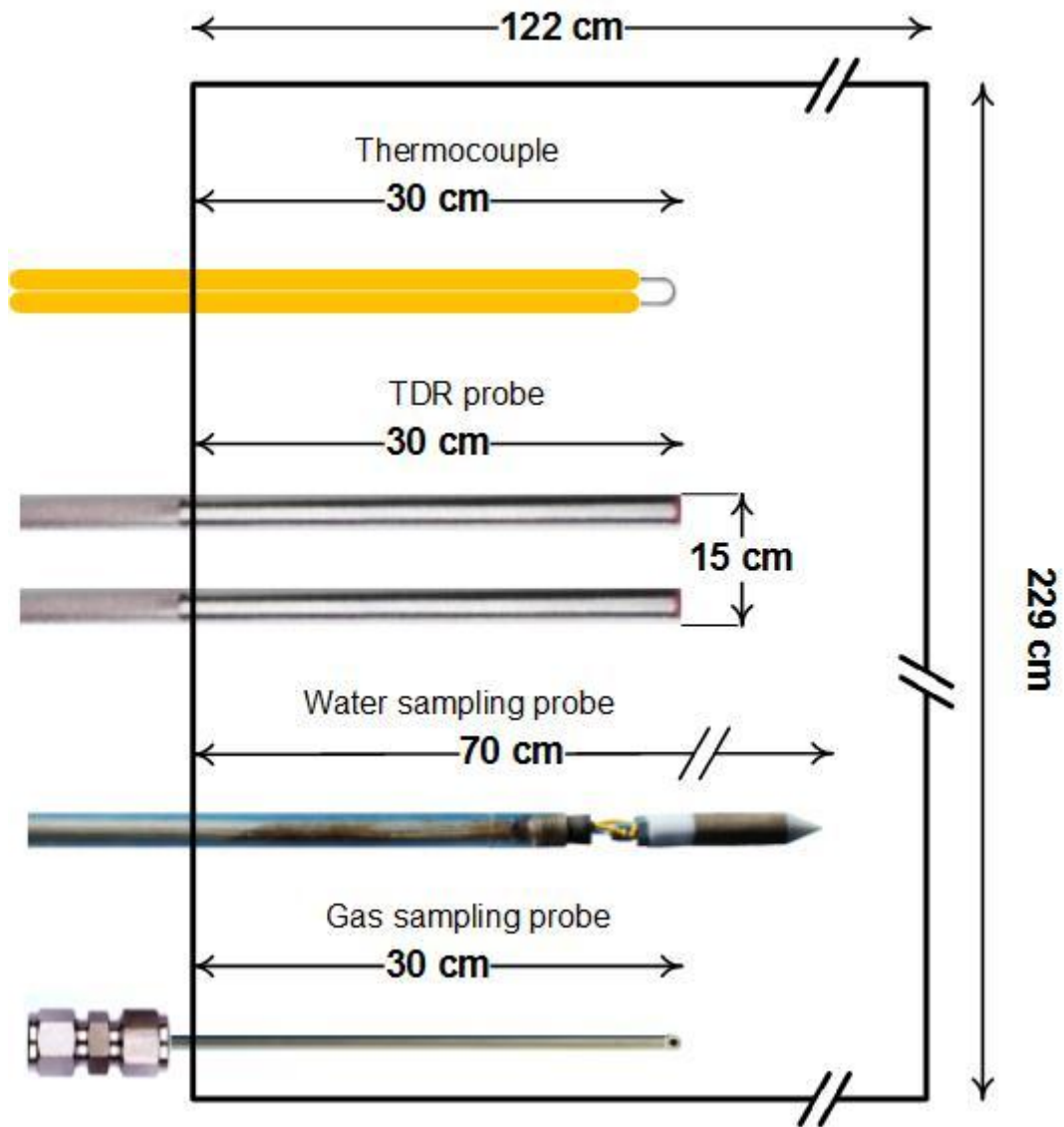


Figure 3.3. Schematic representation (top view) of nondestructive probes in a soil profile layer in a monolith lysimeter.

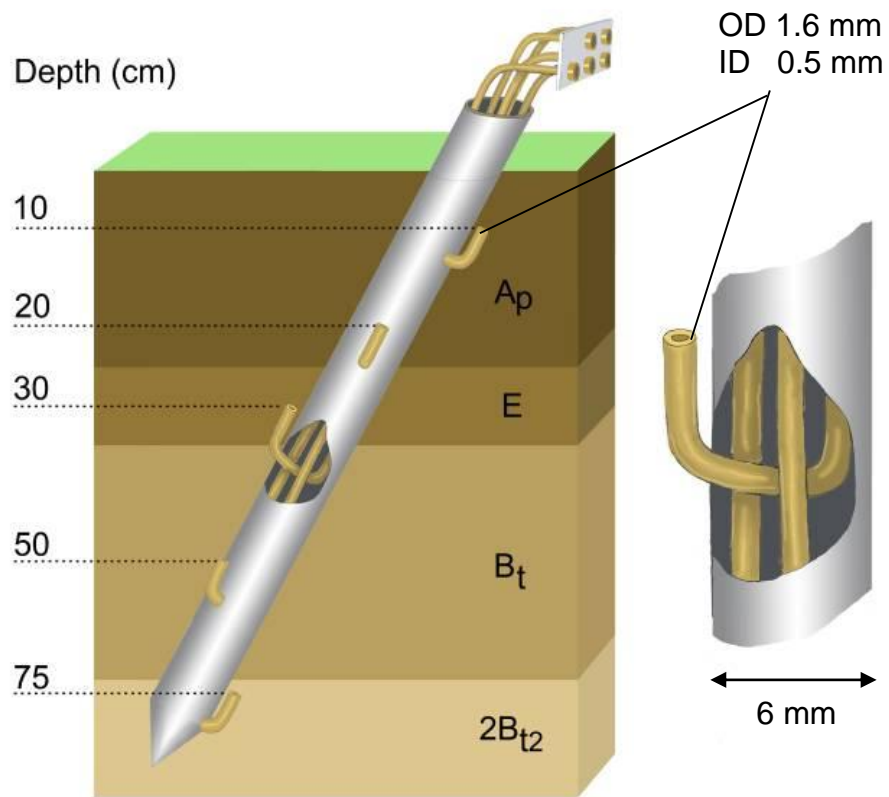


Figure 3.4. Soil profile gas probe installed at 60° angle with sampling depths at 10, 20, 30, 50, and 75 cm (from Shcherbak and Robertson, in press).

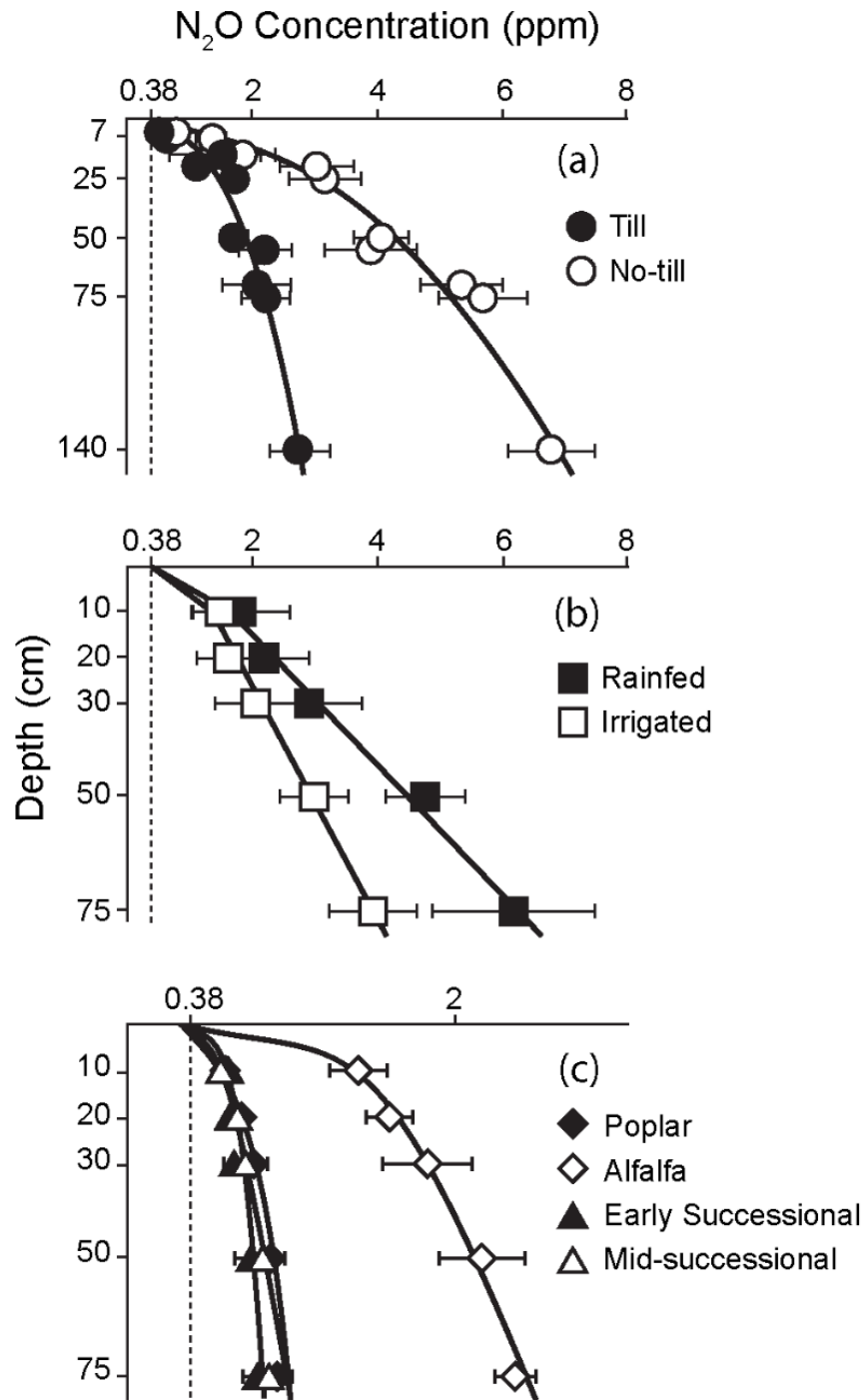


Figure 3.5. Mean seasonal N_2O concentration profiles observed in the experiments. Atmospheric concentration is 0.38 ppm ν . a) Tilled and no-till Monolith Lysimeters treatments. b) Rainfed and irrigated Resource Gradient Experiment treatments. c) Poplar, Alfalfa, Early-successional community, and Mown grassland (never tilled) systems of the LTER Main Cropping System Experiment (MCSE).

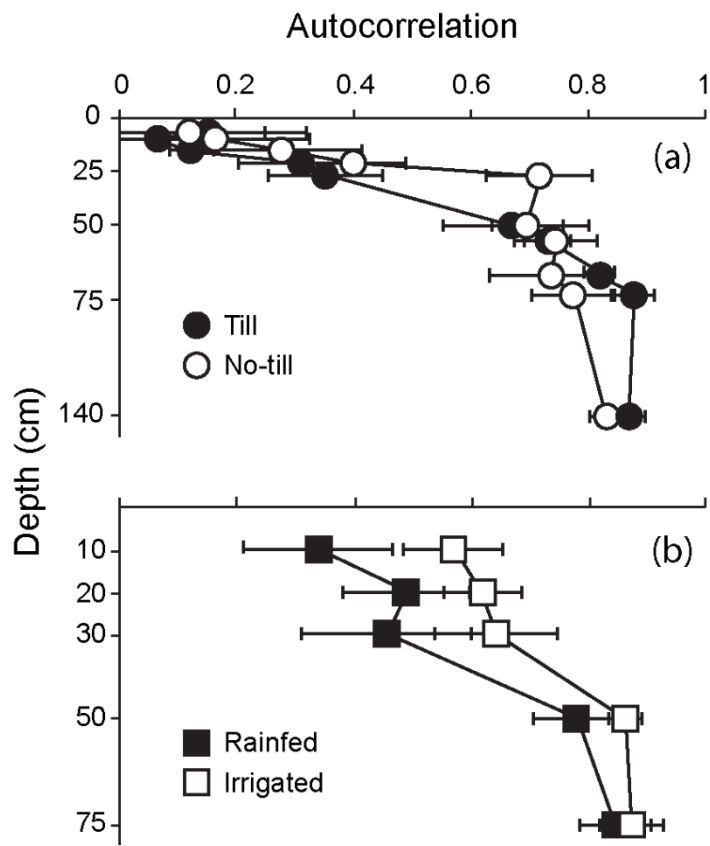


Figure 3.6. Average temporal autocorrelations of concentrations at different depths and temporal autocorrelation of surface fluxes of N₂O. Autocorrelations close to one indicate N₂O concentrations (or fluxes) with low temporal variability, whereas autocorrelations close to or below zero indicate highly variable and unstable values. a) Tilled and no-till Monolith Lysimeter treatments. b) Rainfed and irrigated and Resource Gradient Experiment treatments.

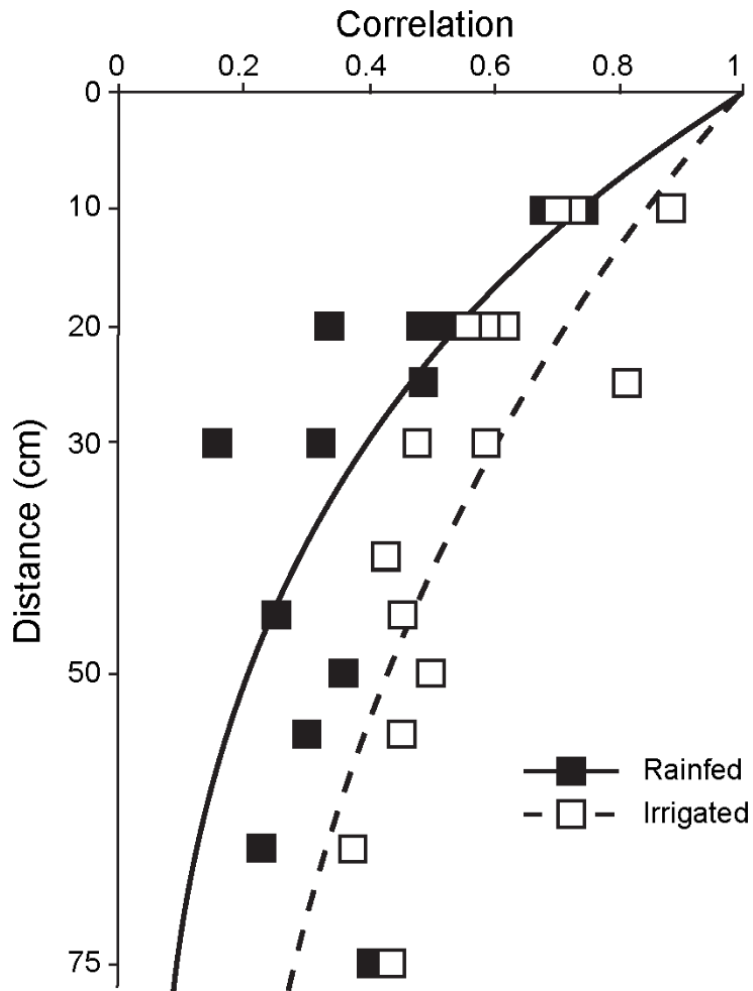


Figure 3.7. Change in correlation between N₂O surface fluxes and soil N₂O concentrations with distance between measurement depths for rainfed and irrigated Resource Gradient Experiment treatments. Each point represents a correlation of N₂O concentrations at two different depths in 2011 vs. absolute differences between the depths.

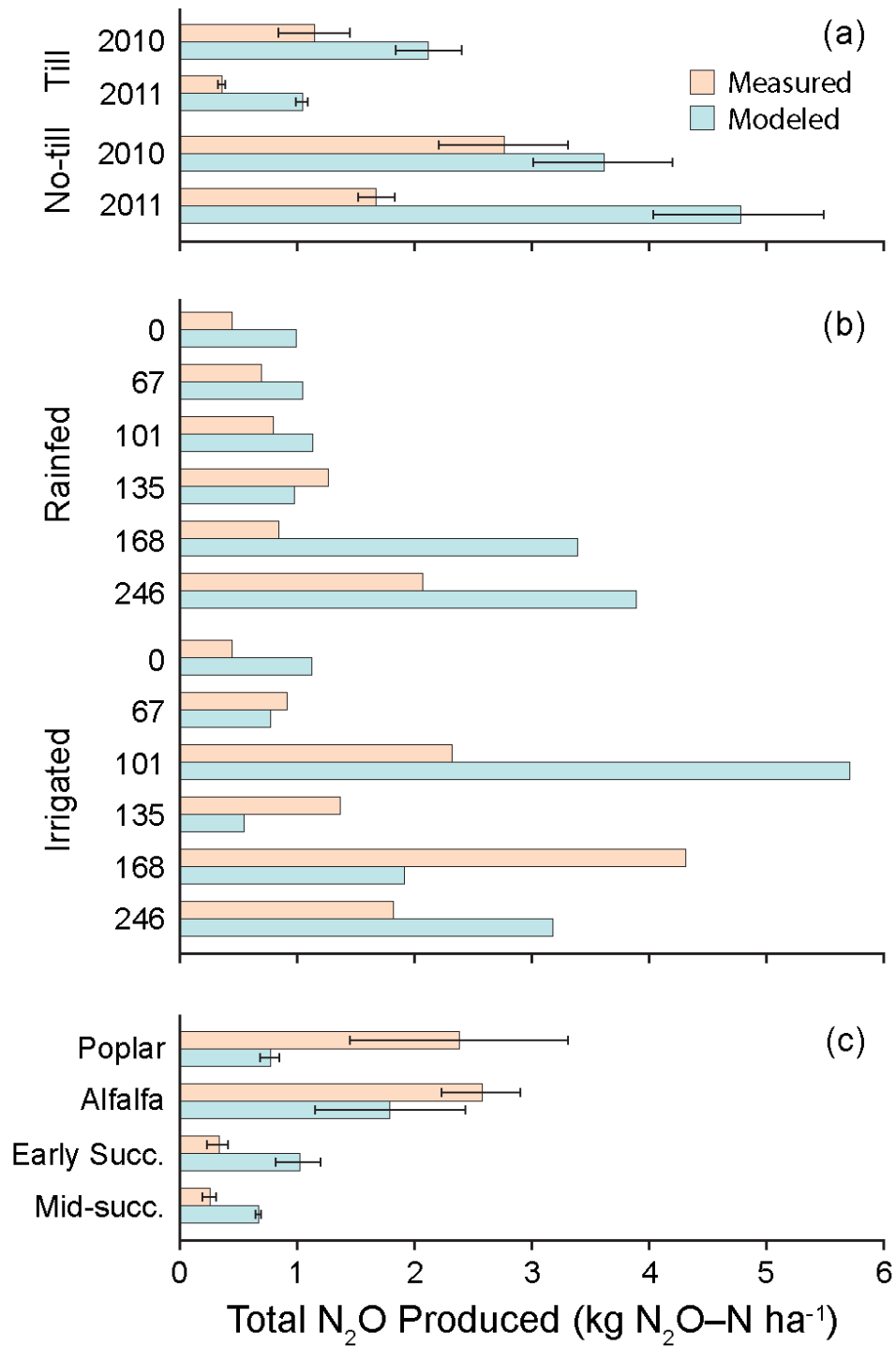


Figure 3.8. Comparison of total seasonal N₂O emissions measured by static or automatic chamber method and modeled from N₂O concentration and diffusivity at 10 cm depth. a) Tilled and no-till Monolith Lysimeter treatments. b) Rainfed and irrigated Resource Gradient Experiment treatments. c) Poplar, Alfalfa, Early-successional community, and Mown grassland (never tilled) systems of the LTER MCSE.

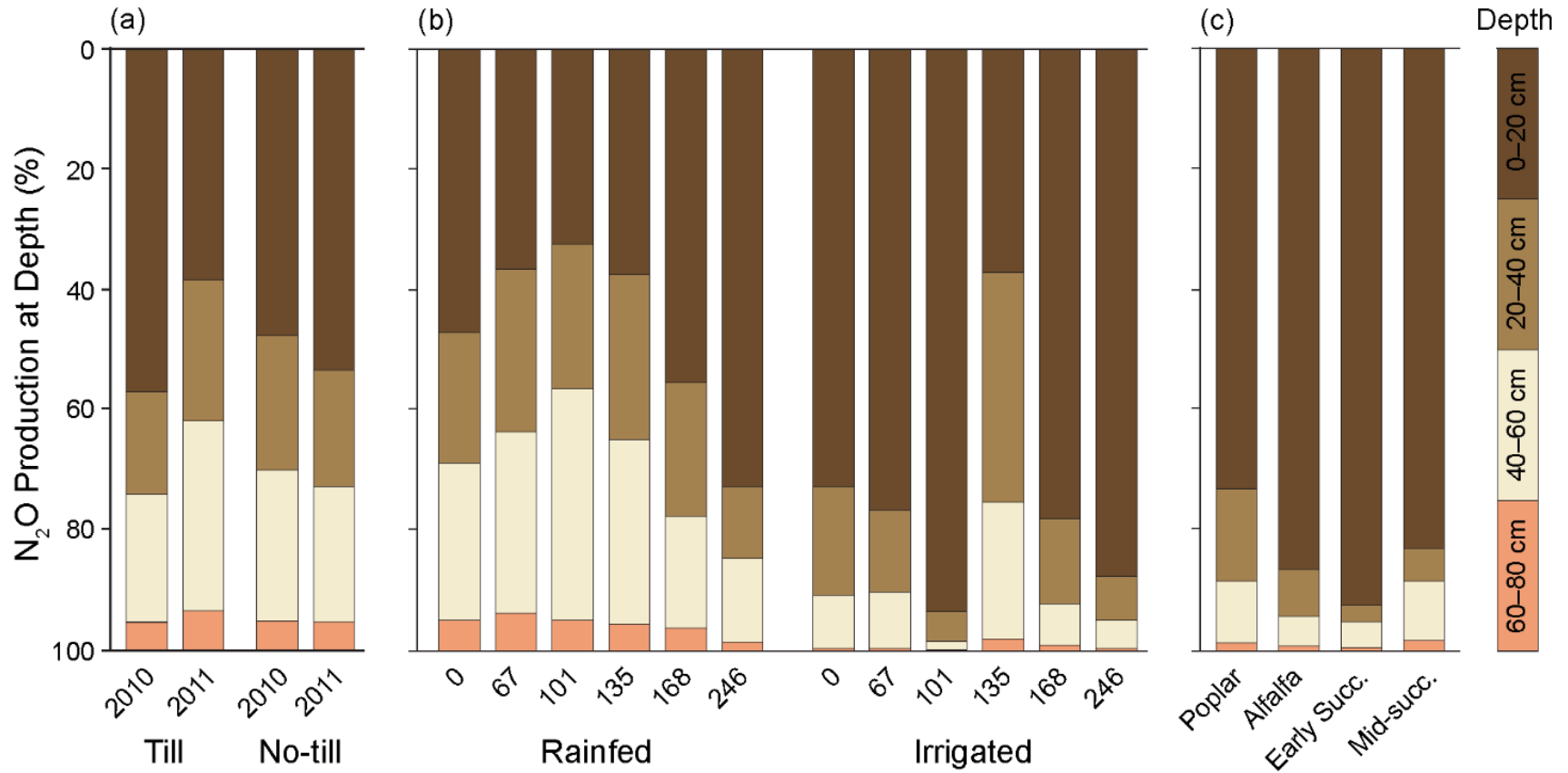


Fig 3.9. Annual relative N₂O production by depth as calculated from concentrations and modeled diffusivity. a) Tilled and no-till Monolith Lysimeter treatments. b) Rainfed and irrigated Resource Gradient Experiment treatments with rate of N input (0-246 kg N ha⁻¹) indicated next to the treatment. c) Poplar, Alfalfa, Early-successional community, and Mown grassland (never tilled) systems of the LTER MCSE.

REFERENCES

REFERENCES

- Addy K., Kellogg D.Q., Gold A.J., Groffman P.M., Ferendo G. and Sawyer C. 2002. In situ push-pull method to determine ground water denitrification in Riparian Zones. *Journal of Environmental Quality* 31:1017–1024.
- Aiken, R. M. 1992. Functional Relations of Root Distributions with the Flux and Uptake of Water and Nitrate. *PhD Dissertation*. Michigan State University, East Lansing.
- Barkle, G., T. Clough, and R. Stenger. 2007. Denitrification capacity in the vadose zone at three sites in the Lake Taupo catchment, New Zealand. *Australian Journal of Soil Research* 45:91-99.
- Barton, L., C. D. A. McLay, L. A. Schipper, and C. T. Smith. 1999. Annual denitrification rates in agricultural and forest soils: a review. *Australian Journal of Soil Research* 37:1073-1093.
- Basso, B., J.T. Ritchie, P.R. Grace, and L. Sartori. 2006. Simulation of tillage systems impact on soil biophysical properties using the SALUS model. *Italian Journal of Agronomy* 1:677-688.
- Bhogal, A. and M. Shepherd. 1997. Effect of poultry manure on the leaching of carbon from a sandy soil as a potential substrate for denitrification in the subsoil. *Journal of the Science of Food and Agriculture* 74:313-322.
- Bradley, R. L., J. Whalen, P. L. Chagnon, M. Lanoix, and M. C. Alves. 2011. Nitrous oxide production and potential denitrification in soils from riparian buffer strips: Influence of earthworms and plant litter. *Applied Soil Ecology* 47:6-13.
- Brown, K.W., C.J. Gerard, B.W. Hipp, and J.T. Ritchie. 1974. Procedure for placing large undisturbed monoliths in lysimeters. *Soil Science Society of America Journal* 38:981-983.
- Castle, K., J. R. M. Arah, and A. J. A. Vinten. 1998. Denitrification in intact subsoil cores. *Biology and Fertility of Soils* 28:12-18.
- Cerny, R. 2009. Time-domain reflectometry method and its application for measuring moisture content in porous materials: A review. *Measurement* 42:329-336.
- Clough, T.J., S.C. Jarvis, E.R. Dixon, R.J. Stevens, R.J. Laughlin, D.J. Hatch. 1999. Carbon induced subsoil denitrification of (15)N-labelled nitrate in 1 m deep soil columns. *Soil Biology & Biochemistry* 31:31-41.
- Clough, T. J., F. M. Kelliher, Y. P. Wang, and R. R. Sherlock. 2006. Diffusion of N-15-labelled

- N₂O into soil columns: a promising method to examine the fate of N₂O in subsoils. *Soil Biology & Biochemistry* 38:1462-1468.
- Clough T.J., K. Addy, D.Q. Kellogg, B.L. Nowicki, A.J. Gold, and P.M. Groffman. 2007. Dynamics of nitrous oxide in groundwater at the aquatic–terrestrial interface. *Global Change Biology* 13:1528-1537.
- Funk, R., F. X. Maidl, and G. Fischbeck. 1996. Denitrification in deeper soil layers of arable land in southern Germany. *Zeitschrift Fur Pflanzenernahrung Und Bodenkunde* 159:207-213.
- Goldberg, S. D., K. H. Knorr, and G. Gebauer. 2008. N₂O concentration and isotope signature along profiles provide deeper insight into the fate of N₂O in soils. *Isotopes in Environmental and Health Studies* 44:377-391.
- Goldberg, S. D. and G. Gebauer. 2009. Drought turns a Central European Norway spruce forest soil from an N₂O source to a transient N₂O sink. *Global Change Biology* 15:850-860.
- van Groenigen, J.W., P.J. Georgius, C. van Kessel, E. Hummelink, G.L. Velthof, and K.B. Zwart. 2005a. Subsoil ¹⁵N-N₂O concentrations in a sandy soil profile after application of ¹⁵N-fertilizer. *Nutrient Cycling in Agroecosystems* 72:13–25
- van Groenigen, J. W., K. B. Zwart, D. Harris, and C. van Kessel. 2005b. Vertical gradients of delta N-15 and delta(18O) in soil atmospheric N₂O-temporal dynamics in a sandy soil. *Rapid Communications in Mass Spectrometry* 19:1289-1295.
- Hashimoto, T. and H. Niimi. 2001. Seasonal and vertical changes in denitrification activity and denitrifying bacterial populations in surface and subsurface upland soils with slurry application. *Soil Science and Plant Nutrition* 47:503-510.
- Hoffmann, C. C., S. Rysgaard, and P. Berg. 2000. Denitrification rates predicted by nitrogen-15 labeled nitrate microcosm studies, in situ measurements, and modeling. *Journal of Environmental Quality* 29:2020-2028.
- IPCC 2000 Land Use, Land-Use Change, and Forestry.
- Jarvis, S. C. and D. J. Hatch. 1994. Potential for denitrification at depth below long-term grass swards. *Soil Biology & Biochemistry* 26:1629-1636.
- Jury W.A., J. Letey, and T. Collins. 1982. Analysis of chamber methods used for measuring nitrous oxide production in the field. *Soil Science Society of America Journal* 46:250–256.
- Kahmark, K. and N. Millar. 2008. Field Gas Sampling Protocol (Bucket Method), research protocol used at LTER KBS <http://lter.kbs.msu.edu/protocols/113>
- Kamewada, K. 2007. Vertical distribution of denitrification activity in an Andisol upland field

- and its relationship with dissolved organic carbon: Effect of long-term organic matter application. *Soil Science and Plant Nutrition* 53:401-412.
- Kammann C., L. Grunhage, and H.J. Jager. 2001. A new sampling technique to monitor concentrations of CH₄, N₂O and CO₂ in air at well defined depths in soils with varied water potential. *European Journal of Soil Science* 52:297–303.
- Khalili, B. and F. Nourbakhsh. 2012. Vertical distribution of soluble organic nitrogen, nitrogen mineralization, nitrification, and amidohydrolase activities in a manure-treated soil. *Journal of Plant Nutrition and Soil Science* 175:265-272.
- Maljanen, M., A. Liikanen, J. Silvola, and P.J. Martikainen. 2003. Measuring N₂O emissions from organic soils by closed chamber or soil/snow N₂O gradient methods. *European Journal of Soil Science* 54:625–631.
- McCarty, G.W. and J.M. Bremner. 1992. Availability of organic-carbon for denitrification of nitrate in subsoils. *Biology and Fertility of Soils* 14:219-222.
- Millar, N., D. W. Rowlings, P. R. Grace, R. J. Gehl, and G. P. Robertson. 2013. Non-linear N₂O response to nitrogen fertilizer in winter wheat using automated chambers. *Plant and Soil*, submitted.
- Millington, R.J. 1959. Gas diffusion in porous media. *Science* 130:100-102.
- Mokma, D. L., and J. A. Doolittle. 1993. Mapping some loamy alfisols in southwestern Michigan using ground-penetrating radar. *Soil Survey Horizons* 34:71-77
- Murray, P. J., D. J. Hatch, E. R. Dixon, R. J. Stevens, R. J. Laughlin, and S. C. Jarvis. 2004. Denitrification potential in a grassland subsoil: effect of carbon substrates. *Soil Biology & Biochemistry* 36:545-547.
- Myrold, D. D. 1988. Denitrification in ryegrass and winter-wheat cropping systems of western Oregon. *Soil Science Society of America Journal* 52:412-416.
- Myrold, D. D. and J. M. Tiedje. 1985. Establishment of denitrification capacity in soil - effects of carbon, nitrate and moisture. *Soil Biology & Biochemistry* 17:819-822.
- Page, K.L., R.C. Dalal, N.W. Menzies, and W.M. Strong. 2002. Nitrification in a Vertisol subsoil and its relationship to the accumulation of ammonium-nitrogen at depth. *Australian Journal of Soil Research* 40:727-735.
- Robertson, G.P. 2000. Denitrification In *Handbook of Soil Science*. M.E. Summer, ed. CRC Press, Boca Raton, Florida, USA. pp. C181-190.
- Robertson, G.P. 2013. Soil greenhouse gas emissions and their mitigation In *The Encyclopedia of Agriculture and Food Systems*. N.K. Van Alfen ed., Academic Press, San Diego, CA.

- Robertson, G.P. and P.M. Groffman. 2013. Nitrogen transformations In *Soil Microbiology, Ecology and Biochemistry*. 4th Edition. E. A. Paul ed., Academic Press, Burlington, MA. In press.
- Robertson, G.P. and S.K. Hamilton. 2014. Conceptual and experimental approaches to understanding agricultural ecosystems: KBS long-term ecological research In *The ecology of agricultural ecosystems: research on the path to sustainability*. Pages xx-xx in S. K. Hamilton, J. E. Doll, and G. P. Robertson, eds., Oxford University Press, New York, New York, USA. In press.
- Robertson, G.P. et al. 2014. Farming for Ecosystem Services: An Ecological Approach to Production Agriculture. *Bioscience*, *in review*
- Rolston, D.E., M. Fried, and D.A. Goldhamer. 1976. Denitrification measured directly from nitrogen and nitrous oxide gas fluxes. *Soil Science Society of America Journal* 40:259–266.
- Scervini, M. 2009. Thermocouples: The Operating Principle. <http://www.msm.cam.ac.uk/UTC/thermocouple/pages/ThermocouplesOperatingPrinciples.html> 03/24/2010
- Shcherbak, I. and G.P. Robertson. 2014. Determining the diffusivity of nitrous oxide in soil using in situ tracers. *Soil Science Society of America Journal*, *in press*.
- Wang, Y. Y., C.S. Hu, Ming, Y.M. Zhang, X.X. Li, W.X. Dong, and O. Oenema. 2013. Concentration profiles of CH₄, CO₂ and N₂O in soils of a wheat-maize rotation ecosystem in North China plain, measured weekly over a whole year. *Agriculture, Ecosystems & Environment* 164:260-272.
- Warncke D., J. Dahl, L. Jacobs, and C. Laboski. 2004. Nutrient Recommendations for Field Crops in Michigan. *Extension Bulletin E2904*, Department of Crop and Soil Sciences, Michigan State University.
- Weier, K. L., I. C. Macrae, and R. J. K. Myers. 1993. Denitrification in a clay soil under pasture and annual crop - losses from ¹⁵N-labeled nitrate in the subsoil in the field using C₂H₂ inhibition. *Soil Biology & Biochemistry* 25:999-1004.
- Well R. and D.D. Myrold. 2002. A proposed method for measuring subsoil denitrification in situ. *Soil Science Society of America Journal* 66:507–518.
- Yeomans, J. C., J. M. Bremner, and G. W. McCarty. 1992. Denitrification capacity and denitrification potential of subsurface soils. *Communications in Soil Science and Plant Analysis* 23:919-927.
- Yoh, M., H. Toda, K. Kanda, and H. Tsurata. 1997. Diffusion analysis of N₂O cycling in a fertilized soil. *Nutrient Cycling in Agroecosystems* 49:29–33.

CHAPTER 4

A Meta-analysis of the Nonlinearity of Direct Annual N₂O Emissions in Response to Nitrogen Fertilization

ABSTRACT

Nitrogen (N) fertilizer rate is the best single predictor of N₂O emissions from agricultural soils, which are responsible for ~50% of the total global anthropogenic N₂O flux, but is a relatively imprecise estimator. More precise knowledge of the fertilizer N₂O emission response could improve global and regional N₂O assessments and help to design more efficient mitigation strategies. Evidence now suggests that the emission response is not linear, as assumed by IPCC methodologies, but rather exponentially increases with fertilization. I performed a meta-analysis to test the generalizability of these findings. I selected published studies with at least three N fertilizer rates and identical soil management. From 78 available studies (231 site-years) I calculated N₂O emission factors (EFs) as a percentage of applied N converted to N₂O emissions. I found that the rate of change in N₂O EF (Δ EF) grew significantly faster than linear for synthetic fertilizers, for a majority of the crop types examined, and for soils with high organic carbon content, low mean annual temperatures, or low pH. Nitrogen-fixing crops had a significantly higher Δ EF than non-fixing crops. A higher Δ EF is also evident in soils with organic carbon content > 1.5%, in acidic soils, and in experiments with a single fertilizer application. My results suggest a general trend of exponentially increasing N₂O emissions as N fertilizer rates increase to exceed crop N needs. Use of this knowledge in global and regional greenhouse gas inventories should provide a more accurate assessment of fertilizer-derived N₂O emissions and help further close the global N₂O cycle.

INTRODUCTION

Nitrous oxide is a major greenhouse gas (GHG) with a global warming potential ~300 times that of CO₂ over a 100 year time period (IPCC 2007). Additionally, N₂O is the largest of all the ozone depleting substances and is projected to remain so for the remainder of this century (Ravishankara et al. 2009). Nitrous oxide emissions from agricultural soils, produced predominantly by the microbial processes of nitrification (oxidation of ammonium to nitrate) and denitrification (reduction of nitrate, via N₂O, to N₂) (Robertson and Groffman, 2014), constitute ~50% of global anthropogenic N₂O emissions (IPCC 2007), primarily as a result of the addition of synthetic nitrogen (N) fertilizers and animal manure to soil (Bouwman et al. 2002a). The total input of N to soil and its subsequent availability is a robust predictor of N₂O fluxes from most soils and has been used to construct most national GHG inventories using an emission factor (EF) approach (de Klein et al. 2006).

The N₂O EF is a percentage of the fertilizer N applied that is transformed into fertilizer-induced emissions, which for IPCC GHG inventories is calculated as the difference in emission between a fertilized and unfertilized soil under otherwise identical conditions. Global EFs for fertilizer-induced direct N₂O emissions have been determined by Eichner (1990), Bouwman (1990, 1996), Mosier et al. (1998), Bouwman et al. (2002a, b), and Stehfest and Bouwman (2006). The current global mean value, derived from over 1000 field measurements of N₂O emissions, is ~0.9% (Bouwman et al. 2002b, Stehfest and Bouwman 2006). This value is an approximate average of synthetic fertilizer (1.0%) and animal manure (0.8%) induced emissions, and was rounded by the IPCC (de Klein et al. 2006) to 1% due to uncertainties and the inclusion of other N inputs such as crop residues (Novoa and Tejeda 2006) and soil organic matter mineralization (IPCC 2007). In short, for every 100 kg of N input, 1.0 kg of N in the form of N₂O is estimated to be emitted directly from soil.

A 1% constant EF assumes a linear relationship between N fertilizer rate and N₂O emissions that is indifferent to biological thresholds that might occur, e.g., when the availability of soil inorganic N exceeds crop N demands. Because the vast majority of studies on N₂O emissions from crops have examined a single fertilizer rate (many without a zero fertilizer rate comparison), there is no power in these studies for detecting such thresholds. Yet results from a growing number of field experiments with multiple N fertilizer rates indicate that emissions of N₂O respond non-linearly to increasing N rates across a range of fertilizer formulations, climates, and soil types (e.g. McSwiney and Robertson 2005, Ma et al. 2010, Hoben et al. 2011, Signor et al. 2013), and that EFs in fact change monotonically with respect to N addition. Incorporating this knowledge into large-scale N₂O models could help to close the gap between bottom-up and top-down estimates of fertilizer N₂O contributions to regional and global fluxes (Crutzen et al. 2008, Smith et al. 2012).

Grace et al. (2011), for example, used a nonlinear N₂O emission function to model total direct emissions of N₂O from the U.S. North Central Region between 1964 and 2005. Their estimate was equivalent to an EF of 1.75% of applied N over this period, substantially higher than the global default IPCC value of 1%. More recently, Griffis et al. (2013) estimated for contemporary fluxes an overall North Central Region EF of 1.8% using a large tower eddy covariance approach.

Global, top down estimates of N₂O from anthropogenic sources of reactive N, including animal manure (Davidson 2009), yield an overall EF of $4 \pm 1\%$ (Crutzen et al. 2008, Smith et al. 2012). Bottom-up models are in broad agreement (del Grosso et al. 2008), but there are large uncertainties and the agreement breaks down at regional and sub-regional scales (Reay et al. 2012). The use of EFs that vary with N input (IPCC Tier 2) may help to reconcile this difference and augment the local to regional insights urgently needed to stem the projected 20% increase in

agricultural N₂O emissions expected by 2030 (Reay et al. 2012).

Response curves for N₂O flux as a function of N rate have recently become more common. McSwiney and Robertson (2005), for example, reported an exponentially increasing N₂O response to fertilizer N along a nine-point fertilizer N gradient for non-irrigated corn in Michigan. In their study N₂O fluxes more than doubled (20 vs. >50g N₂O–N ha⁻¹ day⁻¹) at N rates greater than 100 kg N ha⁻¹, the level at which yield was maximized. Hoben et al. (2011) documented a similar response for five on-farm sites in Michigan under corn–soybean rotation with six fertilizer N rates (0–225 kg N ha⁻¹ yr⁻¹). Others (Ma et al. 2010, Signor et al. 2013) but not all (Halvorson et al. 2008) have since found similar patterns for multi-point N fertilizer gradients. Kim et al. (2013) documented 18 published instances with non-linear responses to four or more N-input levels.

Here I test the generality of these findings globally. While there are very few N₂O response studies with a sufficient number of N-input levels to characterize an exact non-linear response with confidence, I located over 200 studies with more than two levels in addition to a zero-N control. And while it is not possible to define a response curve without additional levels, I compare EFs for nonzero levels to determine the presence of a change, its direction, and an aggregate Δ EF (change in EF with N input). Here I report the results of a meta-analysis on this global dataset, and also investigate the potential interaction of Δ EF with other factors such as crop type, fertilizer source, and soil texture. I also test for possible biases caused by reported differences in measurement characteristics: the duration, number, and frequency of measurements, flux chamber area, number of samples per flux measurement, and numbers of replicates. I then compare results to prior EF determinations, including those used as a basis for current IPCC Tier 1 methodologies (Bouwman et al. 2002a, b) and carbon credit markets (Millar et al. 2010, 2012).

MATERIALS AND METHODS

Study Selection and Data Extraction

I selected field studies from the literature where in-situ measurements of at least three different levels of N fertilizer input including a zero N rate (control) were applied under otherwise identical conditions including site, growing season, crop, fertilizer type, measurement length, frequency, and method. I included in my search all published datasets from the Web of Science (selected from 1330 papers found using keywords “nitrous oxide fertilizer rate” in June 2013), studies identified in reviews by Bouwman (1996), Jungkunst et al. (2006), Kim et al. (2012), and several forthcoming papers. Laboratory and greenhouse studies were excluded from my analysis as were studies where different N fertilizer rates were confounded by differences in management practices.

I used all site-years present in original studies averaged by replicates (if reported). I did not average measurements for a particular site if years, crops, fertilizers, or other significant factors were different. I converted units of fertilizer input, mean N₂O emission, and standard error to kg N ha⁻¹ for the study period.

Papers with data presented only as graphs of total or daily emissions were digitized using Get Data Graph Digitizer (2013). Digitization errors were less than 1% in newer papers to ~3-5% for old graphs with poor image quality or where daily emission values were used.

I include key characteristics for each study in the dataset (Dataset S2): literature reference, location name and coordinates of experiment; mean annual precipitation and temperature; soil texture, organic carbon, organic nitrogen, pH, and bulk density; some crop and management details; year, duration, total number of measurements, and number of replicates; chamber area and number of measurements per sample; and fertilizer type, mode of application, and number of applications per measurement period. Where necessary I contacted corresponding

authors to make this table as complete as possible.

Emission Factor Change Rates (ΔEF s)

I calculated emission factors for every nonzero N application rate as a difference between N₂O emissions (ER_N) at the application rate (N) and control (ER_0) divided by the (N).

$$EF_N = \frac{ER_N - ER_0}{N}$$

The least squares linear relation between the emission factor and N application rate was found for each site-year:

$$EF_N = EF_0 + \Delta EF N$$

EF change rate (ΔEF ; Figure C.1) of this relationship is degree of nonlinearity of emission increase with N input: zero ΔEF indicates that N₂O emissions grow linearly with N input (constant EF), a positive ΔEF indicates a faster than linear emission increase (increasing EF), and a negative ΔEF means that emissions grow at a rate slower than linear (decreasing EF). The model of linear change in EF assumes quadratic growth in emissions with N rate $ER_N = ER_0 + (EF_0 + \Delta EF N)N$, but my goal was to analyze the nonlinear component (ΔEF , Dataset S2) and not to determine the specific shape of the response.

Analysis

Data analysis was performed using Mathematica (2013). I performed a Kolmogorov-Smirnov test and determined that distribution of ΔEF is not normal ($p < 0.0001$). I used nonparametric (resampling) and parametric procedures for further analysis. Resampling procedures (bootstrap, i.e. sampling with replacement of the size equal to initial size of subset repeated N=100,000 times) were used for analysis of means, medians, and confidence intervals

(CIs) for all ΔEF s in the study as well as subsets of ΔEF s and parametric statistics used to compare results.

I removed four outlier ΔEF s with largest absolute values (-0.065, -0.05, 0.077, and 0.108) from further analysis because of their undue influence on subgroup means. The remaining 227 ΔEF s were divided into categories based on type of crop (corn, rice, small grains, vegetables, N-fixing, forage, and woody), fertilizer type (ammonium nitrate – AN, calcium ammonium nitrate – CAN, urea – U, manure – M, and mixed fertilizer), SOC content, soil pH (nonalkaline and alkaline), mean annual amount of rainfall, mean annual temperature, and first nonzero N input rate (0-100 and above 100 kg N ha⁻¹). Mean ΔEF s for subgroups were compared using a bootstrap test for differences (N=100,000 between means obtained by sampling with replacement equal to initial size of the subset) across categories for the same factor. I used Benjamini and Hochberg adjustment to control the false discovery rate (Benjamini and Hochberg 1995). I performed a linear regression analysis of ΔEF relative to mean EF.

I analyzed mean ΔEF s for potential biases due to measurement techniques. I selected the value of a parameter that split the dataset into two categories of similar size. I repeated the above procedure for each of the following factors: number of replicates, study duration, total number of samples, sampling frequency, chamber area, number of samples per flux measurement, number of fertilizer applications, and number of input levels. I performed bootstrap tests for differences as above, but without adjustment for the total number of comparisons. I further selected only site-years with at least four N input levels and that fit a quadratic function. I then divided the dataset into two categories of similar size by quality of the fit ($r^2 < 0.93$ and $r^2 \geq 0.93$) and tested the differences in ΔEF s.

I tested relatedness of pairs of different tested factors to each other to avoid relating the same influence to two different factors. For each pair of experimental and sampling factors I

calculated the phi-coefficient (ϕ), which is a measure of association of the two variables forming a two-by-two contingency table. Phi-coefficient is

$$\phi = \sqrt{\frac{X^2}{n}},$$

where X^2 is derived from Pearson's chi-squared test and n is total number of observations (Everitt, 1992).

Comparison with previous studies

I obtained the average quadratic model and its 95% CI for all the site-years in my dataset excluding sites with N-fixing crops and the single site with bare soil. I compared this CI with 95% CIs for IPCC Tier 1 methodology and for the range of six models in Philbert et al. (2012) including and not including parameter uncertainty.

Selecting only studies with 4 or more N input rates in my dataset, I performed a procedure described in Kim et al. (2013) to classify all site-years into categories of linear, faster-than-linear (exponential), and slower-than-linear (hyperbolic) N₂O emission increase with N input.

I obtained an average quadratic model for all the site-years and a subset of fields planted to corn. I compared this estimate to the Hoben et al. (2011) model and the IPCC 1% EF model. I estimated the differences in emissions reductions predicted by each model under reduction in N fertilizer input from 200 to 150 kg N ha⁻¹, from 150 to 100 kg N ha⁻¹, and from 50 to 0 kg N ha⁻¹.

RESULTS

I identified (Dataset S2) 78 papers, covering 84 locations (Figure 4.1) and 231 site-years

that satisfied my selection criteria of in situ flux measurements from sites fertilized at three or more N rates with a zero N control. A Kolmogorov-Smirnov test confirmed that Δ EFs are not normally distributed ($p < 0.0001$, Figure 4.2). In 155 cases (64%) Δ EFs are positive; in the remainder rates are zero or negative. A resampling procedure on all Δ EFs showed that mean (0.0027) and median (0.0005) Δ EFs (% increase per kg added N) are significantly larger than 0, with 95% confidence intervals (CI) of 0.0011–0.0044 and 0.0003–0.0009, respectively. Removing four outlier site-years from the dataset slightly decreased the average Δ EF (to 0.0024), decreased the standard error substantially (from 8.5×10^{-4} to 5.4×10^{-4}), and did not affect the median Δ EF or its standard error (Figure 4.3 and Table B.1).

Nitrogen-fixing crops, upland grain crops, rice, and forage all had positive Δ EFs significantly different from 0 ($p < 0.01$, Figure 4.3 a and Table B.1). N-fixing crops (including those present in rotation with other crops) had the highest mean Δ EF (0.018), followed by forage (0.0033), upland grain crops (0.0017), and rice (0.001). The Δ EF for bare soil was 0.03 based on a single study (site-year). The only significant difference among land uses was N-fixing crops vs. all others ($p = 0.001$), vs. upland grain crops ($p = 0.001$), vs. rice ($p = 0.0006$), and vs. perennial grasses ($p = 0.004$) (Table B2a). All of these tests remain significant after Benjamini and Hochberg adjustment for the total number of tests.

Synthetic fertilizers ($n = 187$, including organic formulations) dominate other available fertilizer types (manure, $n = 16$; mixture of synthetic and manure, $n = 10$) so their mean Δ EF (0.0027, Figure 4.3 b and Table B.1) is similar to that of all treatments. Among synthetic fertilizers, ammonium nitrate (AN) and urea had significant ($p < 0.002$) positive mean Δ EFs, while calcium-ammonium nitrate (CAN), controlled-release urea (CRU), urea ammonium nitrate (UAN), manure, and mixed fertilizer (Mix) had Δ EFs not different from 0. A difference (t-test) among synthetic fertilizers (Table B.2 b) showed that mean Δ EFs for AN are significantly ($p <$

0.01) different than those of CAN, UAN, and CRU; the ΔEF for urea is significantly different ($p=0.0034$) from that of CRU. Benjamini and Hochberg adjustment leaves all differences significant.

Among the other experimental factors I tested (Figure 4.3 c and Table B.1: soil carbon, precipitation, temperature, pH, and number of fertilizer applications), ΔEF s were all different from 0, except for sites with soil organic carbon (SOC) contents below 1.5%, mean annual temperature above 10 °C, or alkaline soils (pH above 7), which have mean ΔEF s significantly lower than sites with SOC above 1.5%, mean temperature below 10 °C, or nonalkaline soils (pH below 7) ($p<0.03$, Table B.2 c). Benjamini and Hochberg adjustment removes the first two differences, while mean ΔEF s for alkaline and nonalkaline sites remains significant ($p=0.01$). Sites with $pH < 7$ have a variance in ΔEF that is approximately 4 times larger than that for sites with $pH > 7$.

The average EF for site-year was positively correlated with ΔEF (Adjusted $r^2 = 0.22$, Figure C.2), with a slope of 0.0024 (± 0.0003 SE). Site-years with smallest N input rate after control below 100 kg N ha⁻¹ had mean ΔEF (0.0034) significantly larger ($p=0.007$, Figure 4.3 c) than mean ΔEF for the site-years with smallest N input rate after control above 100 kg N ha⁻¹ (0.0009). Both groups have mean ΔEF s larger than 0 ($p=5 \times 10^{-5}$ and 0.01, respectively).

Among sampling-related factors, the annual number of measurements, duration of the experiment, number of replicates, and number of samples per flux measurement did not significantly affect the mean ΔEF at the 95% confidence level (Figure C.3 and Table B.2 d). Chamber area was the exception with large chambers (>0.2 m², equivalent to 45×45 cm square) corresponding to a small but significantly lower mean ΔEF ($p < 0.0003$) as compared to small chambers (<0.2 m²). Sites with three or more nonzero N input rates showed no significant relationship between ΔEF and adjusted r^2 of the quadratic function fit (Figure C.4).

The largest experimental factor associations in contingency tables (Table B.3 a) were between mean annual temperature and SOC ($\phi = -0.59$), SOC and soil pH ($\phi = 0.44$), and between soil pH and mean annual temperature ($\phi = -0.36$). The sampling factor associations (Table B.3 b) were weaker yet, with strongest associations between chamber area and number of replicates ($\phi = -0.56$) and between number of measurements and duration of the experiment ($\phi = 0.45$).

DISCUSSION

My results show that N₂O emissions tend to grow in response to N fertilizer additions at a rate significantly greater than linear, i.e. there is a positive mean ΔEF for all site-years as well as for the majority of groupings by crop, type of N fertilizer applied, and other study and sampling characteristics. This main result is in agreement with results from most sites with five or more N-input levels (McSwiney et al. 2005, Hoben et al. 2011, Kim et al. 2013) and suggests that the current global EF of 1% (de Klein et al. 2006) is too conservative for high N input rates.

That the majority of N₂O ΔEF s are positive (Figure 4.2) means that N₂O emissions grow with N input at a rate that is significantly faster than linear. The significantly larger ΔEF for N-fixing crops compared to upland grain crops, rice, and perennial grasses (Figure 4.3 a) is likely due to crop N saturation without any additional N input. Likewise the ΔEF value for the single bare soil site, lacking all plant uptake, was higher yet (0.03, Table B.1). In contrast, controlled-release urea delivers N at a slower rate than urea, ammonium nitrate, and other synthetic fertilizers and has a lower ΔEF than other fertilizers, which also supports the hypothesis that plant-heterotroph competition exerts control on the N₂O emission rate. Likewise, split fertilizer applications also had a lower ΔEF than single applications. All the outcomes above are consistent with the N surplus approach of van Groenigen et al. (2010). Site-years with pH below 7 or SOC

above 1.5% had both higher mean EF and mean Δ EF, which is consistent with acidic soils and carbon-rich soils having higher average N_2O emissions (Figure 4.3 c) and consistent with a positive correlation between mean EF and mean Δ EF.

There were no significant differences in Δ EF based on sampling factors except for chamber size. Chambers larger than 0.2 m^2 ($\sim 45 \times 45$ cm on a side if square) had somewhat lower Δ EFs than smaller chambers. Contingency tables of experimental and sampling factors did not reveal strong associations among factors (Table B.3 a, B.3 b), which means that tests for different experimental or sampling factors do not rely on the same set of site-years. However, one source of potential bias is that site-years with an initial nonzero N input rate below 100 kg N ha^{-1} are associated with higher Δ EFs compared to site-years with larger initial nonzero N input rates (Figure 4.3 c). This is likely because for a larger portion of these experiments, the crop N saturation point is surpassed with the initial nonzero N application rate. Another potential source of bias is the small number of studies with multiple N rates (Table B.1), which probably explains my inability to detect the difference in Δ EFs with increasing number of N levels (Figure C.3). Quality of data did not decline with increasing Δ EF (Figure C.4).

The significant presence of negative Δ EFs (i.e. a slower than linear emission growth rate with N input, Figure 4.2) does not have a satisfactory theoretical explanation. Such a response might imply higher plant nitrogen use efficiency at higher N rates, which has never been observed, or a higher $\text{N}_2:\text{N}_2\text{O}$ mole ratio at higher N application rates, which conflicts with our understanding of the microbiological basis for N_2O production (Senbayram et al. 2012). The remaining explanation is measurement errors arising from large variability in N_2O emissions both spatially and temporally. Were I to remove studies with negative Δ EFs the emission response to N rate would become even more nonlinear.

My findings agree in general with most prior work. Bouwman et al. (2002b) assumed an

exponential relationship between N₂O emissions and N input rates in their model, but the majority of their site-years had a single N application rate, and only a few had a zero-N control. My work explicitly tests the changes in EF for each experiment with multiple N inputs, arriving at the same general conclusion of a faster than linear N₂O emission increase but with quantitative and higher confidence outcome.

The model with all site-years but excluding N-fixers and the site with bare soil has a much narrower confidence interval compared to IPCC Tier 1 methodology (Figure 4.5). Philbert et al. (2012) show an improved CI for the range of nonlinear and linear models. When not accounting for parameter uncertainty, the lower boundary in Philbert et al. (2012) coincides with mine, while the upper boundary is more conservative than mine for N input levels > 150 kg N ha⁻¹. Parameter uncertainty widens the CI in Philbert et al. (2012) and brings my estimate entirely within for N input values up to 250 kg N ha⁻¹.

Kim et al. (2013) did not estimate the degree of EF nonlinearity in their dataset but provided a robust qualitative assessment of EF behavior that showed 6 linear, 18 exponential, and 2 hyperbolic responses out of 26 total studies. Using the same technique on the subset of my site-years with more than three nonzero N input rates yields 30 linear EF responses, 54 exponential, and 11 hyperbolic – in good agreement.

Hoben et al. (2011) provide a strong case for a faster than linear N₂O emission increase for U.S. Midwest maize crops with a model based on log-transformed values to make emissions more conservative. The model forms the basis for approved methodologies at American Carbon Registry (Millar et al. 2012) and Verified Carbon Standard (Millar et al. 2013):

$$Emis = 6.7(e^{0.0067 N} - 1)/N,$$

with best quadratic approximation of $Emis = (4.00 + 0.026 N)N$. The quadratic model I constructed based on Hoben et al. (2011) untransformed emissions has the form $Emis =$

$(4.36 + 0.025N)N$, where N is N input rate in kg N ha^{-1} , and $Emis$ is $\text{g N}_2\text{O-N ha}^{-1}$. A model based directly on Hoben et al. (2011) measurements is somewhat more nonlinear than a model for upland grain crops derived in this study: $Emis = (6.93 + 0.017N)N$. Models from Hoben et al. (2011) predict lower emissions than the model derived for the average of upland grain crop experiments in this paper for N input rates below 325 kg N ha^{-1} .

Regional budgets might be significantly altered by replacement of the constant IPCC 1% EF with N rate-dependent EF. In particular, this change would likely lower estimated emissions from regions predominantly fertilized at a low N rate, while increasing emissions from highly fertilized areas. This would be consistent with observations that global but not regional bottom-up estimates are consistent with top down estimates of N_2O emissions (del Grosso et al. 2008, Smith et al. 2012, Reay et al. 2012).

The nonlinearity of N_2O EFs means that the IPCC constant global 1% EF is inadequate to capture emission reductions due to lowered N fertilizer input in cases of high baseline N fertilization rates. In Figure 4.4 a I compare modeled estimates derived from measurements in Hoben et al. (2011), from the IPCC 1% EF, and from my ΔEF for upland grain crops for a 50 kg ha^{-1} reduction in N input at 3 baseline application rates: 200, 150, and 50 kg N ha^{-1} (Figure 4.4 b). When reducing from 200 to 150 kg N ha^{-1} the IPCC emission reduction estimate is $0.5 \text{ kg N}_2\text{O-N ha}^{-1}$, 30% below the $0.65 \text{ kg N}_2\text{O-N ha}^{-1}$ estimate for the other two models. For a reduction from 150 to 100 kg N ha^{-1} , all 3 models had about the same emission reduction estimate ($0.5\text{-}0.56 \text{ kg N}_2\text{O-N ha}^{-1}$). For a reduction from 50 kg N ha^{-1} to no fertilizer application, the IPCC model estimated an emission reduction of $0.5 \text{ kg N}_2\text{O-N ha}^{-1}$, whereas the Hoben et al. (2011) and upland grain crop models estimate reductions of 0.28 and $0.39 \text{ kg N}_2\text{O-N ha}^{-1}$, respectively.

When models are to be used to estimate the impact of N fertilizer reductions on N_2O

emissions (e.g. Millar et al. 2010), it will thus be especially important to avoid overestimating the impact of reductions where N is applied at rates close to crop N needs and, conversely, underestimating the impact of reductions where N is over-applied. This means that the largest mitigation gains are to be made where fertilizer N is applied in excess, such as many areas of China, and little mitigation will be gained where fertilizer N is in greatest need, such as many areas of Africa (Vitousek et al. 2009). Regional and global estimates of emissions are thus likely underestimating emission reductions due to lowered N application rates (see example above). This underestimation will not be balanced by overestimating reductions elsewhere, since economical N application reductions (with respect to yield) can only be made in fields where N is currently being applied in excess, so at higher N rates. ΔEF model predicts higher N_2O emission reductions than IPCC Tier 1 model for N applications above 90 kg N ha^{-1} , covering most land in need of N input reduction.

I believe my global default variable EF ($EF_0 + \Delta EF N$, Tier 1, Figure 4.3 a) can be used as a more biologically appropriate value for estimating direct N_2O emissions from agricultural cropland than the current IPCC 1% default. ΔEF s for particular crops and soil types where the dataset is sufficiently abundant can separately function as Tier 2 ΔEF s for these particular conditions (Figure 4.3). The use of one or more of these ΔEF s should improve the accuracy of national and regional inventories for direct N_2O emissions from fertilized agricultural land.

A significant shortcoming of this analysis is the few number of site-years with four or more nonzero N-input levels. With a sufficient number of fully-resolved N_2O response curves, I would be able to generalize the shape of the ΔEF function with higher confidence. More studies with five or more input levels are needed, especially for heavily fertilized crops such as maize and vegetables. Needed especially are additional studies in climate zones other than north temperate, in rice and upland grain crops, and with different fertilizer formulations and

application timings. Further knowledge of the factors and practices that affect N₂O emissions from agricultural soils are crucial for mitigating emissions of this important greenhouse gas (Venterea et al. 2012, Reay et al. 2012, Smith et al. 2012).

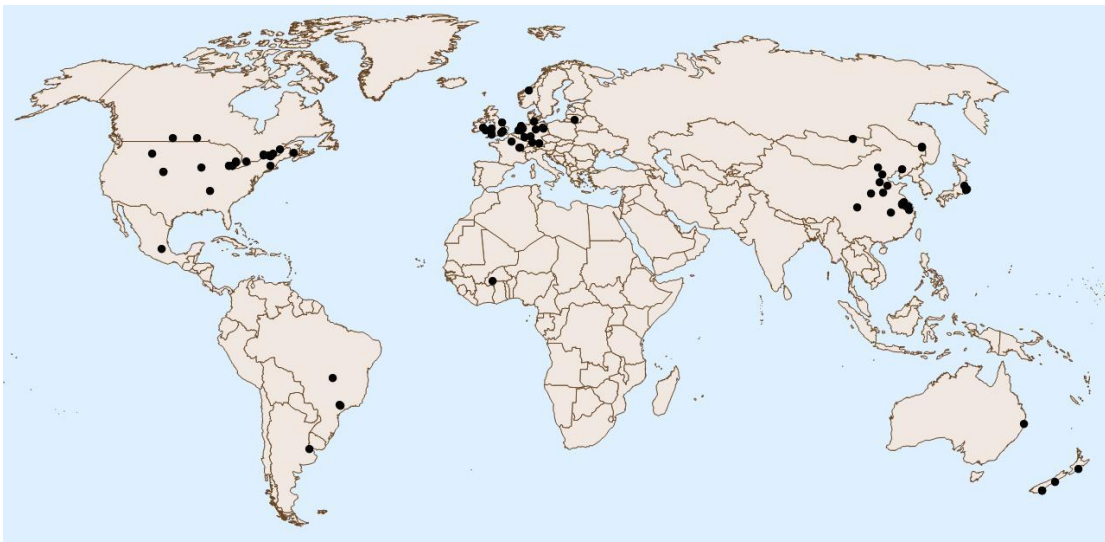


Figure 4.1. Locations for the studies included in the analysis.

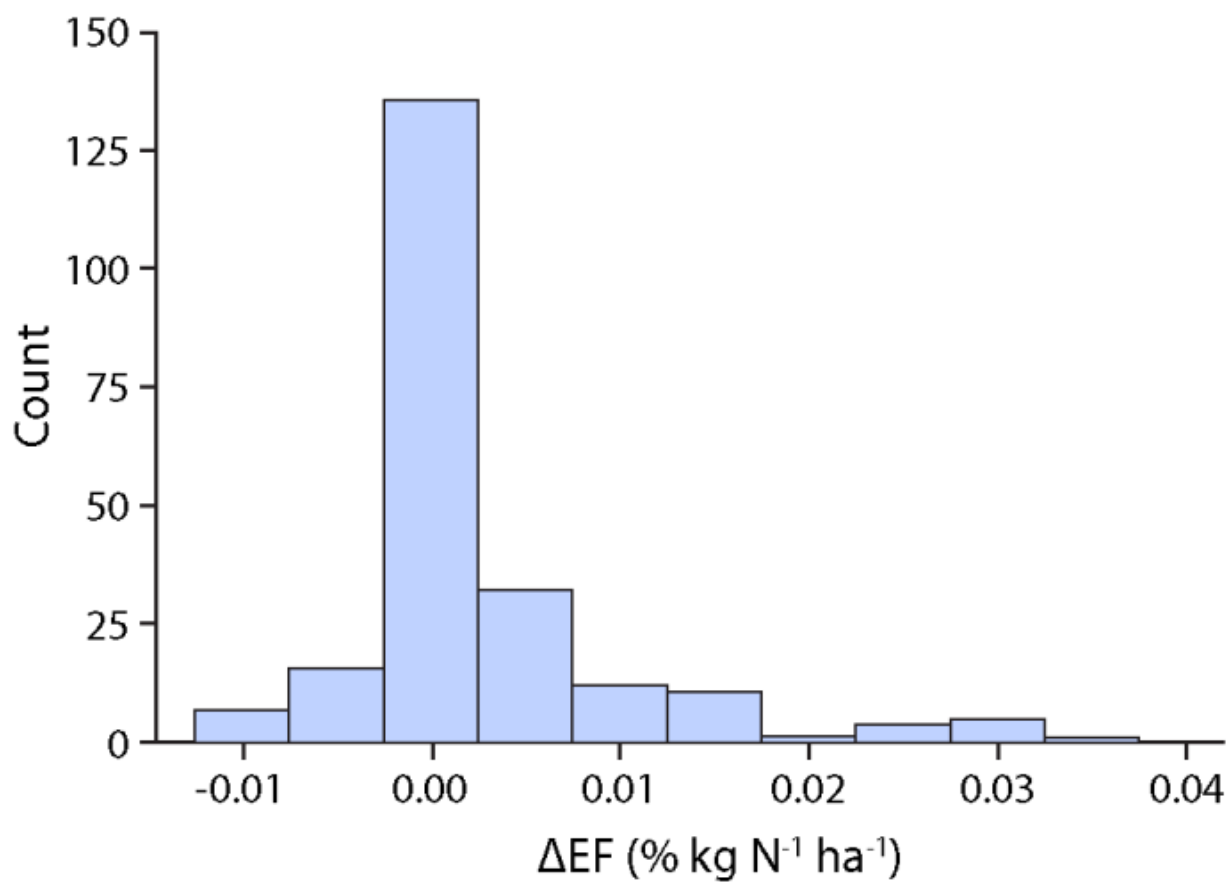


Figure 4.2. Histogram of emission factor change rates (ΔEF s) that indicate percentage of EF change per 1 additional kg N ha^{-1} of fertilizer input. Zero, positive, and negative ΔEF s indicate, respectively, a linear, faster-than-linear, and slower-than-linear rate of N_2O emissions increase with N input. ΔEF s < 0.02 are not shown for clarity.

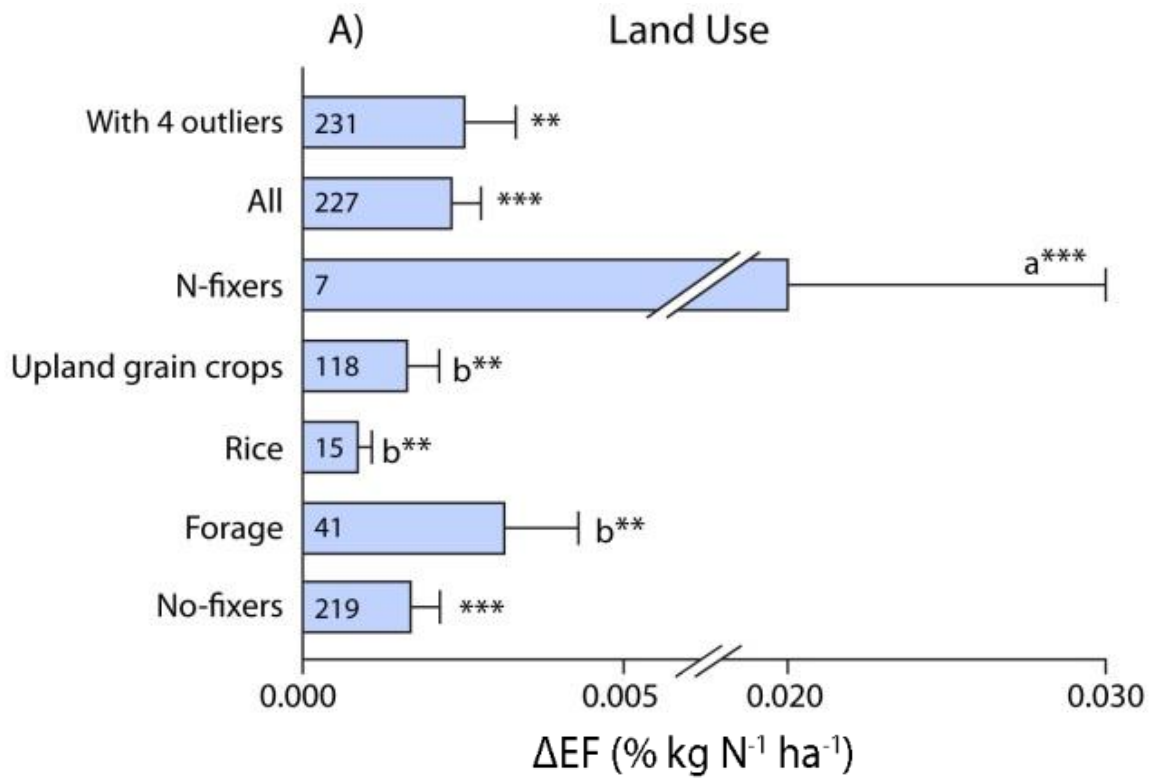
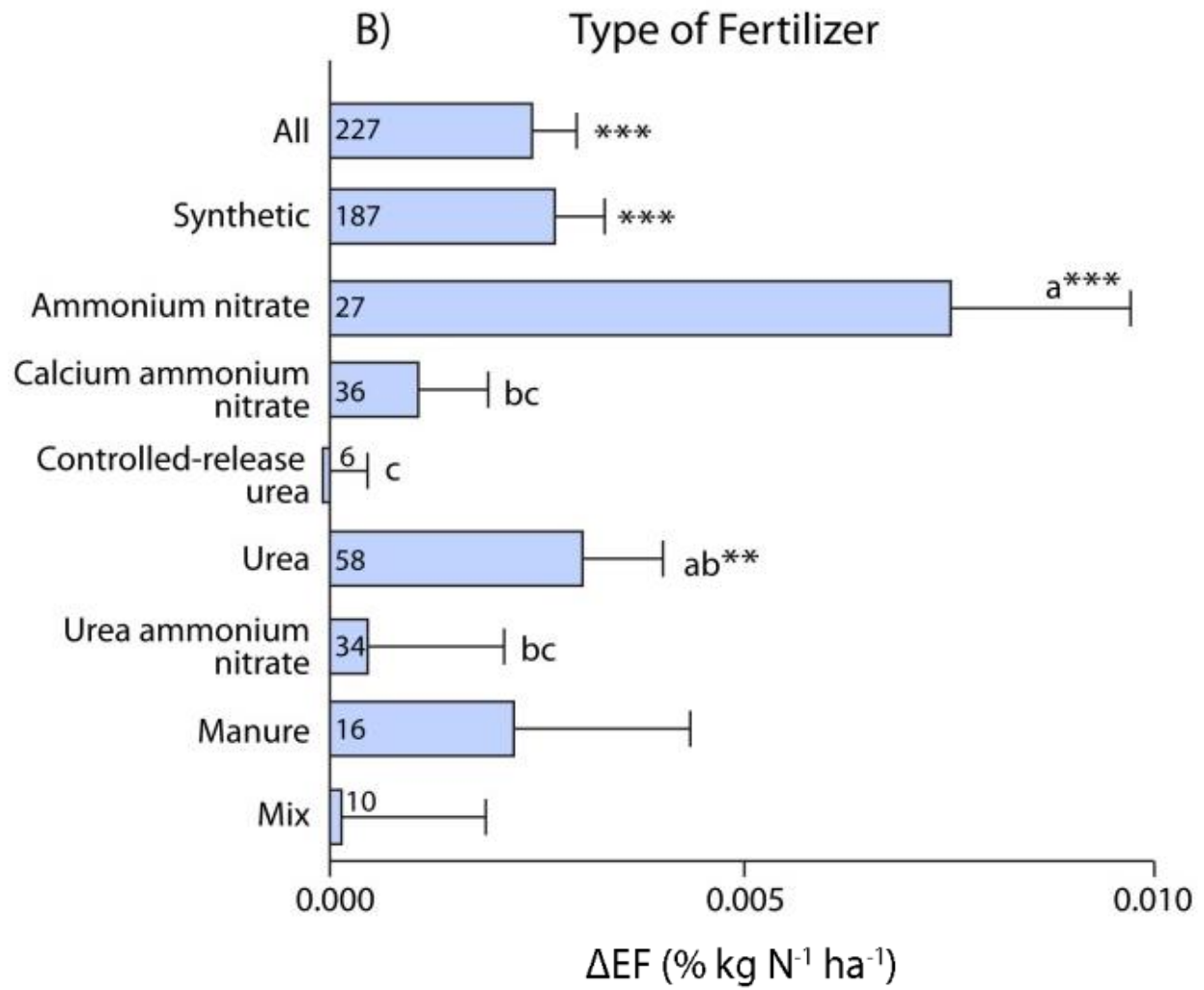


Figure 4.3. Mean Δ EF with standard errors by type of a) crop, b) fertilizer type, and c) other experimental factors. *, **, and *** indicate difference from 0 at $p=0.05$, 0.01 , and 0.001 , respectively. Different letters indicate significant differences between mean Δ EFs for groups of site-years by particular factor.

Figure 4.3. (Cont'd)



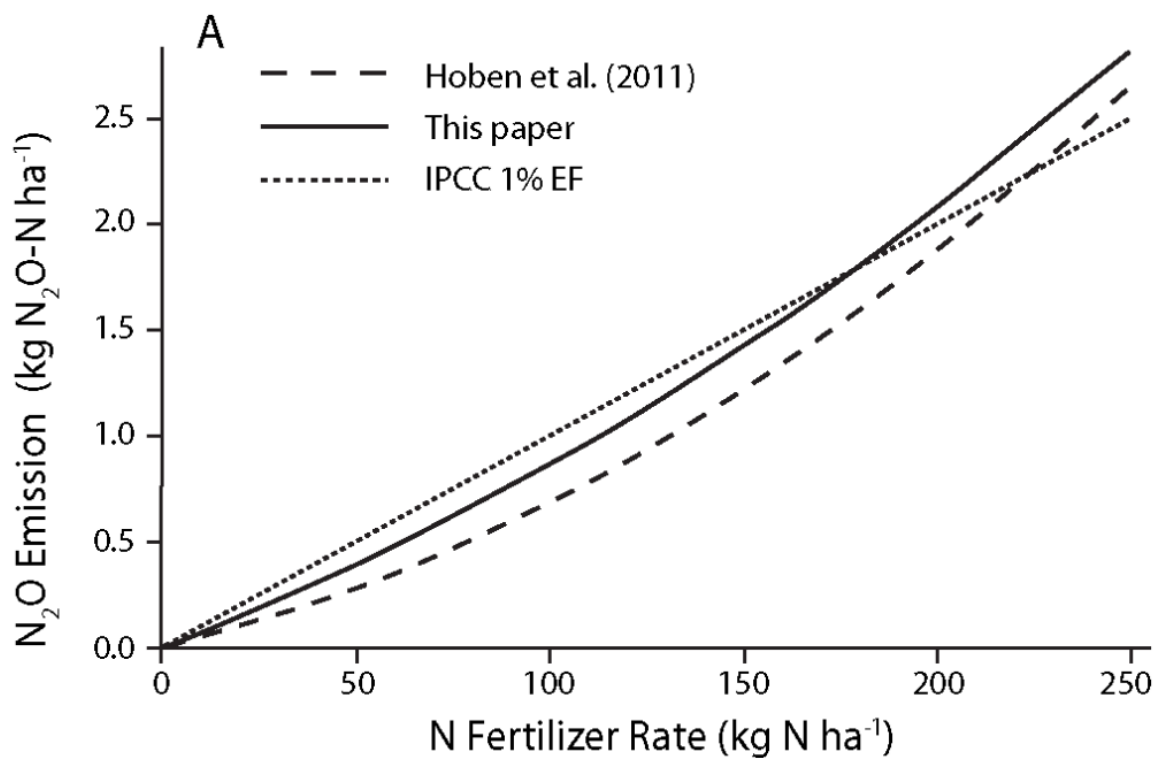
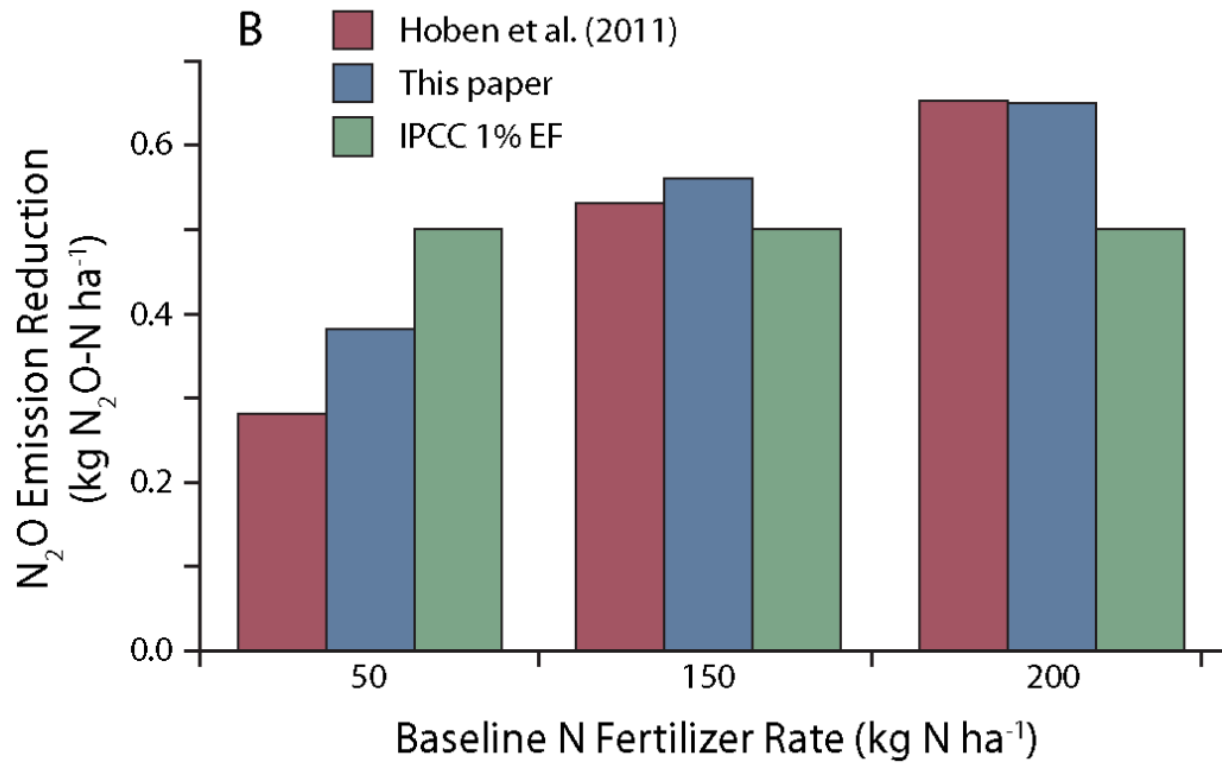


Figure 4.4. a) Comparison of IPCC 1% linear emission model, the Hoben et al. (2011) model, and a model of average upland grain crop emissions from the current meta-analysis; and b) Relative N₂O emission reductions for the three models when N application rates are reduced by 50 kg ha⁻¹ from three baseline N fertilization scenarios: 200, 150, and 50 kg N ha⁻¹.

Figure 4.4. (Cont'd)



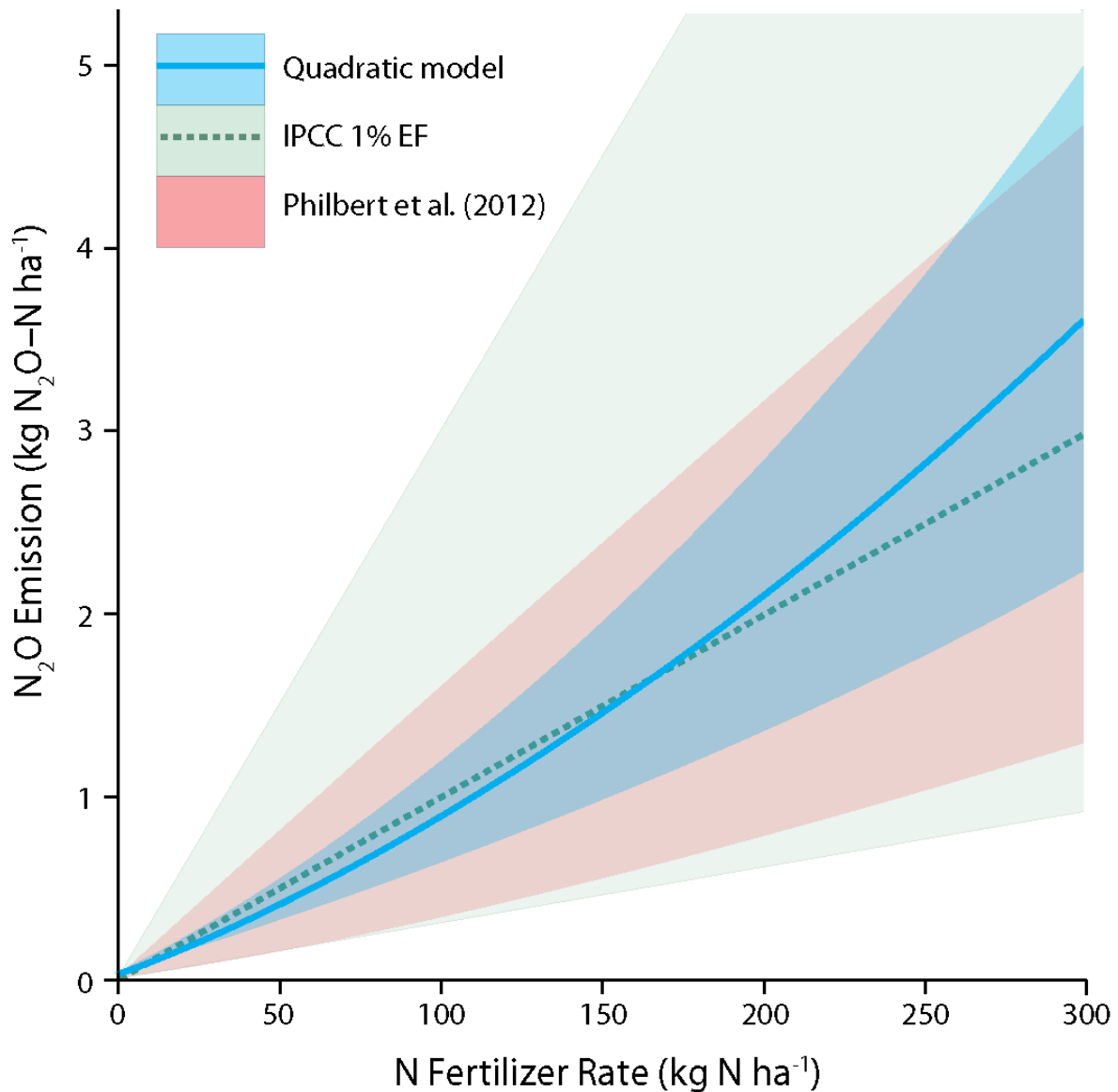


Figure 4.5. Comparison of uncertainties between IPCC Tier 1 (1%), and range of six models from Philbert et al. (2012) and mean quadratic model for all site years without N-fixing crops and the bare soil site. Each of the three models is presented with 95% CI range across 0-300 kg N ha⁻¹ fertilizer input. IPCC Tier 1 95% CI is 0.3-3%. Philbert et al. (2012) 95% CI for model uncertainty is included with and without parameter uncertainty.

REFERENCES

REFERENCES

- Benjamini, Y. and Y. Hochberg. 1995. Controlling the false discovery rate: a practical and powerful approach to multiple testing. *Journal of the Royal Statistical Society Series B-Methodological* 57:289-300.
- Bouwman, A. F. 1990. Exchange of greenhouse gases between terrestrial ecosystems and the 6 atmosphere. Pages 61-127 In *Soils and the greenhouse effect*. A. F. Bouwman, ed., John Wiley and Sons, Chichester, UK.
- Bouwman, A. F. 1996. Direct emission of nitrous oxide from agricultural soils. *Nutrient Cycling in Agroecosystems* 46:53-70.
- Bouwman, A. F., L. J. M. Boumans, and N. H. Batjes. 2002a. Emissions of N₂O and NO from fertilized fields: Summary of available measurement data. *Global Biogeochemical Cycles* 16:6.1-6.13.
- Bouwman, A. F., L. J. M. Boumans, and N. H. Batjes. 2002b. Modeling global annual N₂O and NO emissions from fertilized fields. *Global Biogeochemical Cycles* 16:28.1-28.8.
- Crutzen, P. J., A. R. Mosier, K. A. Smith, and W. Winiwarter. 2008. N₂O release from agro-biofuel production negates global warming reduction by replacing fossil fuels. *Atmospheric Chemistry and Physics* 8:389-395.
- Davidson, E. A. 2009. The contribution of manure and fertilizer nitrogen to atmospheric nitrous oxide since 1860. *Nature Geoscience* 2:659-662.
- de Klein C., R. S. A. Novoa, S. Ogle, K. A. Smith, P. Rochette, and T. C. Wirth, B. G. McConkey, A. Mosier, and K. Rypdal. 2006. In *IPCC guidelines for national greenhouse gas inventories. Volume 4. Agriculture, forestry and other land use*, eds Eggleston HS, Buendia L, Miwa K, Ngara T, Tanabe K (Institute for Global Environmental Strategies (IGES), Kanagawa, Japan), Vol on behalf of the Intergovernmental Panel on Climate Change (IPCC), pp 11.11-11.54.
- Eichner, M. J. 1990. Nitrous-oxide emissions from fertilized soils - summary of available data. *Journal of Environmental Quality* 19:272-280.
- Everitt, B. S. 1992. *The Analysis of Contingency Tables*. Chapman and Hall/CRC Press, London. 2nd edition.
- Grace, P. R., G. P. Robertson, N. Millar, M. Colunga-Garcia, B. Basso, S. H. Gage, and J. Hoben. 2011. The contribution of maize cropping in the Midwest USA to global warming: A

- regional estimate. *Agricultural Systems* 104:292-296.
- Griffis T.J., X. Lee, J. M. Baker, M. P. Russelle, X. Zhang, R. Venterea, D. B. Millet. 2013. Reconciling the differences between top-down and bottom-up estimates of nitrous oxide emissions for the US Corn Belt. *Global Biogeochemical Cycles* 27, doi:10.1002/gbc.20066.
- Halvorson, A. D., S. J. Del Grosso, and C. A. Reule. 2008. Nitrogen, tillage, and crop rotation effects on nitrous oxide emissions from irrigated cropping systems. *Journal of Environmental Quality* 37:1337-1344.
- Hoben, J. P., R. J. Gehl, N. Millar, P. R. Grace, and G. P. Robertson. 2011. Nonlinear nitrous oxide (N₂O) response to nitrogen fertilizer in on-farm corn crops of the US Midwest. *Global Change Biology* 17:1140-1152.
- IPCC Climate Change. 2007. In *The Physical Science Basis. Contribution of Working Group I to the Fourth Assessment Report of the Intergovernmental Panel on Climate Change*. ed Solomon S, D. Qin, M. Manning, Z. Chen, M. Marquis, K.B. Averyt, M. Tignor and H.L. Miller (eds.) (Intergovernmental Panel on Climate Change, Cambridge University Press, Cambridge, United Kingdom and New York, NY).
- Jungkunst, H. F., A. Freibauer, H. Neufeldt, and G. Bareth. 2006. Nitrous oxide emissions from agricultural land use in Germany - a synthesis of available annual field data. *Journal of Plant Nutrition and Soil Science-Zeitschrift Fur Pflanzenernahrung Und Bodenkunde* 169:341-351.
- Kim, D. G., G. Hernandez-Ramirez, and D. Giltrap. 2013. Linear and nonlinear dependency of direct nitrous oxide emissions on fertilizer nitrogen input: A meta-analysis. *Agriculture Ecosystems & Environment* 168:53-65.
- Lokupitiya, E. and K. Paustian. 2006. Agricultural soil greenhouse gas emissions: A review of National Inventory Methods. *Journal of Environ Quality* 35:1413-1427.
- Ma, B. L., T. Y. Wu, N. Tremblay, W. Deen, M. J. Morrison, N. B. McLaughlin, E. G. Gregorich, and G. Stewart. 2010. Nitrous oxide fluxes from corn fields: on-farm assessment of the amount and timing of nitrogen fertilizer. *Global Change Biology* 16:156-170.
- McSwiney, C. P. and G. P. Robertson. 2005. Nonlinear response of N₂O flux to incremental fertilizer addition in a continuous maize (*Zea mays* L.) cropping system. *Global Change Biology* 11:1712-1719.
- Millar, N., G. Robertson, P. Grace, R. Gehl, and J. Hoben. 2010. Nitrogen fertilizer management for nitrous oxide (N₂O) mitigation in intensive corn (Maize) production: an emissions reduction protocol for US Midwest agriculture. *Mitigation and Adaptation Strategies for Global Change* 15:185-204.

- Millar, N., G. P. Robertson, A. Diamant, R. J. Gehl, P. R. Grace, and J. P. Hoben. 2012. Methodology for Quantifying Nitrous Oxide (N₂O) Emissions Reductions by Reducing Nitrogen Fertilizer Use on Agricultural Crops. American Carbon Registry, Winrock International, Little Rock, Arkansas.
- Millar, N., G. P. Robertson, A. Diamant, R. J. Gehl, P. R. Grace, and J. P. Hoben. 2013. Quantifying N₂O emissions reductions in US agricultural crops through N fertilizer rate reduction. Verified Carbon Standard, Washington, DC, USA.
- Mosier, A., C. Kroeze, C. Nevison, O. Oenema, S. Seitzinger, and O. van Cleemput. 1998. Closing the global N₂O budget: nitrous oxide emissions through the agricultural nitrogen cycle - OECD/IPCC/IEA phase II development of IPCC guidelines for national greenhouse gas inventory methodology. *Nutrient Cycling in Agroecosystems* 52:225-248.
- Novoa, R. S. A. and H. R. Tejada. 2006. Evaluation of the N₂O emissions from N in plant residues as affected by environmental and management factors. *Nutrient Cycling in Agroecosystems* 75:29-46.
- Ravishankara, A. R., J. S. Daniel, and R. W. Portmann. 2009. Nitrous Oxide (N₂O): The Dominant Ozone-Depleting Substance Emitted in the 21st Century. *Science* 326:123-125.
- Reay, D. S., E. A. Davidson, K. A. Smith, P. Smith, J. M. Melillo, F. Dentener, and P. J. Crutzen. 2012. Global agriculture and nitrous oxide emissions. *Nature Climate Change* 2:410-416.
- Robertson, G.P. and P.M. Groffman. 2014. Nitrogen transformations. In *Soil Microbiology, Ecology and Biochemistry* ed. Paul EA (4th Ed. Academic Press, Burlington, MA). In press.
- Senbayram, M., R. Chen, A. Budai, L. Bakken, and K. Dittert. 2012. N₂O emission and the N₂O/(N₂O + N₂) product ratio of denitrification as controlled by available carbon substrates and nitrate concentrations. *Agriculture Ecosystems & Environment* 147:4-12.
- Signor, D., C. E. P. Cerri, and R. Conant. 2013. N₂O emissions due to nitrogen fertilizer applications in two regions of sugarcane cultivation in Brazil. *Environmental Research Letters* 8:015013.
- Smith, K. A., A. R. Mosier, P. J. Crutzen, and W. Winiwarter. 2012. The role of N₂O derived from crop-based biofuels, and from agriculture in general, in Earth's climate. *Philosophical Transactions of the Royal Society B: Biological Sciences* 367:1169-1174.
- Stehfest, E. and L. Bouwman. 2006. N₂O and NO emission from agricultural fields and soils under natural vegetation: summarizing available measurement data and modeling of global annual emissions. *Nutrient Cycling in Agroecosystems* 74:207-228.
- van Groenigen, J. W., G. L. Velthof, O. Oenema, K. J. Van Groenigen, and C. Van Kessel. 2010. Towards an agronomic assessment of N₂O emissions: a case study for arable crops.

European Journal of Soil Science 61:903-913.

Venterea, R. T., A. D. Halvorson, N. Kitchen, M. A. Liebig, M. A. Cavigelli, S. J. Del Grosso, P. P. Motavalli, K. A. Nelson, K. A. Spokas, B. P. Singh, C. E. Stewart, A. Ranaivoson, J. Strock, and H. Collins. 2012. Challenges and opportunities for mitigating nitrous oxide emissions from fertilized cropping systems. *Frontiers in Ecology and the Environment* 10:562-570.

Vitousek, P., R. Naylor, T. Crews, M.B. David, L.E. Drinkwater, E. Holland, P.J. Johnes, J. Katzenberger, L.A. Martinelli, P.A. Matson, G. Nziguheba, D. Ojima, C.A. Palm, G.P. Robertson, P.A. Sanchez, A.R. Townsend, and F.S. Zhang. 2009. Nutrient imbalances in agricultural development. *Science* 324:1519-1520.

APPENDICES

APPENDIX A

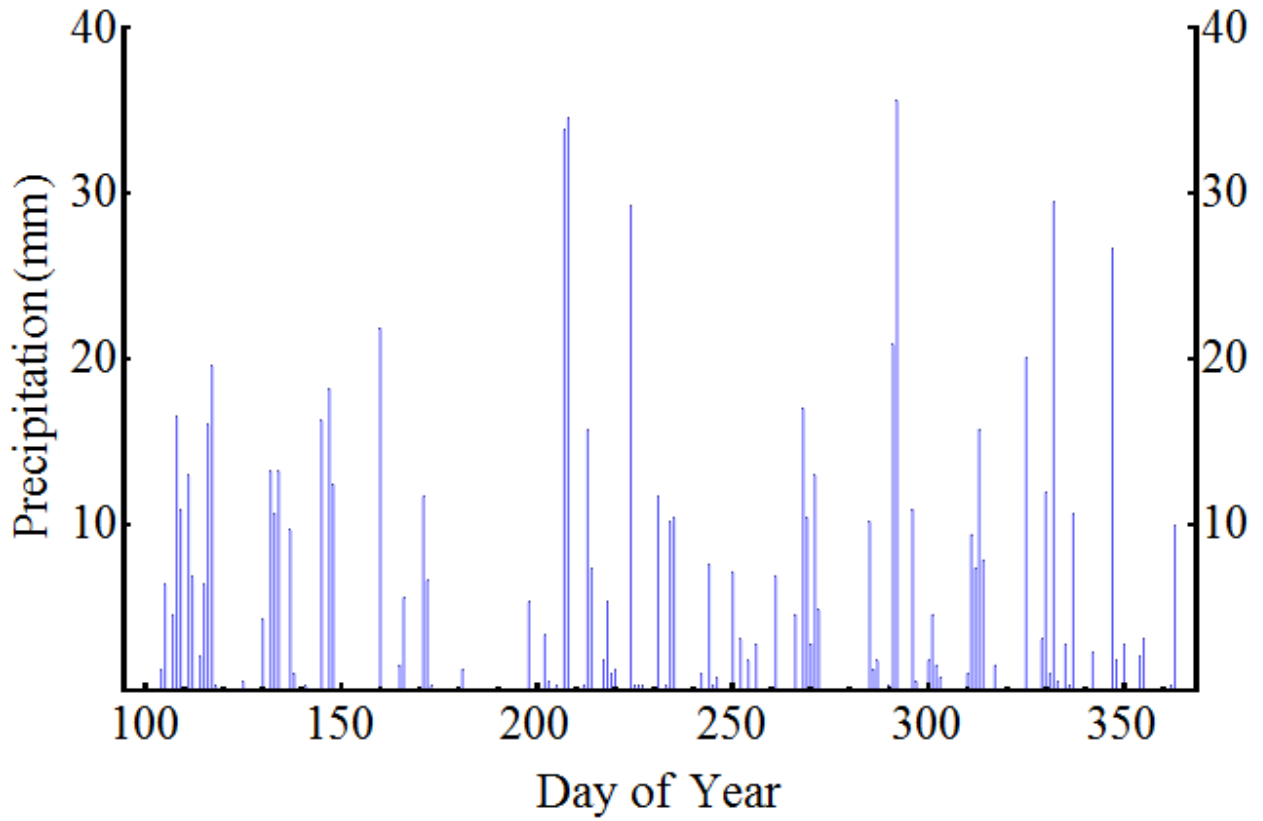


Figure A.1. Daily precipitation measured at Kellogg Biological Station Long-Term Ecological Research Site for 2011.

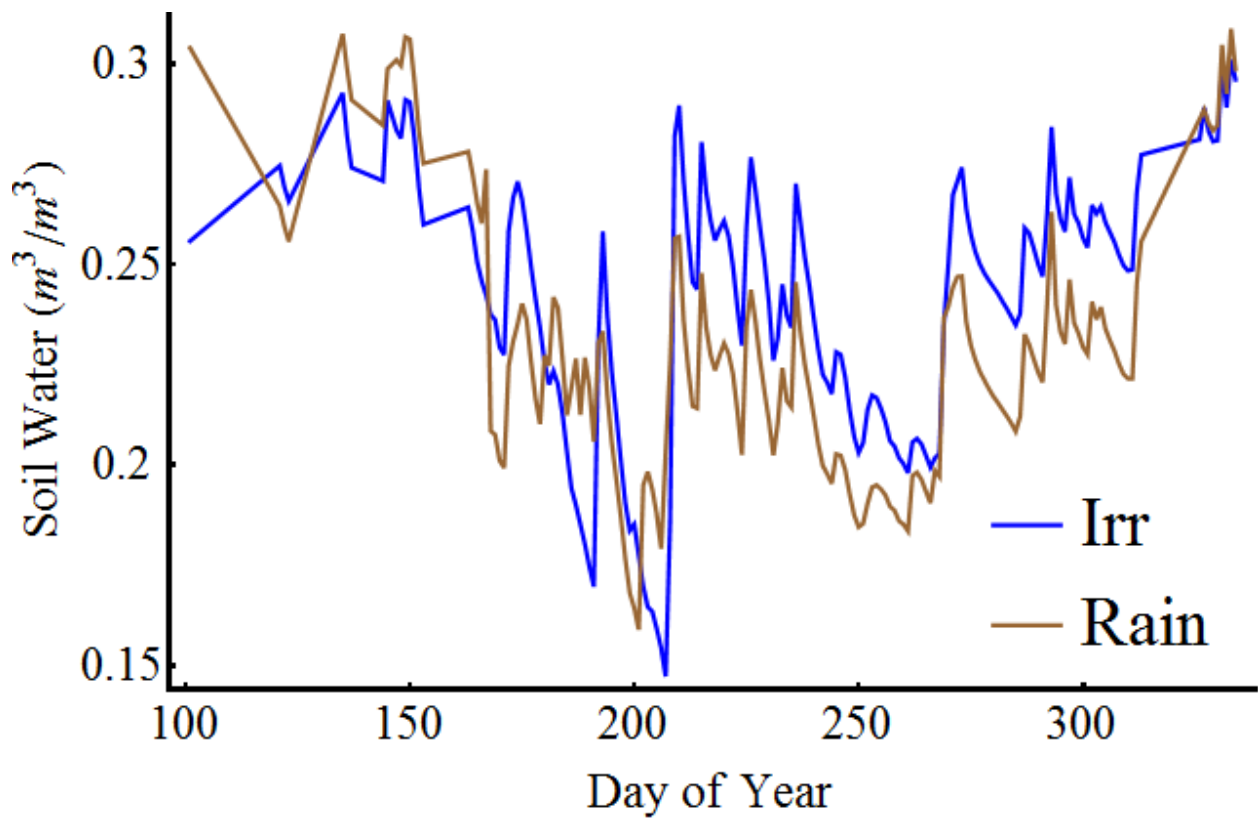


Figure A.2. Average daily soil moisture content for 0-25 depth in rainfed (Rain) and irrigated (Irr) treatments of N fertilizer gradient site for 2011.

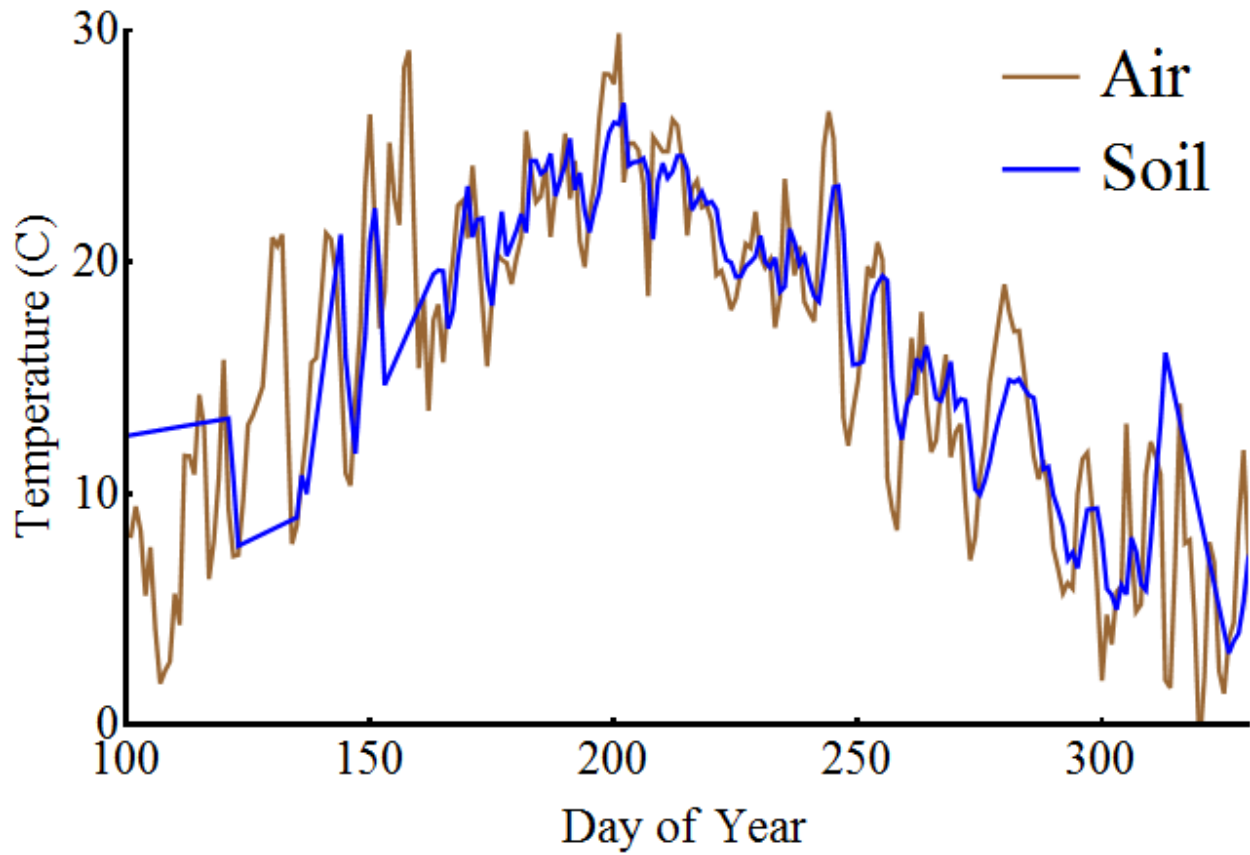


Figure A.3. Mean daily soil temperature at 10 cm depth (Soil) and air temperature (Air) and N fertilizer gradient site in 2011. Differences between rainfed and irrigated treatments are less than 1 °C.

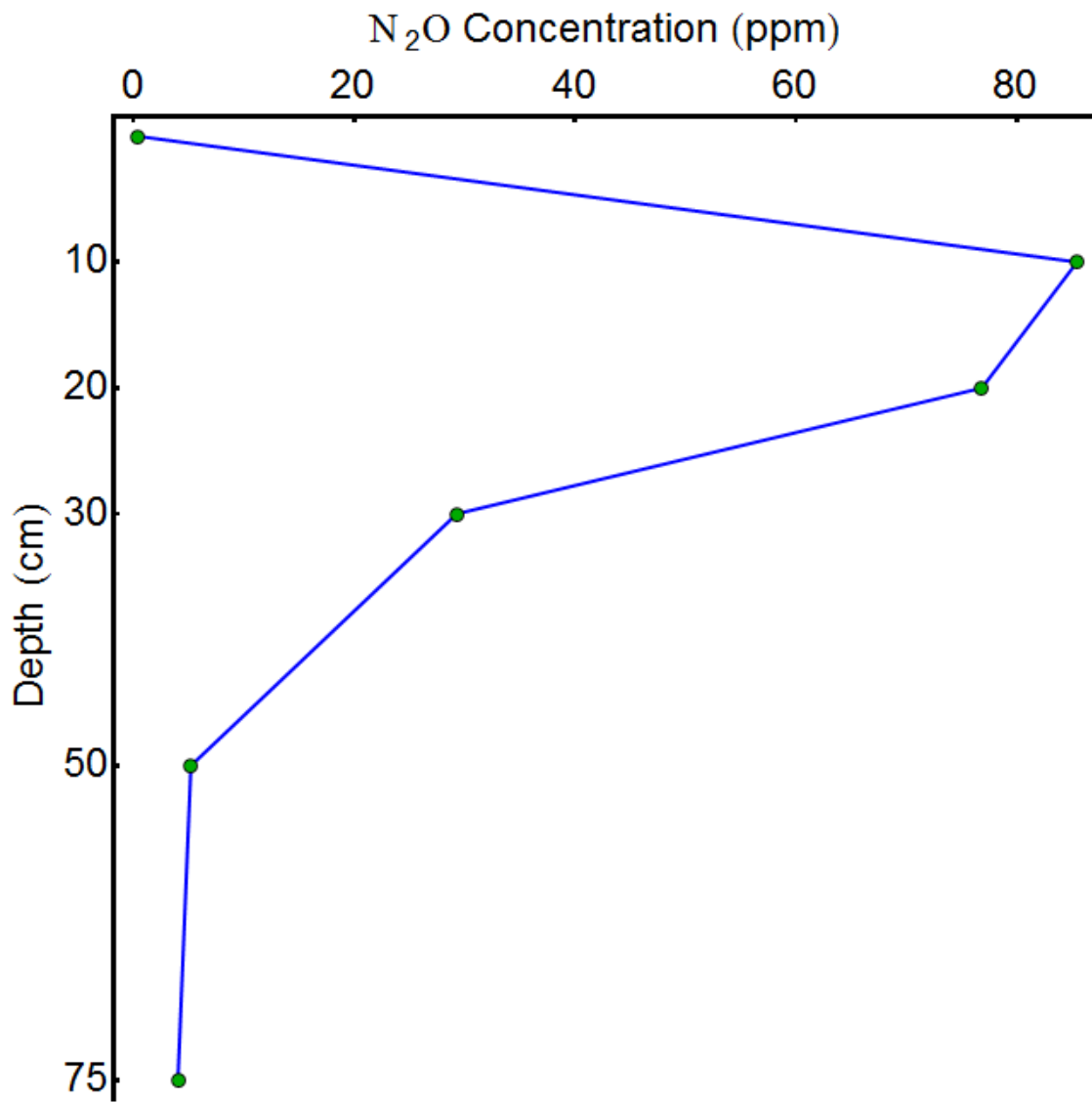


Figure A.4. N₂O concentration profile in Resource Gradient Experiment Irrigated treatment with 101 kg N ha⁻¹ input rate on DOY 172 in 2011.

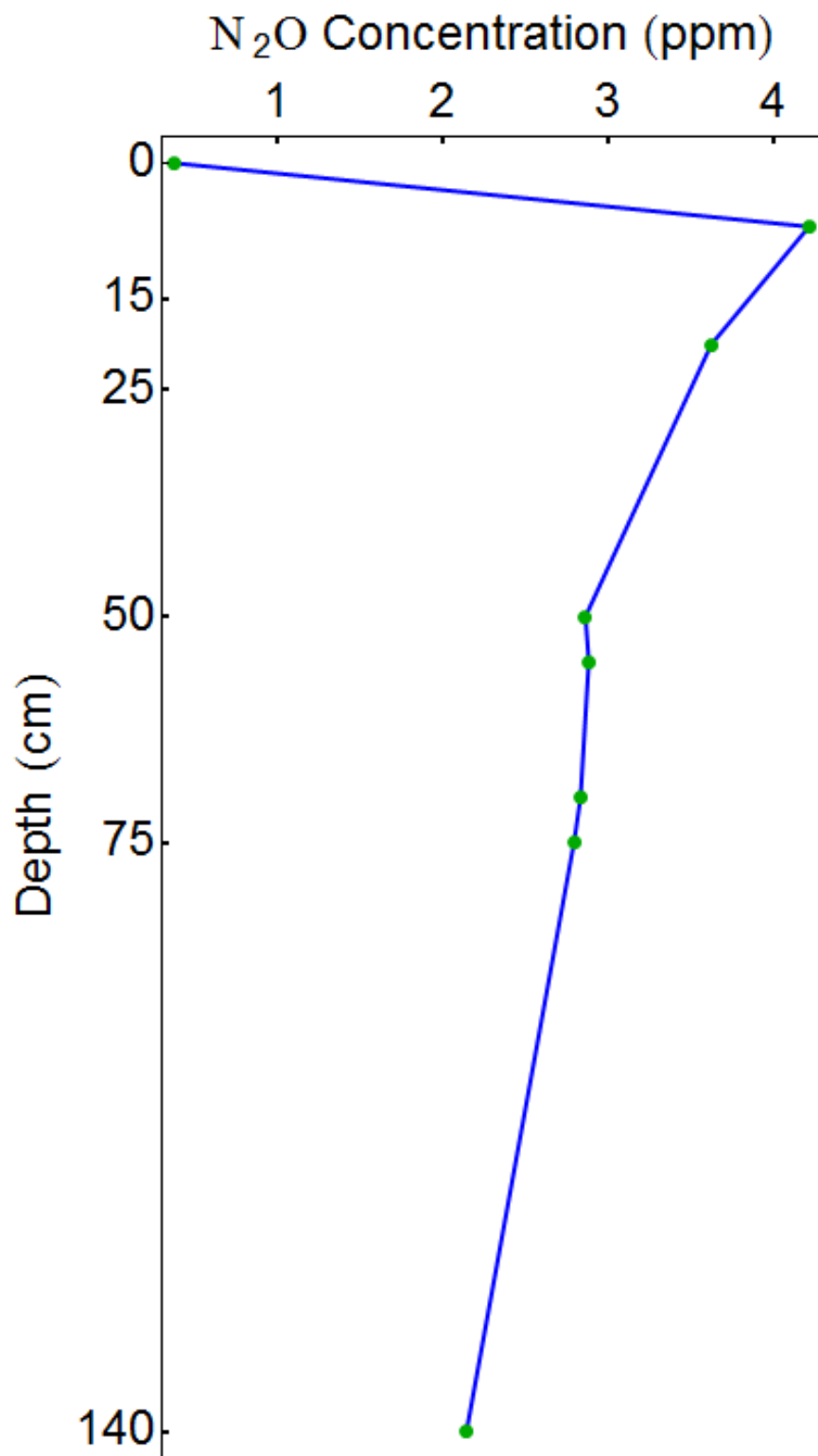


Figure A.5. N₂O concentration profile in Monolith Lysimeter Conventional Tillage treatment with in plot CT6 on DOY 66 in 2011.

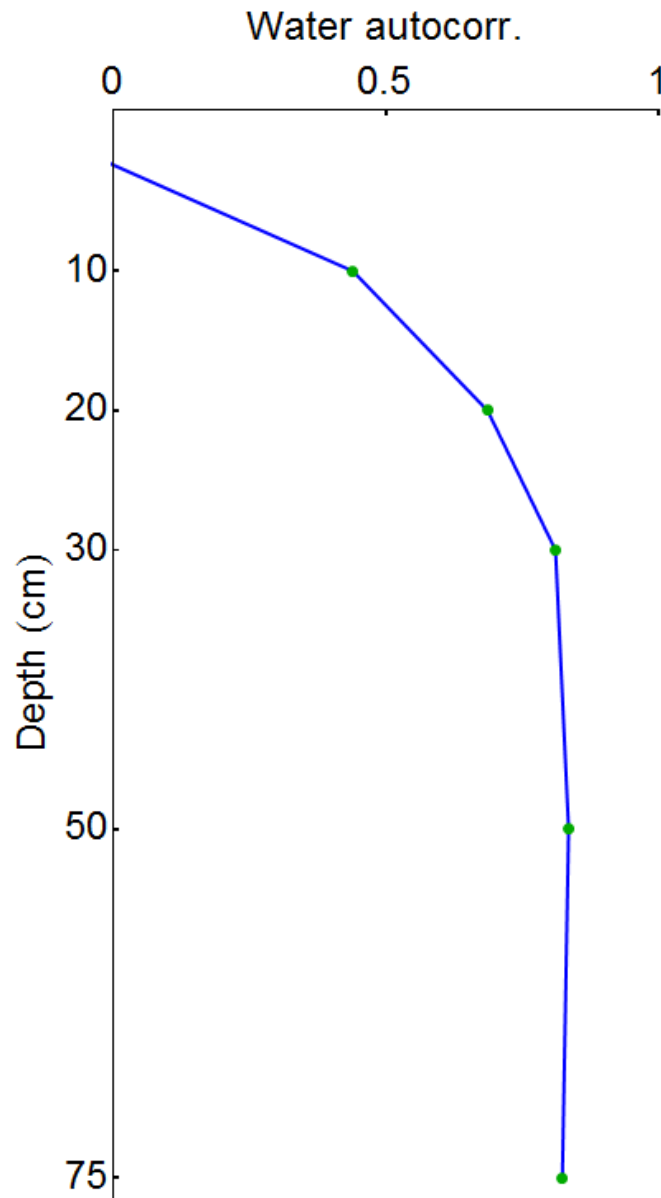


Figure A.6. Temporal autocorrelation with depth of modelled water content for days of N_2O concentration measurements in Monolith Lysimeter No Till treatment in plot CT6 in 2011.

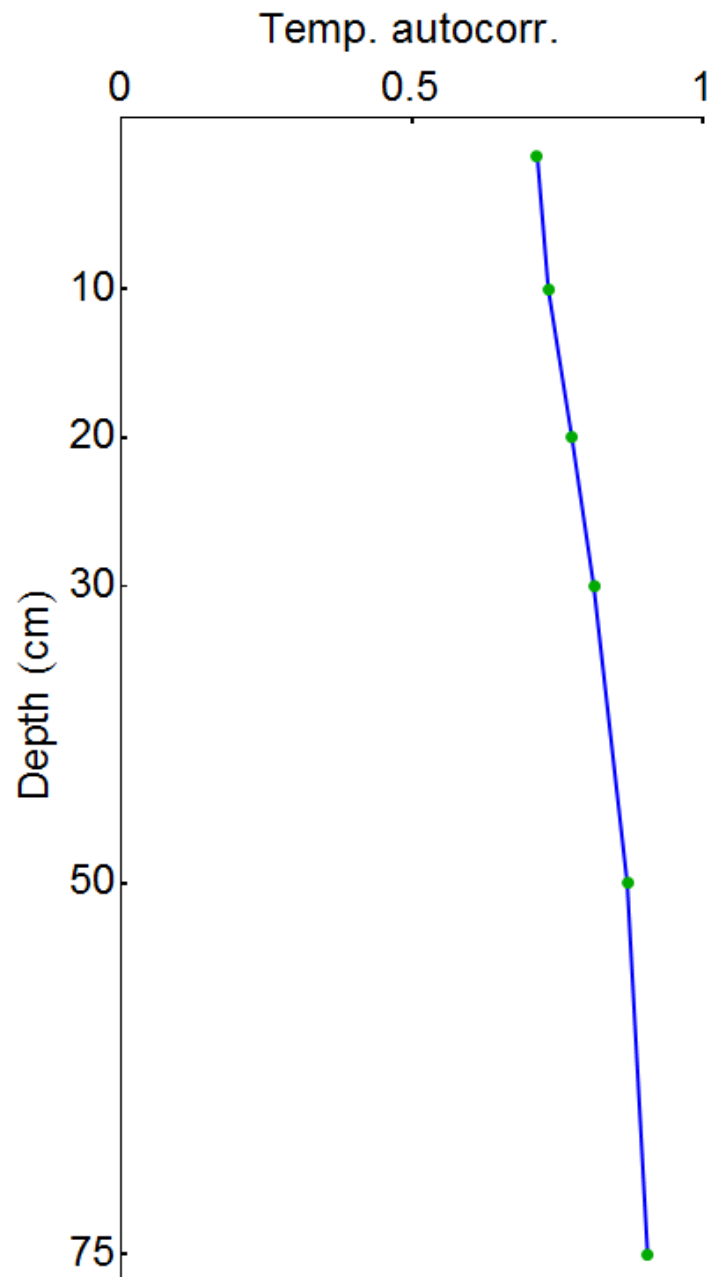


Figure A.7. Temporal autocorrelation with depth of modelled soil temperature for days of N₂O concentration measurements in Monolith Lysimeter No Till treatment in plot CT6 in 2011.

APPENDIX B

Table B.1. Mean and median ΔEF values for different site-year groups by various experimental and sampling factors with the respective standard errors.

Group	n	Mean	STE	Median	STE	p-value	Dif.
<i>Land Use</i>							
With outliers	231	0.0027	0.00085	0.0005	0.00017	0.0015	
All	227	0.0024	0.00054	0.0005	0.00017	0.0000	
No N fixers	219	0.0018	0.00048	0.0005	0.00016	0.0002	
N-fixers	7	0.0181	0.00498	0.0201	0.00964	0.0003	a
Bare Soil	1	0.0311					
Upland Grain Crops	118	0.0017	0.00056	0.0007	0.00027	0.0019	b
Rice	15	0.0009	0.00028	0.0007	0.00028	0.0012	b
Perennial Grasses	41	0.0033	0.00126	0.0003	0.00056	0.0079	b
<i>Fertilizer Type</i>							
Synthetic	187	0.0027	0.00060	0.0006	0.00019	0.0000	
Ammonium Nitrate (AN)	27	0.0075	0.00217	0.0020	0.00339	0.0005	a
Calcium Ammonium Nitrate (CAN)	36	0.0011	0.00084	0.0010	0.00049	0.2052	bc
Controlled-Release Urea (CRU)	6	0.0001	0.00045	0.0002	0.00058	0.8512	c
Urea	58	0.0030	0.00097	0.0005	0.00022	0.0017	ab
Urea Ammonium Nitrate (UAN)	34	0.0005	0.00165	0.0003	0.00054	0.7817	bc
Manure	16	0.0022	0.00213	0.0000	0.00104	0.2932	
Mixed Fertilizer	10	0.0001	0.00174	0.0004	0.00083	0.9361	
<i>Soil Carbon (%)</i>							
≤ 1.5	64	0.0006	0.00087	0.0003	0.00022	0.4730	
> 1.5	100	0.0033	0.00088	0.0006	0.00042	0.0001	
<i>Precipitation (mm)</i>							
≤ 700	58	0.0029	0.00096	0.0009	0.00042	0.0024	
> 700	63	0.0030	0.00102	0.0003	0.00021	0.0030	
<i>Mean Annual Temperature ($^{\circ}C$)</i>							
≤ 10	54	0.0027	0.00102	0.0011	0.00044	0.0093	
> 10	51	0.0008	0.00060	0.0001	0.00019	0.1881	
<i>pH</i>							
Acidic	91	0.0039	0.00110	0.0005	0.00032	0.0004	a
Basic	51	0.0005	0.00027	0.0004	0.00030	0.0521	b

Table B.1. (cont'd)

Group	n	Mean	STE	Median	STE	p-value	Dif.
<i>Fertilizer Application</i>							
One-Time	55	0.0052	0.00136	0.0009	0.00037	0.0001	
Split	90	0.0019	0.00066	0.0004	0.00014	0.0036	
<i>Total Number of Measurements</i>							
≤30	92	0.0034	0.00098	0.0009	0.00034	0.0004	
>30	104	0.0018	0.00075	0.0004	0.00019	0.0136	
<i>Chamber area (m²)</i>							
≤0.2	115	0.0042	0.00079	0.0011	0.00037	0.0000	a
>0.2	95	0.0008	0.00075	0.0003	0.00020	0.2834	b
<i>Number of Measurements per Sample</i>							
≤3	110	0.0030	0.00084	0.0007	0.00029	0.0003	
>3	98	0.0022	0.00073	0.0005	0.00019	0.0027	
<i>Duration of the Experiment (days)</i>							
≤200	110	0.0023	0.00071	0.0007	0.00025	0.0012	
>200	104	0.0029	0.00087	0.0005	0.00027	0.0009	
<i>Number of Replicates</i>							
≤3	110	0.0018	0.00084	0.0004	0.00019	0.0300	
>3	107	0.0034	0.00069	0.0009	0.00028	0.0001	
<i>Lowest N input level above control (kg ha⁻¹)</i>							
≤100	139	0.0034	0.00084			0.0001	a
>100	88	0.0009	0.00036			0.0102	b

Table B.2 a. T-test results for paired differences between mean ΔEF groups by crop

	N-fixers	Upland Grain Crops	Rice	Perennial Grasses
N-fixers	1	0.001	0.000	0.004
Upland Grain Crops		1	0.193	0.231
Rice			1	0.057
Perennial Grasses				1

Table B.2 b. T-test results for paired differences between mean ΔEF groups by N fertilizer type

	Syn	AN	CAN	CRF	Urea	UAN
Syn		0.038	0.095	0.000	0.833	0.182
AN	0.038		0.006	0.001	0.062	0.010
CAN	0.095	0.006		0.228	0.124	0.740
CRF	0.000	0.001	0.228		0.003	0.752
Urea	0.833	0.062	0.124	0.003		0.176
UAN	0.182	0.010	0.740	0.752	0.176	

Table B.2 c. T-test results for paired differences between mean Δ EF groups by experimental factors

Groups of Experiments Tested	p-value
Soil Carbon ($\leq 1.5\%$ vs. $> 1.5\%$)	0.029
Annual Precipitation (≤ 700 mm vs. > 700 mm)	0.931
Mean Annual Temperature (≤ 10 °C vs. > 10 °C)	0.115
pH (Acidic vs. Basic)	0.003
N Applications (One-Time vs. Split)	0.027
Lowest N input level above control (≤ 100 kg ha ⁻¹ vs. > 100 kg ha ⁻¹)	0.007

Table B.2 d. T-test results for paired differences between mean Δ EF groups by sampling factors

Groups of Experiments Tested	p-value
Number of Measurements (≤ 30 vs. > 30)	0.196
Chamber Area (≤ 0.2 m ² vs. > 0.2 m ²)	0.008
Number of Measurements per Sample (≤ 3 vs. > 3)	0.451
Total Duration of Experiment (≤ 200 days vs. > 200 days)	0.594
Number of Replicates (≤ 3 vs. > 3)	0.149

Table B.3 a. Experimental factor associations in contingency tables

Experimental Factors	P	T	C	pH	N App
Annual Precipitation (P)		0.027	0.329	-0.308	-0.063
Mean Annual Temperature (T)	105		-0.585	0.437	0.184
Soil Carbon (C)	81	73		-0.362	-0.021
pH	73	66	140		0.078
Number of Fertilizer Applications (N App)	77	62	120	109	

Table B.3 b. Sampling factor associations in contingency tables

Sampling Factors	Mea	Area	MpS	D	Rep
Measurements (Meas)		0.294	-0.188	0.439	-0.194
Chamber Area (Area)	184		0.151	0.110	-0.554
Measurements per Sample (MpS)	180	198		-0.269	0.013
Duration (D)	189	198	196		0.005
Number of Replicates (Rep)	188	204	205	205	

Table B.4. Locations for the studies included in the analysis.

Reference	Country	Location	Coordinates	
Abdalla et al. 2010	Ireland	Carlow	52.85°N	6.91°W
Allen et al. 2010	Australia	Jacobs Well, Brisbane	27.72°S	153.27°E
Anger et al. 2003	Germany	Daun	50.19°N	6.82°E
Augustin et al. 1999	Germany	Paulinenaue	52.77°N	12.77°E
Balezientiene and Kusta 2012	Lithuania	Kaunas	54.87°N	23.83°E
Breitenbeck and Bremner 1986	USA	Ames, Iowa	41.95°N	93.71°W
Brummer et al. 2008	Burkina Faso	Dano, Ioba	11.16°N	3.08°W
Cai et al. 1997	China	Nanjing, Jiangsu	32.04°N	118.87°E
Cardenas et al. 2010	UK	Aberystwyth, Wales	52.43°N	4.02°W
		Devon	50.77°N	3.90°W
		North Yorkshire	54.11°N	0.67°W
Chang et al. 1998	Canada	Lethbridge	49.70°N	112.75°E
Cheng et al. 2002	Japan	Tsukuba	36.02°N	140.12°E
Chiaradia et al. 2009	Brazil	Capivari, San Paolo	22.93°S	47.57°W
Ciampitti et al. 2005	Brazil	Buenos Aires	34.60°S	58.48°W
Ding et al. 2007	China	Henan	35.00°N	114.40°E
Dong et al. 2005	China	Dianzi, Yucheng	36.95°N	116.63°E
Dusenbury et al. 2008	USA	Bozeman, Montana	45.67°N	111.15°W
Fernandez-Luqueno et al. 2009	Mexico	Otumba, State of Mexico	19.70°N	98.81°W
Gagnon et al. 2011	Canada	Quebec City, Quebec	46.78°N	71.13°W
Gao et al. 2013	Canada	Carberry, Manitoba	49.90°N	99.35°W
Halvorson et al. 2008	USA	Fort Collins, Colorado	40.73°N	104.98°W
Hansen et al. 1993	Norway	Surnadal	63.00°N	8.88°E
Harrison et al. 1995	UK	Harpenden	51.81°N	0.36°W
Henault et al. 1998	France	Chalons, Champagne	48.95°N	2.42°E
		Messigny, Champagne	47.46°N	4.95°E
		Longchamp, Champagne	47.27°N	5.30°E
Hoben et al. 2011	USA	Fairgrove, Michigan	43.52°N	83.64°W
		Hickory Corners, Michigan	42.41°N	85.37°W
		Reese, Michigan	43.45°N	83.65°W
		Mason, Michigan	42.47°N	84.27°W
		Stockbridge, Michigan	42.48°N	84.27°W
Hoffman et al. 2001	Germany	Rengen, Eifel		
		Kleve, Niederrhein		
		Heubach, Munsterland		

Table B.4. (cont'd)

Reference	Country	Location	Coordinates	
Hoogendoorn et al. 2008	New Zealand	Ballantrae, North Island	40.00°S	176.70°E
		Invermay, South Island	46.00°S	170.40°E
Huang et al. 2005	China	Jian Xing, Zhejiang		
Hyde et al. 2006	Ireland	Johnstown Castle, Co.Wexford	52.00°N	6.00°W
Iqbal 2009	China	Zhejiang	30.50°N	120.40°E
Izaurrealde et al. 2004	Canada	Swift Current, Saskatchewan	50.00°N	107.00°W
Ji et al. 2012	China	Jurong, Jiangsu	31.97°N	119.30°E
Kaiser et al. 1998	Germany	Brunswick	52.27°N	10.53°E
Kammann et al. 1998	Germany	Giessen	50.53°N	8.72°E
Kavdir et al. 2008	Germany	Potsdam	52.44°N	13.00°E
Kern et al. 2008	Germany	Potsdam	52.44°N	13.00°E
Khan et al. 2010	New Zealand	Lincoln, Canterbury, South Island	43.64°S	172.50°E
Lampe et al. 2004	Germany	Kiel	54.32°N	10.12°E
Lessard et al. 1996	Canada	Ottawa, Ontario	45.36°N	75.72°W
Letica et al. 2010	New Zealand	Invermay, Otago, South Island	45.86°S	170.40°E
Li et al. 2002	Japan	Matsudo	35.78°N	139.90°E
Lin et al. 2011	China	Heshengqiao, Xianning, Hubei	29.63°N	114.60°E
Liu et al. 2004	China	Beijing	39.95°N	116.30°E
Liu et al. 2005	USA	Fort Collins, Colorado	40.65°N	104.98°W
Liu et al. 2012	China	Yongji, Shanxi	34.93°N	110.72°E
Lou et al. 2012	China	Shenyang	41.52°N	123.40°E
Ma et al. 2007	China	Dapu, Yixing, Jiangsu	31.28°N	119.90°E
Ma et al. 2010	Canada	Guelph, Ontario	43.57°N	80.42°W
		Ottawa, Ontario	45.30°N	75.72°W
		Saint-Valentin, Quebec	45.10°N	73.35°W
MacKenzie et al. 1997	Canada	Ormstown, Quebec	45.13°N	74.00°W
		Sainte-Rosalie, Quebec	45.64°N	72.90°W
MacKenzie et al. 1998	Canada	Ormstown, Quebec	45.13°N	74.00°W
McKenney et al. 1980		Harrow		
McSwiney and Robertson 2005	USA	Hickory Corners, Michigan	42.40°N	85.40°W

Table B.4. (cont'd)

Reference	Country	Location	Coordinates	
Mori and Hojito 2011	Japan	Nasu	36.90°N	139.90°E
Mosier et al. 2006	USA	Fort Collins, Colorado	40.65°N	104.98°W
Pelster et al. 2011	Canada	L'Acadie, Quebec	45.30°N	73.35°W
Pennock and Corre 2001	Canada	southern Saskatchewan		
Pfab et al. 2011	Germany	Stuttgart	48.75°N	9.18°E
		Luancheng, North		
Qin et al. 2012	China	China Plain	37.90°N	114.67°E
Ruser et al. 2001	Germany	Munich	48.50°N	11.35°E
Ryden 1983	UK	Bracknell, Berkshire	51.42°N	0.75°W
Schils et al. 2008	Netherlands	Wageningen	51.95°N	5.66°E
Signor et al. 2013	Brazil	Piracicaba, San Paulo	22.73°S	47.65°W
		Goianesia, Goias	15.33°S	49.12°W
Situala et al. 1995				
Song and Zhang 2009	China	Sanjiang Plain	47.60°N	133.50°E
Thornton and Valente 1996	USA	Jackson, Tennessee	35.62°N	88.80°W
van Groenigen et al. 2004	Netherlands	Wageningen	51.95°N	5.66°E
		Leeuwarden	53.20°N	5.80°E
Velthof et al. 1996	Netherlands	Heino	52.43°N	6.23°E
		Lelystad	52.52°N	5.47°E
		Zegveld	52.12°N	4.83°E
Velthof et al. 1997	Netherlands	Bennekom	52.00°N	5.67°E
Velthof and Mosquera 2011	Netherlands	Wageningen	51.95°N	5.66°E
		Harvard Forest,		
Venterea et al. 2003	USA	Massachusetts	42.50°N	72.67°W
Wang et al. 2011	China	Nanjing, Jiangsu	31.90°N	118.80°E
Xiang et al. 2007	China	Yanting, Sichuan	31.27°N	105.45°E
Yao et al. 2012	China	Yangtze River Delta	32.60°N	119.70°E
		Fredericton, New		
Zebarth et al. 2008	Canada	Brunswick	45.90°N	66.50°W
Zhang et al. 2007	China	Sanjiang Plain	47.35°N	133.31°E
		Duolun County, Inner		
Zhang and Han 2008	China	Mongolia	42.00°N	116.20°E
		Taihu Lake, Yangtze		
Zhao et al. 2009	China	River Delta	31.32°N	120.42°E
Zhou et al. 2013	China	Sichuan Basin	31.16°N	105.28°E
Zou et al. 2005	China	Nanjing, Jiangsu	32.00°N	118.80°E

Table B.5. Variables collected in Dataset S2

Name of Variable	Unit
Reference	-
Location	-
Coordinates (latitude and Longitude)	°
Precipitation	mm y ⁻¹
Mean Annual Temperature	°C
Texture Class	-
Soil Classification	-
Texture (Sand, Silt, and Clay content)	%
Soil Organic Carbon (SOC)	%
Soil Organic Nitrogen (SON)	%
Bulk Density (BD)	g cm ⁻³
pH	-
Crop	-
Management	-
Total Number of Measurements	-
Method (Static, Automatic)	-
Chamber Area	m ²
Number of Measurements per Sample	-
Year	-
Duration	d
Number of Replicates	-
Fertilizer Type	-
Mode of Fertilizer Application	-
Number of Fertilizer Applications	-
Min nonzero nitrogen (N) rate	kg N ha ⁻¹
Max N rate	kg N ha ⁻¹
N rate	kg N ha ⁻¹
Total N ₂ O Emission	kg N ₂ O-N ha ⁻¹
Standard Error of N ₂ O Emission	kg N ₂ O-N ha ⁻¹
Emission Factor (EF)	%
Emission Factor Change Rate (ΔEF)	% kg N ⁻¹ ha
Remarks	-

APPENDIX C

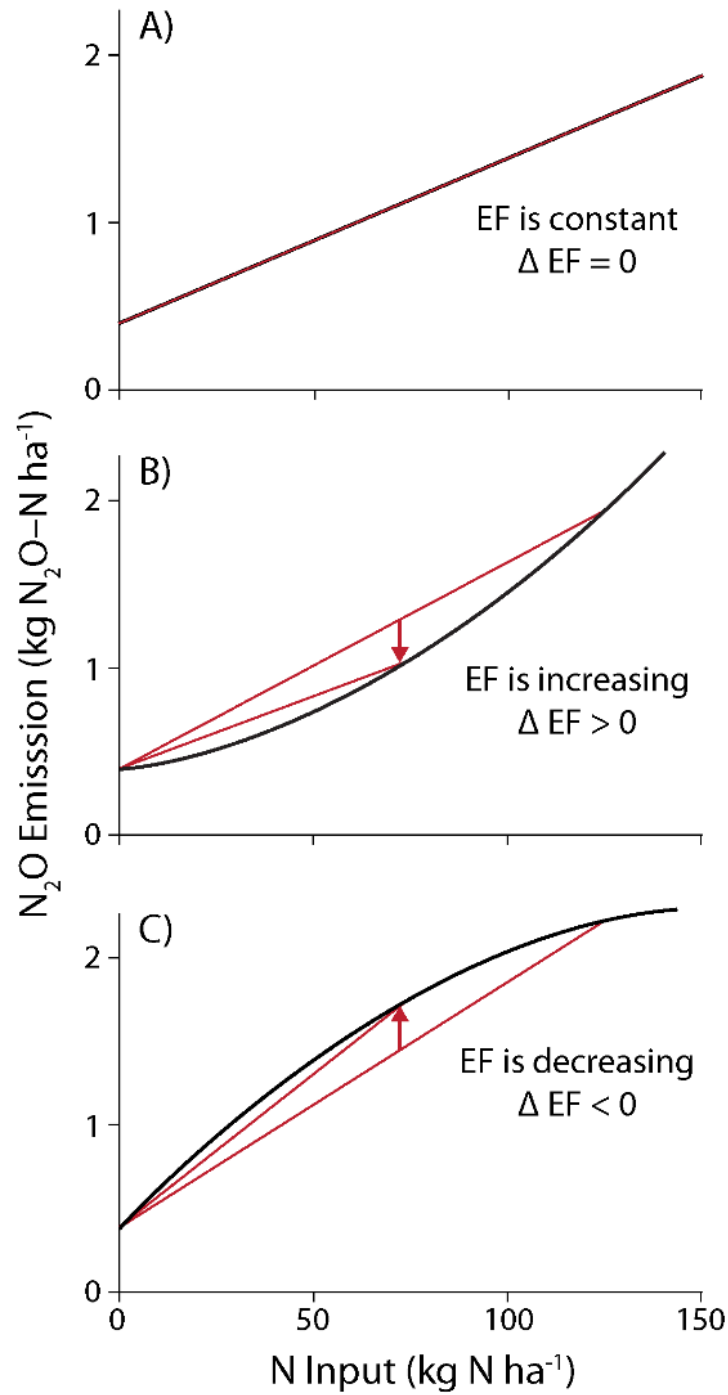


Figure C.1. Effect of nitrogen (N) input rate on the total N₂O emissions and emission factors (EFs) for a) linear, b) slower-than-linear, and c) faster-than-linear response type.

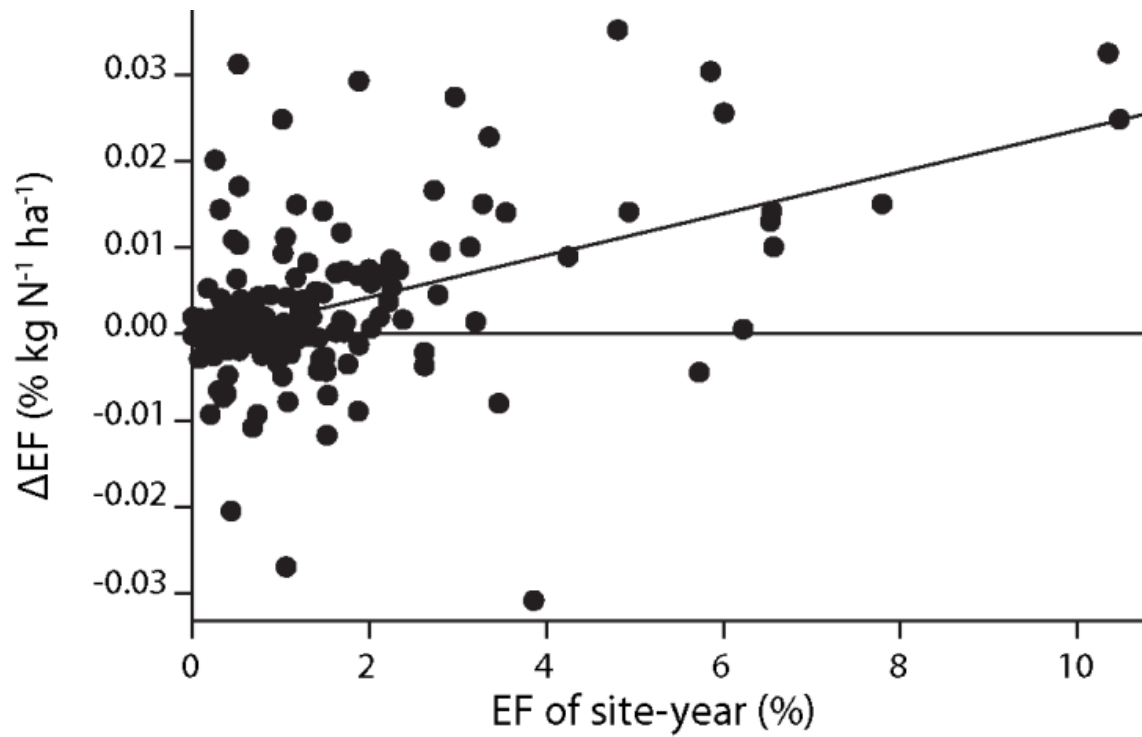


Figure C.2. ΔEF plotted against mean EF for each site-year in meta-analysis. Best linear regression line is plotted $\Delta EF = -0.00045 + 0.0024EF$. Standard error of the linear parameter is 0.0003.

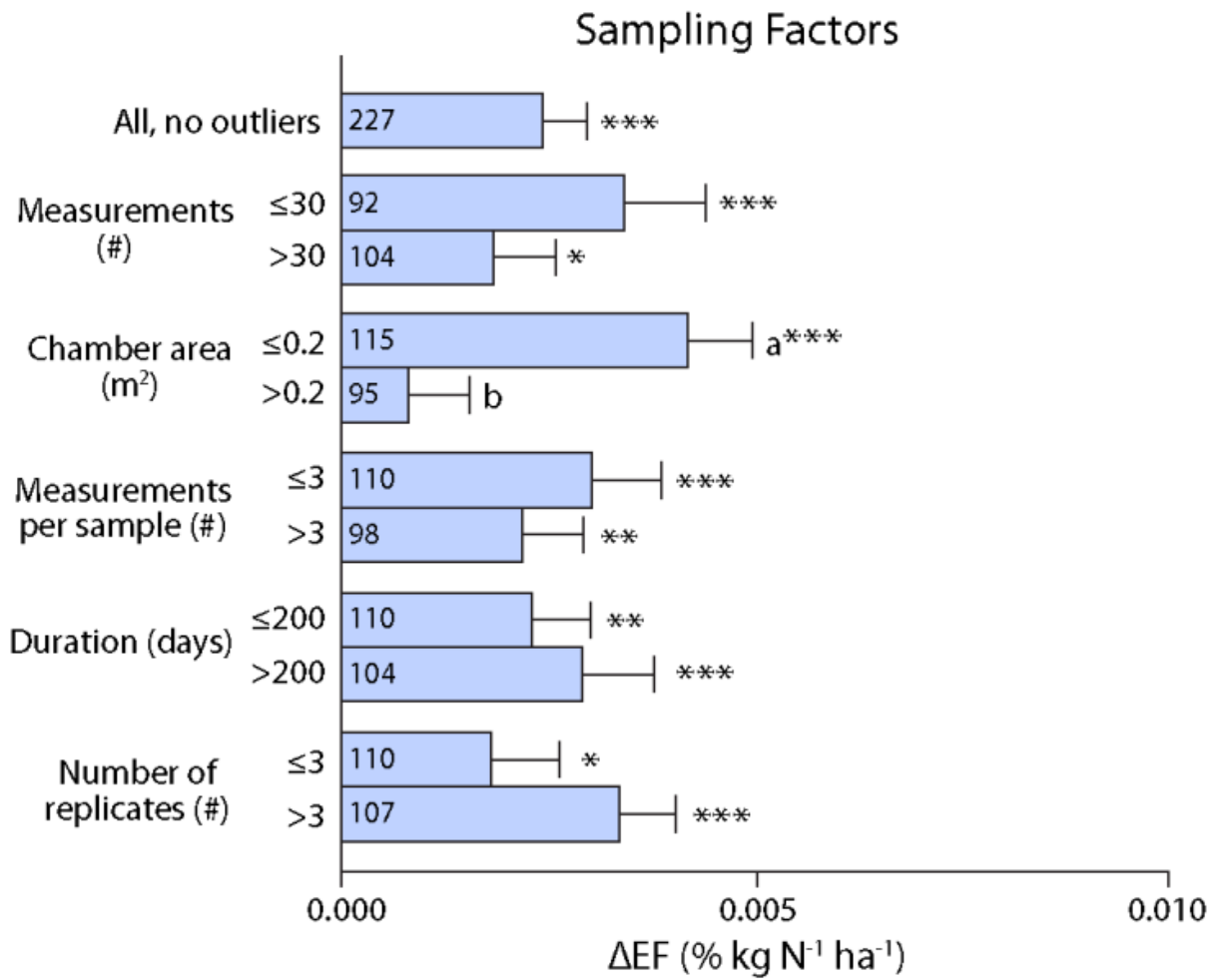


Figure C.3. Graph of mean ΔEF by type of sampling factor.

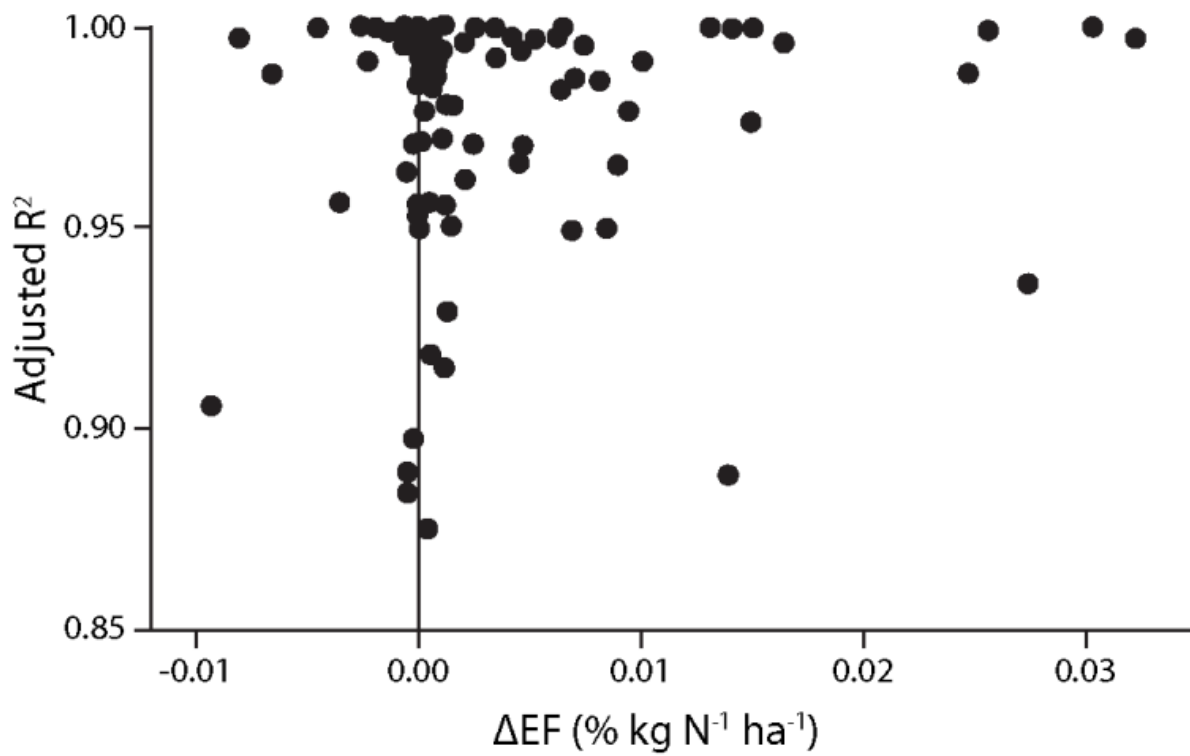


Figure C.4. Relationship between ΔEF and adjusted r^2 of the quadratic function fit is absent.

APPENDIX D

REFERENCES FOR STUDIES INCLUDED IN META-ANALYSIS

- Abdalla, M., M. Jones, P. Ambus, and M. Williams. 2010. Emissions of nitrous oxide from Irish arable soils: effects of tillage and reduced N input. *Nutrient Cycling in Agroecosystems* 86:53-65.
- Allen, D. E., G. Kingston, H. Rennenberg, R. C. Dalal, and S. Schmidt. 2010. Effect of nitrogen fertilizer management and waterlogging on nitrous oxide emission from subtropical sugarcane soils. *Agriculture Ecosystems & Environment* 136:209-217.
- Anger, M., C. Hoffmann, and W. Kuhbauch. 2003. Nitrous oxide emissions from artificial urine patches applied to different N-fertilized swards and estimated annual N₂O emissions for differently fertilized pastures in an upland location in Germany. *Soil Use and Management* 19:104-111.
- Augustin, J., W. Merbach, and J. Rogasik. 1999. Factors influencing nitrous oxide and methane emissions from minerotrophic fens in northeast Germany. *Biology and Fertility of Soils* 28:1-4.
- Balezientiene, L. and A. Kusta. 2012. Reducing Greenhouse Gas Emissions in Grassland Ecosystems of the Central Lithuania: Multi-Criteria Evaluation on a Basis of the ARAS Method. *Scientific World Journal* 2012:908384
- Breitenbeck, G. A. and J. M. Bremner. 1986. Effects of rate and depth of fertilizer application on emission of nitrous-oxide from soil fertilized with anhydrous ammonia. *Biology and Fertility of Soils* 2:201-204.
- Brummer, C., N. Bruggemann, K. Butterbach-Bahl, U. Falk, J. Szarzynski, K. Vielhauer, R. Wassmann, and H. Papen. 2008. Soil-atmosphere exchange of N₂O and NO in near-natural savanna and agricultural land in Burkina Faso (W. Africa). *Ecosystems* 11:582-600.
- Cai, Z. C., G. X. Xing, X. Y. Yan, H. Xu, H. Tsuruta, K. Yagi, and K. Minami. 1997. Methane and nitrous oxide emissions from rice paddy fields as affected by nitrogen fertilisers and water management. *Plant and Soil* 196:7-14.
- Cardenas, L. M., R. Thorman, N. Ashlee, M. Butler, D. Chadwick, B. Chambers, S. Cuttle, N. Donovan, H. Kingston, S. Lane, M. S. Dhanoa, and D. Scholefield. 2010. Quantifying annual N₂O emission fluxes from grazed grassland under a range of inorganic fertiliser nitrogen inputs. *Agriculture, Ecosystems & Environment* 136:218-226.

- Chang, C., H. H. Janzen, and C. M. Cho. 1998. Nitrous Oxide Emission From Long-Term Manured Soils. *Soil Science Society of America Journal* 62:677-682.
- Cheng, W., Y. Nakajima, S. Sudo, H. Akiyama, and H. Tsuruta. 2002. N₂O and NO emissions from a field of Chinese cabbage as influenced by band application of urea or controlled-release urea fertilizers. *Nutrient Cycling in Agroecosystems* 63:231-238.
- Chiaradia, J. J., M. K. Chiba, C. A. de Andrade, J. B. do Carmo, C. de Oliveira, and A. Lavorenti. 2009. CO₂, CH₄ and N₂O fluxes in an ultisol treated with sewage sludge and cultivated with castor bean. *Revista Brasileira De Ciencia Do Solo* 33:1863-1870.
- Ciampitti, I. A., E. A. Ciarlo, and M. E. Conti. 2005. Nitrous oxide emission during a soybean *Glycine max* (L.) Merrill culture: inoculation and nitrogen fertilization effects (in Spanish) Emisiones de oxido nitroso en un cultivo de soja *Glycine max* (L.) Merrill : efecto de la inoculacion y de la fertilizacion nitrogenada. *Ciencia del Suelo* 23(2):123-131
- Ding, W. X., Y. Cai, Z. C. Cai, K. Yagi, and X. H. Zheng. 2007. Nitrous oxide emissions from an intensively cultivated maize-wheat rotation soil in the North China Plain. *Science of The Total Environment* 373:501-511.
- Dong, Y. H., Z. Ouyang, and S. L. Liu. 2005. Nitrogen transformation in maize soil after application of different organic manures. *Journal of Environmental Sciences-China* 17:340-343.
- Dusenbury, M. P., R. E. Engel, P. R. Miller, R. L. Lemke, and R. Wallander. 2008. Nitrous oxide emissions from a northern great plains soil as influenced by nitrogen management and cropping systems. *Journal of Environmental Quality* 37:542-550.
- Fernandez-Luqueno, F., V. Reyes-Varela, C. Martinez-Suarez, R. E. Reynoso-Keller, J. Mendez-Bautista, E. Ruiz-Romero, F. Lopez-Valdez, M. L. Luna-Guido, and L. Dendooven. 2009. Emission of CO₂ and N₂O from soil cultivated with common bean (*Phaseolus vulgaris* L.) fertilized with different N sources. *Science of The Total Environment* 407:4289-4296.
- Gagnon, B., N. Ziadi, P. Rochette, M. H. Chantigny, and D. A. Angers. 2011. Fertilizer Source Influenced Nitrous Oxide Emissions from a Clay Soil under Corn. *Soil Science Society of America Journal* 75:595-604.
- Gao, X. P., M. Tenuta, A. Nelson, B. Sparling, D. Tomaszewicz, R. M. Mohr, and B. Bizimungu. 2013. Effect of nitrogen fertilizer rate on nitrous oxide emission from irrigated potato on a clay loam soil in Manitoba, Canada. *Canadian Journal of Soil Science* 93:1-11.
- Halvorson, A. D., S. J. Del Grosso, and C. A. Reule. 2008. Nitrogen, tillage, and crop

- rotation effects on nitrous oxide emissions from irrigated cropping systems. *Journal of Environmental Quality* 37:1337-1344.
- Hansen, S., J. E. Mæhlum, and L. R. Bakken. 1993. N₂O and CH₄ fluxes in soil influenced by fertilization and tractor traffic. *Soil Biology and Biochemistry* 25:621-630.
- Harrison, R. M., S. Yamulki, K. W. T. Goulding, and C. P. Webster. 1995. Effect of fertilizer application on NO and N₂O fluxes from agricultural fields. *Journal of Geophysical Research-Atmospheres* 100:25923-25931.
- Henault, C., X. Devis, S. Page, E. Justes, R. Reau, and J. C. Germon. 1998. Nitrous oxide emissions under different soil and land management conditions. *Biology and Fertility of Soils* 26:199-207.
- Hoben, J. P., R. J. Gehl, N. Millar, P. R. Grace, and G. P. Robertson. 2011. Nonlinear nitrous oxide (N₂O) response to nitrogen fertilizer in on-farm corn crops of the US Midwest. *Global Change Biology* 17:1140-1152.
- Hoffmann, C., M. Anger, and W. Kuhbauch. 2001. N₂O emissions from true meadows dependent on location and N fertilization. *Journal of Agronomy and Crop Science* 187:153-159.
- Hoogendoorn, C. J., C. A. M. de Klein, A. J. Rutherford, S. Letica, and B. P. Devantier. 2008. The effect of increasing rates of nitrogen fertiliser and a nitrification inhibitor on nitrous oxide emissions from urine patches on sheep grazed hill country pasture. *Australian Journal of Experimental Agriculture* 48:147-151.
- Huang S., W. Jiang, J. Lu, and J. Cao. 2005. Influence of nitrogen and phosphorus fertilizers on N₂O emissions in rice fields. *China Environmental Science* 25:540-543
- Hyde, B. P., M. J. Hawkins, A. F. Fanning, D. Noonan, M. Ryan, P. O'Toole, and O. T. Carton. 2006. Nitrous oxide emissions from a fertilized and grazed grassland in the South East of Ireland. *Nutrient Cycling in Agroecosystems* 75:187-200.
- Iqbal, M. T. 2009. Effects of nitrogen and phosphorous fertilisation on nitrous oxide emission and nitrogen loss in an irrigated rice field. *Malaysian Journal of Soil Science* 13:105-117.
- Izaurrealde, R. C., R. L. Lemke, T. W. Goddard, B. McConkey, and Z. Zhang. 2004. Nitrous oxide emissions from agricultural toposequences in Alberta and Saskatchewan. *Soil Science Society of America Journal* 68:1285-1294.
- Ji, Y., G. Liu, J. Ma, H. Xu, and K. Yagi. 2012. Effect of controlled-release fertilizer on nitrous oxide emission from a winter wheat field. *Nutrient Cycling in Agroecosystems* 94:111-122.

- Kaiser, E. A., K. Kohrs, M. Kucke, E. Schnug, O. Heinemeyer, and J. C. Munch. 1998. Nitrous oxide release from arable soil: Importance of N-fertilization, crops and temporal variation. *Soil Biology & Biochemistry* 30:1553-1563.
- Kammann, C., L. Grunhage, C. Muller, S. Jacobi, and H. J. Jager. 1998. Seasonal variability and mitigation options for N₂O emissions from differently managed grasslands. *Environmental Pollution* 102:179-186.
- Kavdir, Y., H. J. Hellebrand, and J. Kern. 2008. Seasonal variations of nitrous oxide emission in relation to nitrogen fertilization and energy crop types in sandy soil. *Soil & Tillage Research* 98:175-186.
- Kern, J., H. J. Hellebrand, and V. Scholz. 2008. Variability of N₂O emissions during the production of poplar and rye. Central theme, technology for all: sharing the knowledge for development. *Proceedings of the International Conference of Agricultural Engineering, XXXVII Brazilian Congress of Agricultural Engineering, International Livestock Environment Symposium - ILES VIII, Iguassu Falls City, Brazil, 31st August to 4th September, 2008:unpaginated.*
- Khan, S., T. Clough, K. Goh, and R. Sherlock. 2010. In situ determination of NO and N₂O from cow-urine applied to a pasture soil under summer conditions. *Proceedings of the 19th World Congress of Soil Science: Soil solutions for a changing world, Brisbane, Australia, 1-6 August 2010. Congress Symposium 4: Greenhouse gases from soils:125-127.*
- Lampe, C., K. Dittert, M. Wachendorf, B. Sattelmacher, and F. Taube. 2004. Nitrous oxide fluxes from grassland soils with different fertiliser regimes. vdf Hochschulverlag AG an der ETH Zurich, Zurich, Switzerland.
- Lessard, R., P. Rochette, E. G. Gregorich, E. Pattey, and R. L. Desjardins. 1996. Nitrous oxide fluxes from manure-amended soil under maize. *Journal of Environmental Quality* 25:1371-1377.
- Letica, S. A., C. A. M. de Klein, C. J. Hoogendoorn, R. W. Tillman, R. P. Littlejohn, and A. J. Rutherford. 2010. Short-term measurement of N₂O emissions from sheep-grazed pasture receiving increasing rates of fertiliser nitrogen in Otago, New Zealand. *Animal Production Science* 50:17-24.
- Li, X., K. Inubushi, and K. Sakamoto. 2002. Nitrous oxide concentrations in an Andisol profile and emissions to the atmosphere as influenced by the application of nitrogen fertilizers and manure. *Biology and Fertility of Soils* 35:108-113.
- Lin, S., J. Iqbal, R. G. Hu, J. S. Wu, J. S. Zhao, L. L. Ruan, and S. Malghani. 2011. Nitrous oxide emissions from rape field as affected by nitrogen fertilizer management: A case study in Central China. *Atmospheric Environment* 45:1775-1779.

- Liu, X. J., M. Walsh, X. T. Ju, F. S. Zhang, D. Schimel, and D. Ojima. 2004. NO and N₂O fluxes from agricultural soils in Beijing area. *Progress in Natural Science* 14:489-494.
- Liu, X. J., A. R. Mosier, A. D. Halvorson, and F. S. Zhang. 2005. Tillage and nitrogen application effects on nitrous and nitric oxide emissions from irrigated corn fields. *Plant and Soil* 276:235-249.
- Liu, C., K. Wang, and X. Zheng. 2012. Responses of N₂O and CH₄ fluxes to fertilizer nitrogen addition rates in an irrigated wheat-maize cropping system in northern China. *Biogeosciences* 9:839-850.
- Lou, Y., M. Xu, X. He, Y. Duan, and L. Li. 2012. Soil nitrate distribution, N₂O emission and crop performance after the application of N fertilizers to greenhouse vegetables. *Soil Use and Management* 28:299-306.
- Ma, J., X. L. Li, H. Xu, Y. Han, Z. C. Cai, and K. Yagi. 2007. Effects of nitrogen fertiliser and wheat straw application on CH₄ and N₂O emissions from a paddy rice field. *Australian Journal of Soil Research* 45:359-367.
- Ma, B. L., T. Y. Wu, N. Tremblay, W. Deen, M. J. Morrison, N. B. McLaughlin, E. G. Gregorich, and G. Stewart. 2010. Nitrous oxide fluxes from corn fields: on-farm assessment of the amount and timing of nitrogen fertilizer. *Global Change Biology* 16:156-170.
- MacKenzie, A. F., M. X. Fan, and F. Cadrin. 1997. Nitrous oxide emission as affected by tillage, corn-soybean-alfalfa rotations and nitrogen fertilization. *Canadian Journal of Soil Science* 77:145-152.
- MacKenzie, A. F., M. X. Fan, and F. Cadrin. 1998. Nitrous oxide emission in three years as affected by tillage, corn-soybean-alfalfa rotations, and nitrogen fertilization. *Journal of Environmental Quality* 27:698-703.
- McKenney, D. J., K. F. Shuttleworth, and W. I. Findlay. 1980. Nitrous-oxide evolution rates from fertilized soil - effects of applied nitrogen. *Canadian Journal of Soil Science* 60:429-438.
- McSwiney, C. P. and G. P. Robertson. 2005. Nonlinear response of N₂O flux to incremental fertilizer addition in a continuous maize (*Zea mays* L.) cropping system. *Global Change Biology* 11:1712-1719.
- Mori, A. and M. Hojito. 2011. Nitrous oxide and methane emissions from grassland treated with bark- or sawdust-containing manure at different rates. *Soil Science and Plant Nutrition* 57:138-149.
- Mosier, A. R., A. D. Halvorson, C. A. Reule, and X. J. J. Liu. 2006. Net global warming

- potential and greenhouse gas intensity in irrigated cropping systems in northeastern Colorado. *Journal of Environmental Quality* 35:1584-1598.
- Pelster, D. E., F. Larouche, P. Rochette, M. H. Chantigny, S. Allaire, and D. A. Angers. 2011. Nitrogen fertilization but not soil tillage affects nitrous oxide emissions from a clay loam soil under a maize-soybean rotation. *Soil & Tillage Research* 115:16-26.
- Pennock, D. J. and M. D. Corre. 2001. Development and application of landform segmentation procedures. *Soil & Tillage Research* 58:151-162.
- Pfab, H., I. Palmer, F. Buegger, S. Fiedler, T. Muller, and R. Ruser. 2011. N₂O fluxes from a Haplic Luvisol under intensive production of lettuce and cauliflower as affected by different N-fertilization strategies. *Journal of Plant Nutrition and Soil Science* 174:545-553.
- Qin, S. P., Y. Y. Wang, C. S. Hu, O. Oenema, X. X. Li, Y. M. Zhang, and W. X. Dong. 2012. Yield-scaled N₂O emissions in a winter wheat summer corn double-cropping system. *Atmospheric Environment* 55:240-244.
- Ruser, R., H. Flessa, R. Schilling, F. Beese, and J. C. Munch. 2001. Effect of crop-specific field management and N fertilization on N₂O emissions from a fine-loamy soil. *Nutrient Cycling in Agroecosystems* 59:177-191.
- Ryden, J. C. 1983. Denitrification loss from a grassland soil in the field receiving different rates of nitrogen as ammonium-nitrate. *Journal of Soil Science* 34:355-365.
- Schils, R. L. M., J. W. van Groenigen, G. L. Velthof, and P. J. Kuikman. 2008. Nitrous oxide emissions from multiple combined applications of fertiliser and cattle slurry to grassland. *Plant and Soil* 310:89-101.
- Signor, D., C. E. P. Cerri, and R. Conant. 2013. N₂O emissions due to nitrogen fertilizer applications in two regions of sugarcane cultivation in Brazil. *Environmental Research Letters* 8:015013.
- Sitaula, B. K., L. R. Bakken, and G. Abrahamsen. 1995. N-fertilization and soil acidification effects on N₂O and CO₂ emission from temperate pine forest soil. *Soil Biology and Biochemistry* 27:1401-1408.
- Song, C. C. and J. B. Zhang. 2009. Effects of soil moisture, temperature, and nitrogen fertilization on soil respiration and nitrous oxide emission during maize growth period in northeast China. *Acta Agriculturae Scandinavica Section B-Soil and Plant Science* 59:97-106.
- Thornton, F. C. and R. J. Valente. 1996. Soil emissions of nitric oxide and nitrous oxide from no-till corn. *Soil Science Society of America Journal* 60:1127-1133.

- van Groenigen, J. W., G. J. Kasper, G. L. Velthof, A. van den Pol-van Dasselaar, and P. J. Kuikman. 2004. Nitrous oxide emissions from silage maize fields under different mineral nitrogen fertilizer and slurry applications. *Plant and Soil* 263:101-111.
- Velthof, G. L., A. B. Brader, and O. Oenema. 1996. Seasonal variations in nitrous oxide losses from managed grasslands in The Netherlands. *Plant and Soil* 181:263-274.
- Velthof, G. L. and J. Mosquera. 2011. The impact of slurry application technique on nitrous oxide emission from agricultural soils. *Agriculture Ecosystems & Environment* 140:298-308.
- Velthof, G. L. and O. Oenema. 1997. Nitrous oxide emission from dairy farming systems in the Netherlands. *Netherlands Journal of Agricultural Science* 45:347-360.
- Velthof, G. L., O. Oenema, R. Postma, and M. L. v. Beusichem. 1997. Effects of type and amount of applied nitrogen fertilizer on nitrous oxide fluxes from intensively managed grassland. *Nutrient Cycling in Agroecosystems* 46:257-267.
- Venterea, R. T., P. M. Groffman, L. V. Verchot, A. H. Magill, J. D. Aber, and P. A. Steudler. 2003. Nitrogen oxide gas emissions from temperate forest soils receiving long-term nitrogen inputs. *Global Change Biology* 9:346-357.
- Wang, J. Y., J. X. Jia, Z. Q. Xiong, M. A. K. Khalil, and G. X. Xing. 2011. Water regime-nitrogen fertilizer-straw incorporation interaction: Field study on nitrous oxide emissions from a rice agroecosystem in Nanjing, China. *Agriculture Ecosystems & Environment* 141:437-446.
- Xiang H., B. Zhu, F. Kuang, K. Li, Y. Wangy, and X. Zheng. 2007. Effects of nitrogen fertilizer application on N₂O emission in a purple soil and maize root system. *Acta Scientiae Circumstantiae* 27:413-420
- Yao, Z. S., X. H. Zheng, H. B. Dong, R. Wang, B. L. Mei, and J. G. Zhu. 2012. A 3-year record of N₂O and CH₄ emissions from a sandy loam paddy during rice seasons as affected by different nitrogen application rates. *Agriculture Ecosystems & Environment* 152:1-9.
- Zebarth, B. J., P. Rochette, and D. L. Burton. 2008. N₂O emissions from spring barley production as influenced by fertilizer nitrogen rate. *Canadian Journal of Soil Science* 88:197-205.
- Zhang, J. and X. Han. 2008. N₂O emission from the semi-arid ecosystem under mineral fertilizer (urea and superphosphate) and increased precipitation in northern China. *Atmospheric Environment* 42:291-302.
- Zhang, L. H., C. C. Song, D. X. Wang, and Y. Y. Wang. 2007. Effects of exogenous nitrogen on freshwater marsh plant growth and N₂O fluxes in Sanjiang Plain, Northeast China.

Atmospheric Environment 41:1080-1090.

Zhao, X., Y. X. Xie, Z. Q. Xiong, X. Y. Yan, G. X. Xing, and Z. L. Zhu. 2009. Nitrogen fate and environmental consequence in paddy soil under rice-wheat rotation in the Taihu lake region, China. *Plant and Soil* 319:225-234.

Zhou, M. H., B. Zhu, K. Butterbach-Bahl, X. H. Zheng, T. Wang, and Y. Q. Wang. 2013. Nitrous oxide emissions and nitrate leaching from a rain-fed wheat-maize rotation in the Sichuan Basin, China. *Plant and Soil* 362:149-159.

Zou, J. W., Y. Huang, Y. Y. Lu, X. H. Zheng, and Y. S. Wang. 2005. Direct emission factor for N₂O from rice-winter wheat rotation systems in southeast China. *Atmospheric Environment* 39:4755-4765.